1506
UNIVERSITÀ
DEGLI STUDI
DI URBINO
CARLO BO

DIPARTIMENTO DI SCIENZE PURE E APPLICATE (DiSPeA)

CORSO DI DOTTORATO IN SCIENZE DI BASE E APPLICAZIONI

Curriculum B - Scienze della Terra

XXX CICLO

STRUCTURAL SETTING AND FLUID DYNAMICS IN CARBONATE MASSIFS OF UMBRIA-MARCHE APENNINES

Settore Scientifico Disciplinare: GEO/03 e GEO/05

RELATORE
Chiar.mo Prof. MARCO MENICHETTI

DOTTORANDO
Dott. ANDREA TAMBURINI

ANNO ACCADEMICO 2016/2017

What is harder than rock, or softer than water?

Yet soft water hollows out hard rock.

Ovidio

Contents

Acknowledgments

I wish to express my sincere appreciation to those who have contributed to this thesis.

Firstly, I would like to express my sincere gratitude to my supervisor Prof. Marco Menichetti for the continuous support of my Ph.D study and related research, for his patience, motivation, and knowledge.

Similar, profound gratitude goes to Ph.D Daniela Piacentini. I am particularly indebted to Daniela for her constant support when whenever I approached her.

My colleagues, Matteo Roccheggiani and Emanuela Tirincanti, have all extended their support in a very special way, and I gained a lot from them, through their personal and scholarly interactions, their suggestions at various points of my research programme.

Last but not the least, I would like to thank my family: my wife, mom, dad and my brother for providing me with unfailing support and continuous encouragement throughout my years of study and through the process of researching and writing this thesis.

Abstract

The aim of this research is to understand the hydrogeological mechanisms of groundwater circulation and their relationship with the structural setting in carbonate massifs of Umbria-Marche Apennines. Karst aquifers are characterized by a strong heterogeneity in their physical properties. Hence, in order to define the dynamics of fluid circulation in these environments is necessary to integrate different investigative approaches.

Umbria-Marche carbonatic ridge is characterized by three hydrogeological complexes: a basal complex (Massiccio aquifer), an intermediate complex (Maiolica aquifer) and an upper complex (Scaglia aquifer). The carbonatic lithotypes covered about the 67% of the study area and only the 4.3% and 28.8% are represented by the Massiccio complex (the main aquifer of Apennine ridge) and Maiolica complex, respectively. On the contrary, the sub-basins showing higher percentage values of outcropping of Massiccio and Maiolica complexes. These results, indicate as the basal groundwater circulation is controlled exclusively by Massiccio and Maiolica complex.

Analysis of fracture systems exposed in different outcrops of Massiccio and Maiolica complexes, have defined a conceptual model of structural and hydraulic properties of the main aquifers. There are two main fracture sets oriented at SW-NE (dip-direction of N115) and NNE-SSW (dip-direction of N20), that probably the main pathways for the water-circulation from infiltration zone to spring outlet. Discrete Fracture Network (DFN) models of representative geocellar volumes builted to compute fracture porosity and correspondent permeability (K*xx*, K*yy*, K*zz*), show that the fracture porosity of Calcare Massiccio Formation is much greater than Maiolica Formation (4.3% and 1.7%, respectively), and also the permeability values result well correlated with this trend.

From hydrogeological point of view, recession analysis and time series analysis (auto- and cross-correlation functions) applied at daily discharge of six karst springs highlighted the presence of two type of karst aquifers: aquifer with unimodal behaviour and aquifers with bimodal behaviour. These results indicate that Maiolica Formation is characterized by high fracturation degree and a slightly karstification, controlling the infiltration and percolation processes, whereas Calcare Massiccio Formation regulate the groundwater circulation in the deeper zones of aquifer characterized by a high karstification degree through a rather developed conduit networks.

List of figures

List of tables

1. Introduction

Carbonate rocks crop over approximately 10% of the ice-free continental areas and underly much more, and 25% of the planet human population supplied by karst water (Ford and Williams, 1989). Although this number is probably over-estimate, karst groundwater constitutes a crucial freshwater resource for many countries, regions and cities around the world. For example, in Europe, where 35% of the land surface is occupied by carbonates, certain countries such as Slovenia and Austria obtain over 50% of the total water supply from karst aquifers (Kovacs, 2003). At the same time, karst aquifers are commonly highly vulnerable to contamination and are impacted by a wide range of human activities (Drew and Hötzl, 1999). Hence, the exploitation, maintenance of water quality, and the protection of karst aquifers are of a vital importance in these regions.

More than half of the surface area of the continents is covered with hard rocks of low permeability. These rocks may acquire moderate to good permeability on account of fracturing and hence are broadly grouped under the term fractured rocks, in the context of hydrogeology.

From the hydrogeological point of view, fractures and discontinuities are amongst the most important geological structures. Most rocks possess fractures and other discontinuities which facilitate storage and movement of fluids through them. On the other hand, some discontinuities, e.g. faults and dykes may also act as barriers to water flow. Porosity, permeability and groundwaters flow characteristics of fractured rocks, particularly their quantitative aspects, are rather poorly understood. Main flow paths in fractured rocks are along joints, fractures, shear zones, faults and other discontinuities.

Besides conventional survey techniques, such as geological mapping, structural analysis, hydrograph analysis, time-series analysis, chemical and physical water analysis, etc., the quantitative characterization of karst hydrogeological systems increasingly important (Kovacs, 2003).

1.1. Geological and hydrogeological framework of Umbria-Marche Apennines

The geology of Central Italy has been shaped predominantly by the continental Cenozoic collision of the Corsica/Sardinia and the now subducted Adriatic plates. Geological and geophysical data highlight two main sectors within this region: a western, Tyrrhenian sector dominated by Neogene-Quaternary, active, back-arc extensional tectonics and an eastern Adriatic sector dominated by an active compressional stress field (Cavazza and Wezel, 2003).

The study area is located in the northern portion of the Umbria-Marche Apennines, corresponding to the innermost carbonate ridge (**Fig.1.1**.). This chain has developed since late Messinian time, involving a Mesozoic-Cenozoic sedimentary sequence. From hydrostratigraphic point of view this Apennine sector is represented by typical Meso-Cenozoic Umbria-Marche sedimentary sequence (Carloni, 1964; Calamita et al., 1990, 1999; Menichetti, 1991; Marchegiani et al., 1999; Deiana et al.,

2002; Mazzoli et al., 2002), characterized by four major mechanical units: (*1*) a Triassic thick sequence f alternating of dolostones, anhydrites and limestones (Anidriti di Burano Formation and Calcari ad Rhaetavicula Contorta Formation); (*2*) lower Jurassic, poorly layered platform limestones (Calcare Massiccio Formation); (*3*) a lower Jurassic-Miocene pelagic sequence including mainly well-bedded limestones, marly limestones and marls (from Corniola to Bisciaro Formations); (*4*) a Miocene to Pliocene siliciclastic sequence consisting of mainly sandstones and marls (Schlier and Marnoso-Arenacea Formations) (Centamore et al., 1972, 1975).

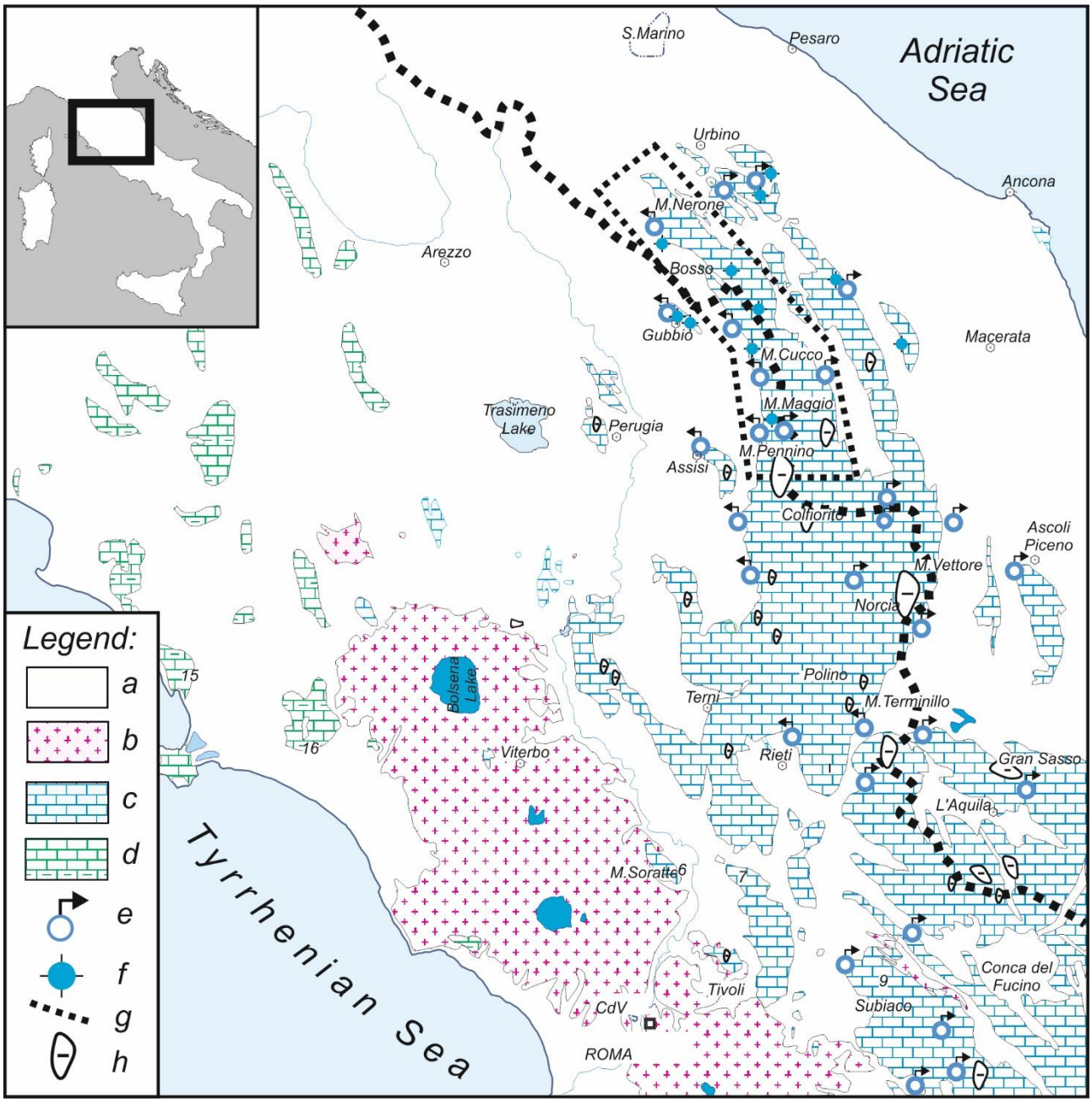

Fig.1.1. Schematic illustration of aquifer complexes in central Italy. (a) Cenozoic succession, (b) Quaternary volcanic complex, (c) mainly carbonatic Mesozoic complex, (d), larger karst springs, (f) deep-wells, (g) Apennine watershed and (h) sinkholes.

The main phase of the Apennine chain uplift, relevant to cave development, took place within the Pleistocene (Mayer et al., 2003). The primary tectonic features controlling the underground Apennine karst morphology and the carbonate reservoir groundwater drainages are a system of N-S transpressive faults and networks of conjugated joint sets distributed in a primary NE-SW and secondary NW-SE directions. Specifically, the N-S faults are associated with the main passages and rooms, and control the development of the larger underground voids while solutional morphologies are associated with joint systems (Menichetti, 1987; Mayer et al., 2003).

Therefore, the regional drainage network is quite complex due the discrepancy between the highest elevations and the drainage divide in consequence of the eastward migration, since Neogene, of the compressional and extensional tectonic stress field (Cavazza and Wezel, 2003). In many cases there is the presence of superimpositions, antecedences and regressions of the river networks with respect to the anticline structures.

The regional aquifers are located in the Jurassic carbonate banks and the groundwater supplies the springs located in the lower valleys or in the main fault zones with an average base flow discharge of 22 l/sec/km^2 (Boni and Bono, 1986; Galdenzi and Menichetti, 1995). In fact, the largest caves in the area are located in a 1000 m thick Jurassic carbonate bank, where syngenetic porosity in sedimentary facies of packstone and grainstone is well developed. Occasionally, small caves are hosted in Cenozoic marly-limestone successions confined by sandstone and marl formations (Menichetti, 1987). Aquicludes are represented by marly layers distribute at the different levels in the stratigraphic succession. Groundwater flow in the transfer zone is controlled by karst conducts and fissures while faults and fractures characterize the drainage of the regional carbonate reservoirs. The hydrodynamics of larger springs is regulated mainly by the base flow, while in some cases quick flows mark the transfer zone. All karst systems have a basal input points through faults and fracture, at the bottom of the oxidizing zone, where mineralized water rises up from deep seated hydrogeological circuits with recharge times of many months. The groundwater flow in the vadose zone is controlled by conduit systems, with transfer time of few weeks (Sarbu et al., 2000).

Finally, in the basal regions of aquifers, the hydrothermal circuit can reach the Triassic anhydrites at depth, and after a journey of some decades, rises up in the springs located close to the master faults along the border of the main karstic structures (Menichetti et al., 2008).

1.2. Characteristics of karst aquifers

The most important feature of karst aquifers from a hydrogeological perspective, that makes them different from any other kind of hydrogeological systems, is the high flow heterogeneity. From geochemical point of view of the flow medium water, can reacts with the host rocks (Kovacs, 2003). Groundwater flow dissolves the carbonates around interconnected voids (mainly primary porosity and fractures), enlarging aperture and increasing the hydraulic conductivity of rock matrix. The amount of dissolved limestone depends on the chemical composition/aggressiveness of the rock and of the water, but the relative karstification degree of the various fracture families depends mainly on the direction and the magnitude of groundwater flux density vector (Kiràly et al., 1971, 2002).

Carbonate rocks thus acquire a range of void of different origin that affect their capacity to store and transmit water.

Karst aquifers are therefore commonly differentiated into three end-member types, according the nature of the voids in which the water is stored and through which it is transmitted, namely *matrix*, *fracture* and *conduit*. Conduit may range from cm-wide solutionally enlarged fractures to huge cave passages (Mangin, 1975; Goldscheider and Drew, 2007). Therefore, karst aquifers can be described as a network of conduits embedded in, and interacting with, a matrix of less karstified rock. Flow in the conduits is rapid and often turbulent, while flow velocities in the matrix are much lower. On the contrary, water storage in the conduits is often limited, while significant storage may occur in the matrix, and in other parts of system (Drogue, 1980).

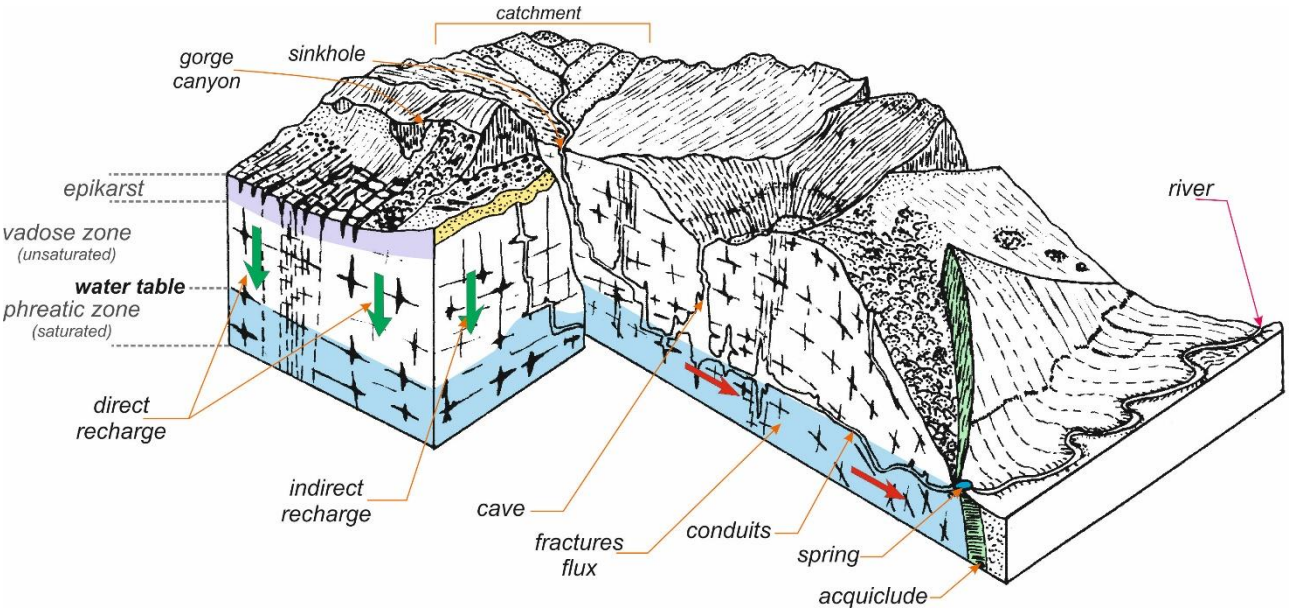

Fig.1.2. Schematic illustration of heterogeneous karst aquifer system characterised by duality of recharge (allogenic and autogenic), infiltration (point and diffuse) and porosity/flow (conduits, fractures and matrix).

Groundwater divides in karst regions can have other complication in both space and time. While these are often indicated as two-dimensional lines drawn on maps, they are perhaps better characterized as complex, three-dimensional surfaces within the subsurface.

Recharge to karst aquifers can occur in several ways (**Fig.1.2**). *Autogenic* recharge results from precipitation directly onto a karst surface where carbonate rocks are exposed this surface which then infiltrates enters the aquifer directly. In contrast, in more heterogeneous geological setting where karst rocks may adjacent to non-carbonate units, headwater areas may be dominated by surface flow high collects, and then upon reaching the soluble carbonates can enter the aquifer at discrete points, *allogenic* input.

1.3. Conceptual models of karstic groundwater flow

There are two main reasons for trying to model karst aquifers: (*i*) to characterize and understand the system (usually as an aid to improving management of groundwater resources) and (*ii*) to try to reproduce the evolution of its characteristics. The karst system connects the recharge area to the outflow spring (or springs), and karst processes direct groundwater towards the spring(s) along flow paths that have a hierarchical order. The physical system is defined by its structure (organization of flow paths), hydraulic behaviour (response to recharge) and its evolution (stage of development), and the framework of the system is the rock mass in which it is developed (Ford and Williams, 2007).

Therefore, every reasonable conceptual model of karst systems incorporates heterogeneity and accordingly the duality of hydraulic flow processes: duality of infiltration processes ("diffuse" or "concentrated"), duality of the groundwater flow field (low flow velocities in the fractured volumes vs high flow velocities in the channel network), duality of the discharge conditions (diffuse seepage from the low permeability volumes vs concentrated discharge from the channel network at the springs) (Kovàcs and Sauter, 2007).

1.3.1. Mangin conceptual model

According to the conceptual model of Mangin (1975), the main conduit system transmits infiltration waters towards a karst spring, but is poorly connected to large voids in the adjacent rocks, referred to "Annex-to-drain system". Active conduit system develops along one, well defined horizon (**Fig.1.3**). Although deep phreatic conduits may exist, the majority of the conduit flow takes place near the saturated and unsaturated zone interface. Mangin (1975) introduce the concept of the epikarst. This being a shallow, high-permeability karstified zone below the aquifer surface, where water rapidly drains through enlarged vertical shafts, reaching the saturated zone and contributing at a diffuse recharge.

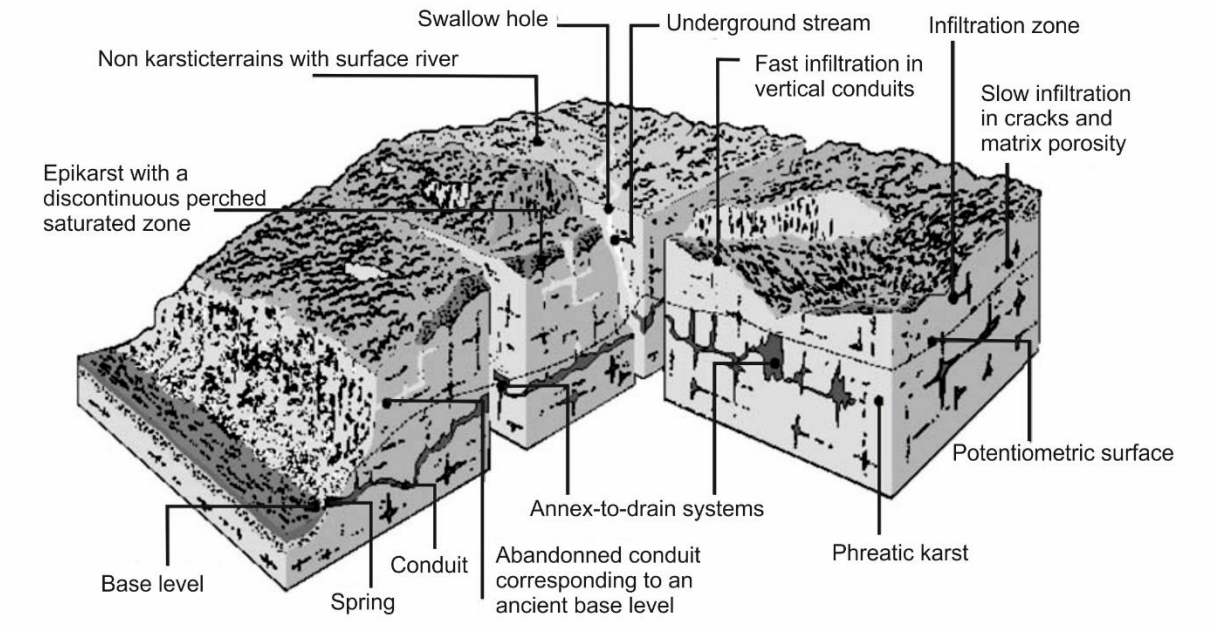

Fig.1.3. Conceptual model of a karst aquifer according to Mangin (1975).

It is believed to act as a temporary storage and distribution system for infiltrating water, similar to a perched aquifer. It is assumed to channel infiltrating water toward enlarged vertical shafts, thereby enhancing concentrated infiltration (Kovàcs and Sauter, 2007).

1.3.2. Drogue conceptual model

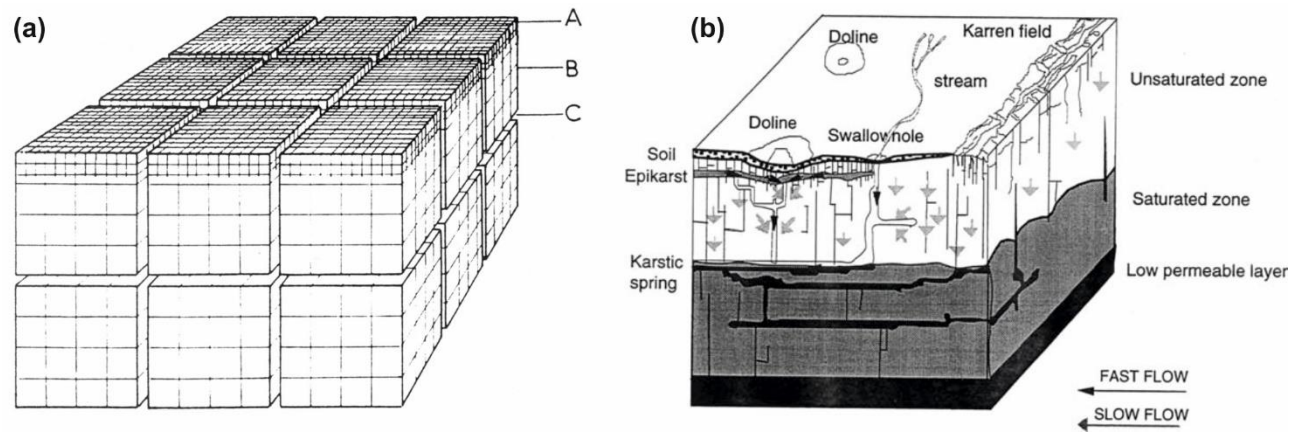

Fig.1.4. (a) Conceptual model of a karst aquifer according to Drogue (1980). A: highly permeable upper zone, B: blocks with low-permeability cracks with slow flow, C: high-permeability karst conduits with rapid flow; (b) Doerfliger and Zwahlen (1995) conceptual model.

Drogue (1974, 1980) assumes, that the geometric configuration of karst networks follows original rock fracture pattern. Joints constitute a double-fissured porosity system. This network consists of fissured blocks with a size in the order of several hundred meters, separated by high-permeability low storage conduits. Every block is dissected by small scale fissures or fracture with considerably larger storage, with low bulk permeability (**Fig.1.4a**).

The uppermost part of the aquifer is more intensely fissured than subjacent rock because of decompression phenomena. This increased permeability zone is responsible for enhanced infiltration of rainwater.

1.3.3. Kiràly conceptual model

The conceptual model proposed by Kiràly (1975, 2002) and Kiràly et al. (1995) combines the conceptual model of Mangin (1975) and Drogue (1980). This model involves the epikarst and a hierarchical organization of the conduit networks. It also comprises the hydraulic effect of nested groups of different discontinuities. This means that the aquifer permeability is determined by the fracture intersections, and the effective porosity is determined by fractures plains. Carbonate aquifers can be considered as interactive units of high-conductivity hierarchically organised karst channel network with a low-permeability fissured rock matrix. The main characteristics of this model have been synthesized in a conceptual model by Doerfliger and Zwahlen (1995) (**Fig.1.4b**).

Finally, Drogue (1971) and Kiraly (1975) proposed a structural approach. The karst aquifer is represented by a network of high permeability conduits embedded in a fissured media of low permeability. Such a representation is adapted for simulating karst spring hydrographs by the mean of physically based models. Kiraly (1998) developed a three dimensional numerical model where groundwater flow is simulated by the resolution of laminar flow equations in finite elements.

The major drawback of this approach is that a thorough knowledge of the aquifer geometry (dimensions and conduit location) is necessary to reproduce a real temporal evolution of discharge at the spring. Another limitation is the use of Darcian flow only, when it is established that flow in the conduits is mainly turbulent.

1.4. Objective of thesis

The principal aim of this thesis is to characterized the fluid circulation in the carbonate aquifer of Umbria-Marche Apennines (Central Italy) by acquiring quantitative information concerning the geometric and structural data and physical and hydraulic parameters of the basal aquifers.
These goals have been achieved by applying two different investigation approach:

1.4.1. Structural analysis and modelling of fractured carbonate formations

Fractures are the most important hydrogeological element in almost any setting and especially in hardrock environments. They control the hydraulic characteristics and solute transport. Without fractures, except for the upper-weathered zone, there is no significant groundwater flow in hard rocks. Therefore, understanding of the fluid-transit properties in fractures is important for production of critical natural resources and environmental protection as well as understanding of natural processes, such as formation of mineral and petroleum deposits, sediment diagenesis, mass wasting, movement of nutrients and chemical in soil zone.
Hence, a structural survey of several outcrops of carbonate formations (Calcare Massiccio and Maiolica) has allowed to define the geometrical and spatial properties of fractured rock mass. The characterization procedures used are well documented and corresponds to classical geomechanics analysis usually used. It has been necessary to evaluate how these properties vary with geological heterogeneity, scale, changing *in situ* stress.
The results were implemented for built discrete fracture models. These models input as much detail as possible, based upon field data, about the geometry and properties of individual fractures, sets, and zones into 3D networks (Sahimi, 1995; Zhang et al., 2003; Neuman, 2005). Each transmissive fracture has been assigned a uniform aperture and hydraulic conductivity. Since quantitative field data on fracture spacing and hydraulic properties are generally lacking, semi-quantitative estimates has been made of expected hydraulic properties (Marrett et al., 1999).

1.4.2. Hydrogeological investigations of several monitored karst springs

The measurements of discharge with time at the outlet of a karst aquifer makes the integral characterization of the hydraulic behaviour of the entire system possible (Kovàcs, 2003). The following two types of spring hydrograph analytical methods can be distinguished (Jeannin and Sauter, 1998):

a. *Single Events Methods* deal with the global hydraulic response of the aquifer to a single rainfall event. It widely accepted, that three basic attributes manifest in the global response of a karst aquifer: recharge, storage and transmission. Existing spring hydrograph analytical techniques make the characterization of these properties possible in a qualitative sense, but not quantitatively.

However, most of these methods are based on simple, or sometimes more complex cascades of reservoirs, and involve physical phenomena.

In this study, has been used two classical exponential expressions: classical equation provided by Maillet (1905) based on the emptying of a reservoir, and supposes that the spring discharge is a function of the volume of water held in storage; the composite exponential equation provides by Forkasiewitz and Paloc (1967), which assume that different segments of a spring hydrograph peak represent different parallel reservoirs, all contributing to the discharge of the spring.

b. Time Series Analysis deal with the global hydraulic response of karst systems to a succession of rainfall events. Univariate time series analytical methods are capable of identifying the cyclic variations. Bivariate time series analyses are very suitable for analysing the relation between the input (recharge) and output (discharge) parameters of different karst systems. These methods are based on pure mathematical operations, and they cannot be directly related to physical phenomena (Mangin and Pulido Bosch, 1983). Time series analyses provide limited information concerning the physical properties of the system itself.

1.5. Thesis structure

This thesis includes five separate studies focusing on different subjects. However, these studies follow a logical succession, and approach the principal goal step-by-step:

Chapter 2 provides the results of a systematic study carried out on the fracture systems exposed in different outcrops of fractured carbonate formations in the Umbria-Marche Apennines (central Italy). This chapter provides the conceptual models of structural and hydraulic properties of the main aquifers of northern Apennine ridge (Calcare Massiccio and Maiolica Formations).

Chapter 3 dealing with a classification of the different karst complexes presents in Umbria-Marche Apennine, defining the hydrogeological watershed. This is achieved summarizing the results in the Karst aquifers of the Umbria-Marche carbonatic ridge (central Apennines, Italy) map, at scale of 1:70000. This chapter also provides detailed maps having more information about the recharge/discharge areas of each hydrostructures considered.

Chapter 4 aim to define the hydrogeological mechanism of groundwater circulation and their relation between structural and stratigraphic setting of each aquifer considered. This is achieved by using the recession analysis and time series analysis applied at several hydrographs of karst springs monitored for about eight years (from 2007 to 2015).

Chapter 5 is a case study of a karst aquifer located in the Umbria-Marche Apennine (central Italy), relating to analysis of spring discharge and structural setting. This chapter provide a new method to define the geometrical and hydrogeological properties of a karst aquifer, based on relationship between recession coefficients and effective porosity of fractured rock mass.

Chapter 6 provides an analyses of the temporal relationships between a karst spring discharge and groundwater temperature, defining the residence time and structural organisation of karst aquifer and flow patterns. This is achieved applying time series analysis on two spring outlet monitored data belonging to the same karst system.

2. Karst aquifers of the umbria-marche carbonatic ridge (northern Apennines, Italy)

Abstract

Hydrogeological mapping is a powerful instrument improving the hydrogeological interpretation and understanding of the processes and dynamics of water flow both in the streams/river and in groundwater. Moreover, hydrogeological mapping is the first step for an adequate management and sustainability of the water resource, having a multiplicity of end-users, from politicians and planners to hydraulic engineers, well drillers and hydrogeologists. Hence, the present paper aims to present the karst aquifers of the Umbria-Marche carbonatic ridge (northern Apennines) from a hydrogeological point of view, in order to define the different karst complexes, the hydrogeological watershed and the regional dynamic of groundwater circulation within northern Apennines. The map proposed provides a range of hydrogeological information with different details: a regional map at a scale of 1:70000, summarizes the distribution of main hydrological structures and karst aquifers in Apennine ridge, and local detailed maps at a scale of 1:25000, summarize the recharge areas of sub-basins and their related karst springs.

The carbonatic lithotypes covered about the 67% of the study area and only the 4.3% and 28.8% are represented by the Massiccio complex (the main aquifer of Apennine ridge) and Maiolica complex, respectively. On the contrary, the sub-basins showing higher percentage values of outcropping of Massiccio and Maiolica complexes. These results, indicate as the basal groundwater circulation is controlled exclusively by Massiccio and Maiolica complex.

2.1.Introduction

The water resources in karst aquifers are of increasing interest since represent an important amount of water supply for the world's population (20-25 %; Ford and Williams, 2007). Karst aquifer represent the larger reservoirs with a rapid recharge time, nevertheless, they are known for the high vulnerability due to short residence time unable to degrade completely the organic matter and chemicals due to pressure of urbanization and intensive agricultural use (Heinz et al., 2009).

The umbria-marche Apennine ridge constitutes one of the most important karst reservoir of Central Italy, where rainfall water infiltrate and circulate into carbonate formations and flow through spring outlets, the discharge of which, with relative hydrographs analysis, adequately monitored provide important data (e.g. storage capacity, time response after a recharge event, water volumes available during wet and dry periods) to evaluate the characteristics of aquifer (Boni et al., 1986). This can be obtained through different analysis techniques widely used in hydrogeology not only for scientific research but also for land planning and land use management (e.g. preventing aquifer contamination and overexploitation).

Equally important is the definition of the characteristics of the catchment area because the groundwater refers to the replenishment of an aquifer with water from the land surface.

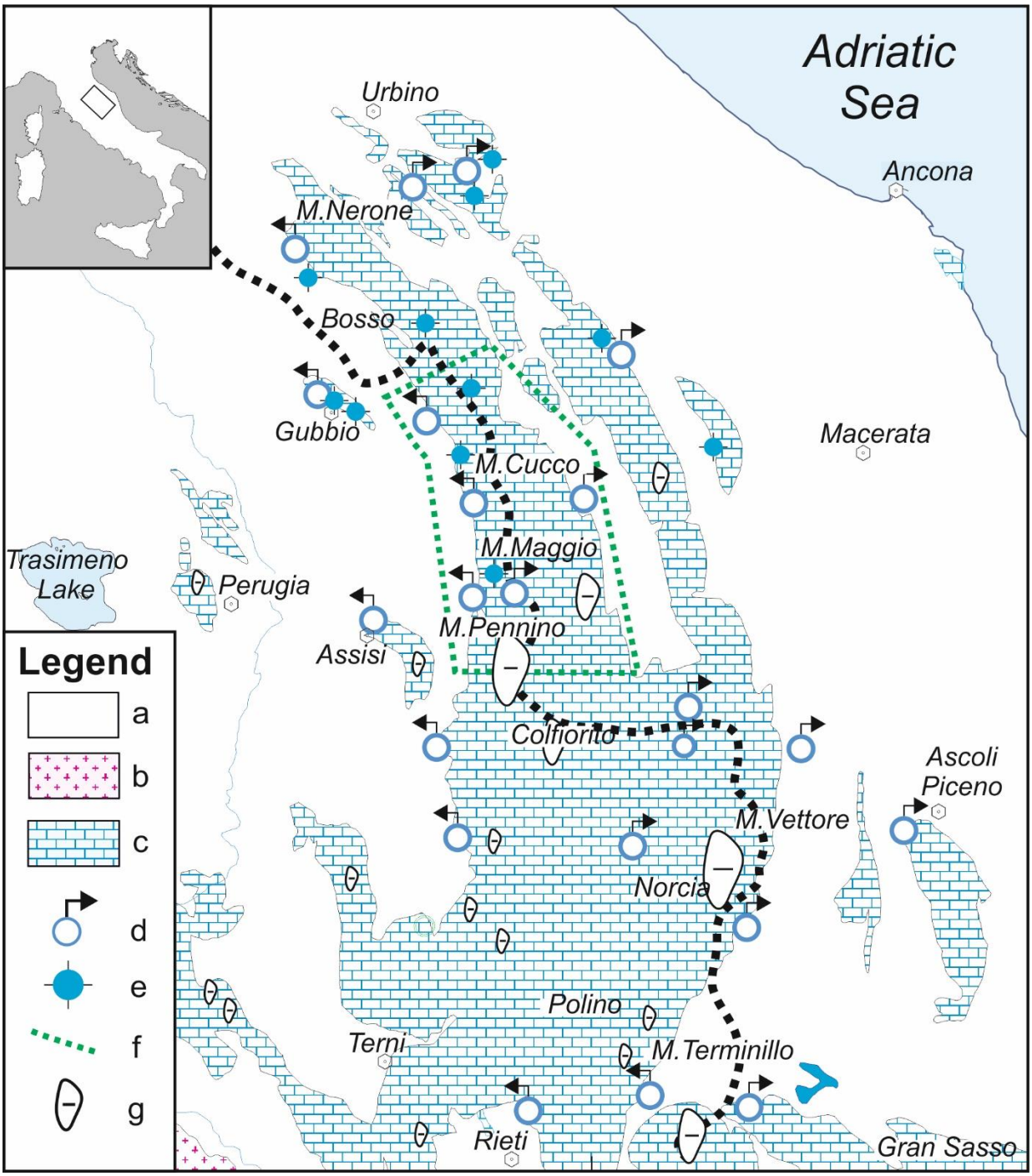

Fig.2.1. Schematic illustration of karstic aquifer in the Umbria-Marche Apennines. Legend: (a) Stratigraphic succession from Quaternary to Cretaceous; (b) Quaternary volcanic rocks; (c) Main calcareous stratigraphic succession from Jurassic to Cretaceous; (d) main karstic spring; (e) deep well reaching basal reservoir; (f) Apennines water divide; (g) karstic intermountain basin (from Menichetti, 2008).

Forest hydrologists and watershed managers have often dealt with uncertainty in quantifying the amount of the baseflow or recharge (Guardiola-Albert et al., 2015). Therefore, identifying and mapping karst landscape represents a fundamental step for understanding the role of each hydrostructure and dealing with the issue of water consumption and water supply. Demek et al. (1972) mentioned that detailed geomorphological maps are of special interest in planning and effective use

of the various geomorphological environment, because they take into consideration the laws controlling the development of relief and understanding of the whole natural environment.

Geomorphological maps allow for the accurate recording of landform information in a map form that can be utilised in further derivative studies such as environmental surveys, site or resource planning, hazard mapping and engineering design (Cooke and Doornkamp, 1990).

Paloc and Margat (1985) pointed out that two complementary approaches to mapping have been proposed, one more hydro-geolithological in emphasis and the other more hydro-geodynamic. In particular, for karst areas, Paloc and Margat (1985) emphasized the importance of classifying baseflow discharges of springs and surface streams. The hydro-geolithological approach superimposes three kinds of information: (*i*) lithological types that are assumed to represent permeability classes; (*ii*) piezometric data from which groundwater flow may be inferred; (*iii*) surface hydrography with data on sites of water exploitation (Ford and Williams, 2007). The hydro-geodynamic approach presents information concerning: (*i*) the constitution of aquifer systems, based on the distinction between disposition of and location of the principal rock bodies (taking into account the degree to which they are water-bearing and their possible layering); (*ii*) the boundary conditions of aquifers, distinguishing between the direction of water flow (input, output, or static) and flow conditions as opposed to potential conditions (Ford and Williams, 2007).

In this contest, the karst aquifers within the central Apennine ridge, located between Umbria and Marche regions (Italy), have been investigated (**Fig.2.1**).

A first approach on the same area which considered the quantitative evaluation of effective infiltration in the karst system of Central Apennines was proposed by Boni and Bono (1982). Other study of hydrogeological mapping of Central Italy has been introduced by Boni et al*ii* (1986). The authors edited three maps at different scale: (*i*) hydrogeological map and hydrological map at 1:500000; (*ii*) water balance and groundwater resources at 1:1000000, highlighting the relationships between geology and regional hydrogeology. These hydrogeological maps provide fundamental information such as the delineation of the groundwater divides and the definition of the basal circulation of groundwater for future comparison on the resource maintenance and management.

The main objectives of the present study were: (1) classify the different karst complexes; (2) define the hydrogeological watershed and (3) highlight the relationship between different carbonate hydrological complexes and their role in groundwater circulation within UM Apennines. The results achieved were summarized in the *Karst aquifers of the umbria-marche carbonatic ridge (central Apennines, Italy)* map, at scale of 1:70000. In addition, detailed maps have been elaborated to provide a more detailed information about the recharge/discharge areas of each hydrostructures considered.

The hydrogeological map covers a sector of umbria-marche Apennine, from Mt Cucco at north to Mt Pennino at south, including the different anticline structures and their associated karst springs.
Such a map, including hydrogeological, geo-structural and geomorphological data, represents the basis for dam and reservoir construction in any geological environment including karst. The key investigation targets in karst are watershed zones, the evolution process of karst aquifer, depth of the base of karstification, location of karst conduits, and groundwater regime.

2.2.Study area

2.2.1. Geological setting

The study area encompasses the western part of UM Apennines, an arcuate fold and thrust belt verging towards ENE (De Feyter et al., 1987; Barchi et al., 1998), displaced by several thrusts fault systems striking NNW-SSE and strike slip faults with N-S and E-W orientation. Several rootless anticlines, elongated for about 20 km along the axe-oriented NW-SE are arranged in a dextral step. This structural configuration is formed in the framework of the convergence between the European continental crust (the Corsica-Sardinia block) and Adria (considered as a promontory of the African Plate or as an independent microplate) and three morpho-structural provinces can be recognised (Bally et al., 1986; Deiana and Pialli, 1994), from west to east: the Umbria pre-Apennines, the Umbria-Marche ridge and the Outer Marche Foothills (Menichetti, 1991).

2.2.2. Hydrogeological setting

This structural setting forces a parallel-to-the-ridge circulation of groundwaters, and the ridge itself has been considered as an isolated hydrogeological system, where the Meso-Cenozoic sequence is closed at the bottom by the Triassic Anhydrite (Anidriti di Burano Fm.) acting as regional basal aquiclude. The presence of lithotypes with different permeabilities allowed the formation of three superimposed hydrogeological complexes which alternate groundwater circulation mainly due to fissures, joints and karst conduits (Boni et al., 1986; Caprari et al., 2002; Nanni and Vivalda, 2005) and low permeable formations (aquicludes). These hydrostratigraphic complexes are (**Fig.2.2** and main map):

- *Basal (or Massiccio) aquifer* (**Baq**), characterized by a stratified limestone of the *Corniola Fm.* and massive limestones of the *Massiccio Fm.*, representing the most important hydrogeological complex in the Umbria-Marche limestone ridges, with a thickness ranging from 800 to 1200 m. The groundwater circulation occurs in very well-developed fissures and karst conduits and it's overlying by the Jurassic marly-limestones sequence acting as top aquiclude. This aquifer is the loci for the main known karstic systems (Galdenzi and Menichetti, 1995).

- *Maiolica aquifer* (**Maq**), consists of micritic limestones and dolomitic limestones of *Maiolica Fm.*, having a thickness ranging between 200 and 400 m, and is overlayed by marlstones and clayey-marlstones of *Marne a Fucoidi Fm.* (the most important aquiclude at a regional scale). This complex is characterized by a high fracturation degree and a karst network poorly developed. Locally, Maiolica aquifer can be in hydraulic connections with the basal aquifer because the lack of the interposed Jurassic marly-limestones formations (Rosso Ammonitico and Calcari Diasprini) that are replaced by Bugarone Fm. (nodular limestones) (Centamore et al., 1976).
- *Scaglia aquifer* (**Saq**), characterized by limestones and marly-limestones of the "Scaglia Rossa" and "Scaglia Bianca" formations of about 300 m of thickness. The hydraulic behaviour of the complex is not homogeneous (Giacopetti et al., 2017) and the groundwater circulation is mainly controlled by joints and fissures, showing a very low karstification degree. Upward, the aquifer is confined by the low permeable formation of the "Scaglia Cinerea".

Considering that a hydraulically closed system (i.e. the groundwater exchange does not occur between adjacent structures (Boni and Bono, 1982) can be defined as a hydrostructure, in the study three different hydrogeological structures can be individuated: Mt Cucco (**MC**), Mt Maggio-Mt Penna (**MM-MP**) and Mt Pennino (**MPn**) (**Fig.2.2** and main map).

In the hydrogeological units hydraulically independent, the unknown term is represented by the effective infiltration.

Boni et al*ii* (1986) estimated the effective infiltration in the Umbria-Marche carbonate domain range from 25 to 32 l/s per km^2 (basal aquifer of Corniola-Calcare Massiccio complex), and about 17.5 l/s per km^2 in the pelagic domain (Maiolica and Scaglia aquifers). Furthermore, for the Corniola-Calcare Massiccio complex, the same authors consider a very low runoff, less than 1% of precipitation (Boni et al., 1986).

In detail, each hydrostructures was subdivided in more sub-basins in function of the different hydraulic parameters and geological conditions, defining the location of karst springs and their related limits of recharge areas, at a scale of 1:25.000 (main map).

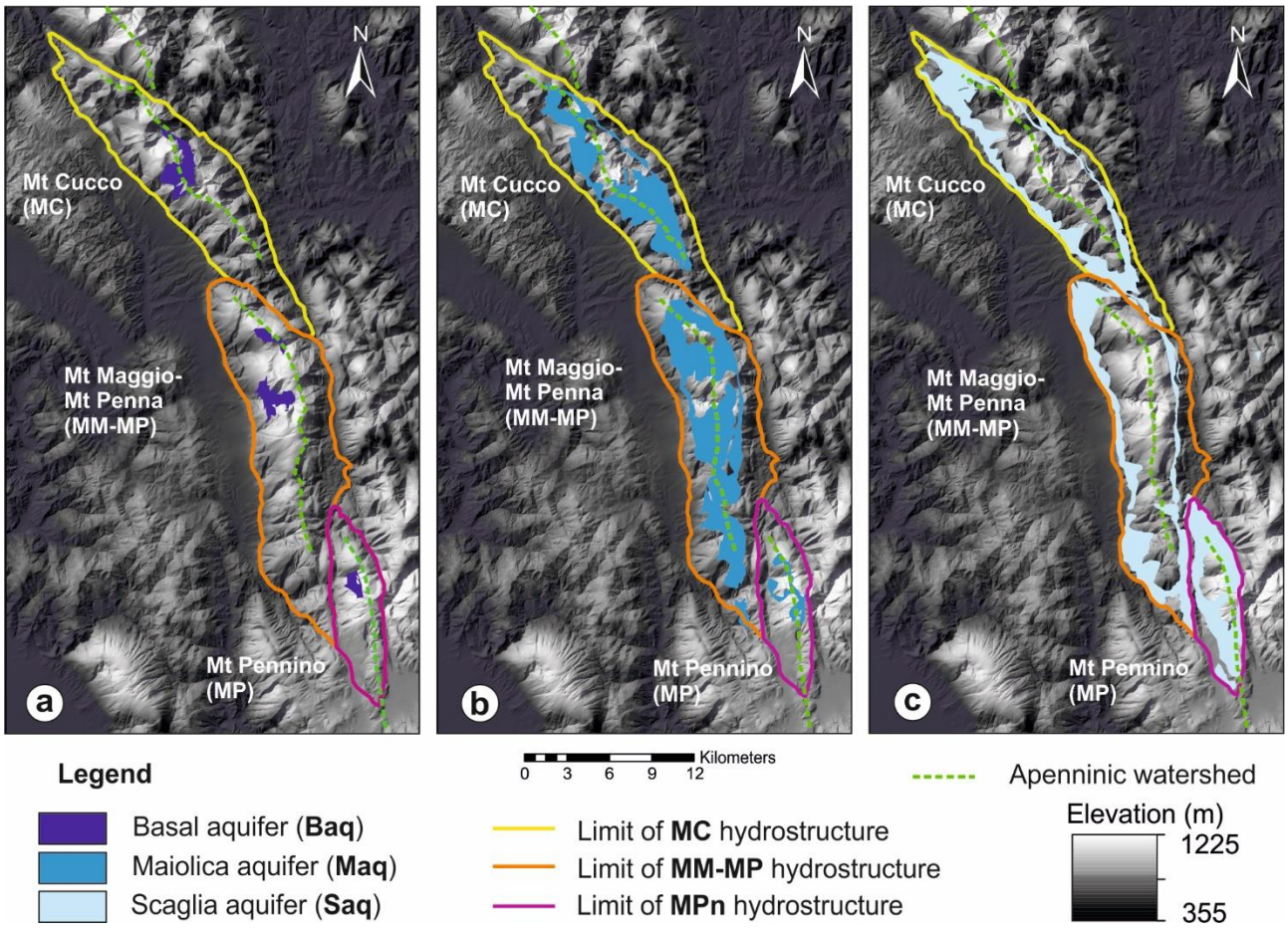

Fig.2.2. Outcrops of carbonate aquifers that occur in the hydrostructures surfaces of Umbria-Marche ridge (Mt Cucco, Mt Maggio-Mt Penna and Mt Pennino); (a) Basal aquifer (Baq) outcrops; (b) Maiolica aquifer (Maq) outcrops; (c) Scaglia aquifer (Saq) outcrops.

2.2.3. Water balance analysis

Groundwater resources are known to be related to climate change through hydrological processes, such as precipitation and evapotranspiration, and through interaction with surface water (Chen et al., 2004). Hence, at a drainage scale an analysis of water input in the system was necessary to assess the input of the systems and to evaluate the so-called *water balance.* A water budget states that the rate of change in water stored in area, such as a spring drainage area, is balanced by the rate at which water flows into and out of the area (Kresic and Stevanovic, 2010).

The precipitation and temperature data are related to three gauge stations (provided by www.regione.umbria.it) located at Mt Cucco, Gualdo Tadino and Nocera Umbra respectively (see location in the main map), during the hydrological year 2010-2011 (from 10 October 2010 to 4 October 2011) has been chosen this hydrological year for reason of completeness of the meteorological data-series.

The region is located in a typical subcontinental climate characterised by dry and warm summers and a wet period that occurs during autumn, winter and spring.

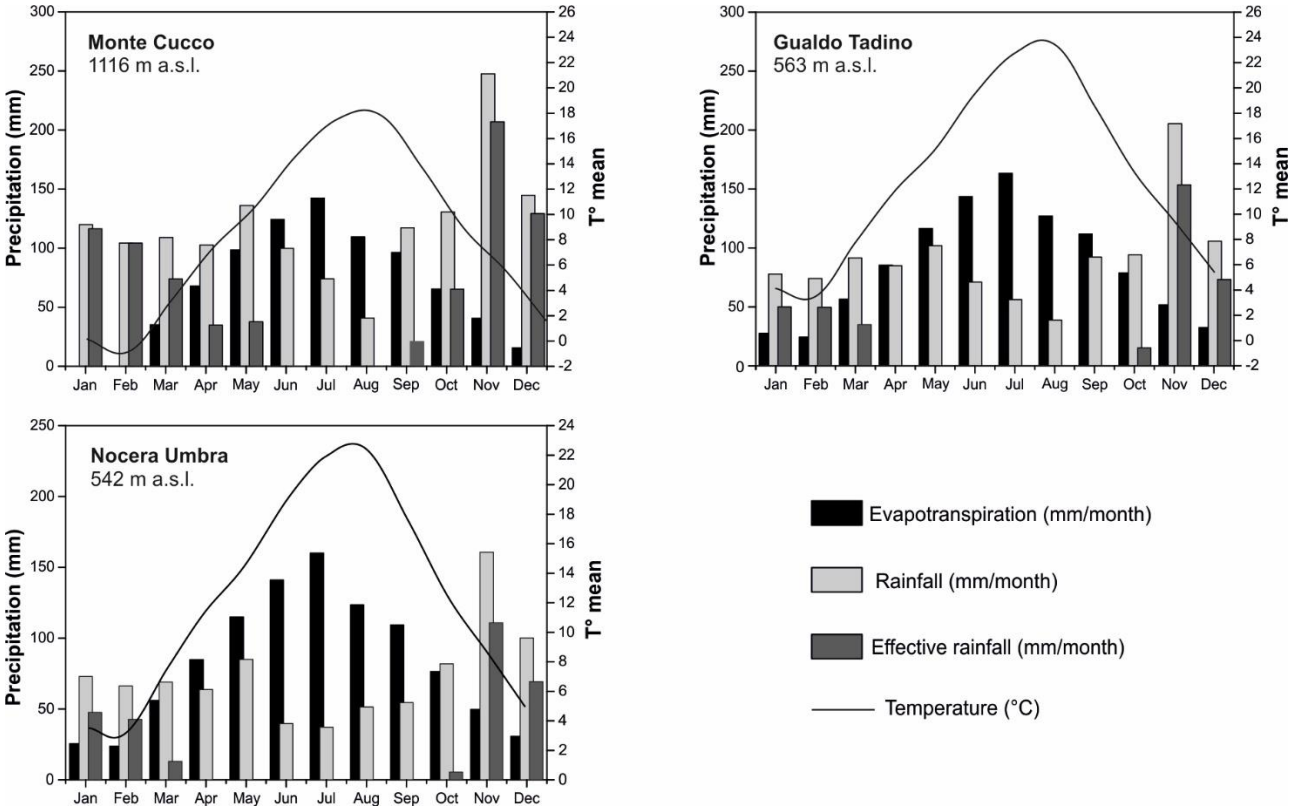

Fig.2.3. Monthly rainfall, potential evapotranspiration and effective rainfall of gauge stations of Monte Cucco, Gualdo Tadino and Nocera Umbra for the hydrological year 2010-2011.

The monthly rainfall reaches a maximum during November and a minimum in August (**Fig.2.3**). The pattern of potential evapotranspiration computed was found to be almost completely opposite to that of rainfall, reaching a maximum in July and a minimum in December-January (**Fig.2.3**).

In a karstic environment, assessing the effective infiltration rate is closely related to the evaluation of potential evapotranspiration, because rainfall primarily occurs during a non-warm season. Hence, its distribution allows a higher infiltration into the aquifer. Because of their simplicity, the Thornthwaite method for estimating potential evaporation was used (Thornthwaite, 1948). Moreover, runoff can be considered almost null in the study area, and the difference between monthly rainfall and monthly potential evapotranspiration appears very similar to the amount of effective infiltration. These amounts, reported in **Tab.2.1**, were considered in order to define the effective rainfall, that reaches the maximum during autumn-winter season, and appears to be null during May-September.

In groundwater studies, the term effective rainfall is sometimes used to describe actual infiltration, indicating any water movement from the land surface into the subsurface, i.e. only a portion of water that reach the saturated zone (Kresic and Stevanovic, 2010). This water is sometimes called potential recharge or effective infiltration that describes the portion of precipitation that reaches surfaces streams via direct overland flow or near surface flow (interflow).

Tab.2.1. Water balance of three-gauge stations (mean temperature, annual precipitation, evapotranspiration and effective infiltration).

Gauge stations	Elevation (m a.s.l.)	T (°C)	P (mm/y)	Epi (mm/y)	Eff. Rainfall (mm/y)
Mt Cucco	1116	8.2	1285.5	587	824.8
Gualdo Tadino	563	13.1	900.8	806	390.4
Nocera Umbra	542	12.4	929.7	767	413.8

The mean annual rainfall calculated in the study area is about 1038.7 mm/y, whereas the average evapotranspiration (Epi) using temperature data range with altitude from 767 mm/y at 542 m a.s.l. (Nocera Umbra gauge station) to 587 mm/y at 1116 m a.s.l. (Mt Cucco gauge station). The average value is 720 mm/y. Therefore, the effective rainfall should range from 390.4 mm/y (12.3 l/s per km^2) to 824.8 mm/y (26.2 l/s per km^2), that correspond approximately at 50% of annual precipitations.

In the highly-elevated zones (above 1000 m a.s.l.) this period is shorter and the precipitation can be snowy during winter (December-February), which can have significant effect on groundwater aquifer recharge.

As discussed by Healy et al. (2007) the understanding of the water budget and underlying hydrologic processes provides foundations for effective spring management and for protection of recharge areas. Boni and Bono (1982) and Boni et al*ii* (1986) proposed a direct method to assess the effective infiltration, based on the principle that the amount of discharge from a hydraulically closed hydrogeological structure is equivalent to the average amount of water entering the recharge area. The average effective infiltration, expressed in millimeters/year, is calculated by dividing the average volume of water discharged by a hydrogeological structure by the extent of its recharge area; the latter is identified based on a detailed reconstruction of the local geological-structural setting (Mastrorillo and Petitta, 2010).

This method encounters some difficulties of application, if the investigated hydrogeological units have deep groundwater but no know springs and are hydraulically linked to nearby structures. The unknown term is represented by hydraulic exchanges, which are evaluated by comparison between theoretical spring discharge respect to measured spring discharge, evidencing deficit or surplus (Mastrorillo et al., 2009).

Detailed hydrostructural studies are used to identify the recharge areas of the individual springs, and the same method may be used to assess local effective infiltration of hydrogeological complexes that outcrop in the investigated area. In this way, effective infiltration data were collected for the individual hydrogeological complexes.

2.3.Materials and methods

Hydrogeological map of karst aquifer was obtained through the combination of different approaches: (*i*) geological field surveys, (*ii*) interpretation of multitemporal orthophotography and (*iii*) comparison between effective infiltration values estimated. The acquired data have been processed using *QGIS 2.18 Las Palmas* in the reference system WGS 1984 UTM Zone 33N.

The geological interpretation from hydrogeological point of view, was derived considering the information available from Italian geological mapping project (CARG – Cartografia Geologica) at 1:50000 scale: sheets Foglio 291 "Pergola" (Jacobacci et al., 1974) and Foglio 301 "Fabriano" (Centamore et al., 1979). A Digital Elevation Model having a resolution image of 10 m was available (*tinitaly* DEM map - http://tinitaly.pi.ingv.it).

Tab.2.2. Statistical characteristics of record discharge of karst springs analysed.

Karst spring	**Hydrostructure**	**Minimum, Q_{min} (l/s)**	**Mean, Q_{av} (l/s)**	**Maximum, Q_{max} (l/s)**
Scirca	MC	50.6	214.9	463.5
Vaccara	MM-MP	32.8	119.1	505.3
Boschetto	MM-MP	23.6	185.4	885.7
Capo d'acqua	MM-MP	33.7	94.2	160.2
San Giovenale	MM-MP	72.0	397.5	1134.6
Bagnara	MPn	1.0	106.2	359.4

Discharge time series measured at six karst springs are monitored by ARPA Umbria (www.arpa.umbria.it) and minimum, mean and maximum daily discharge records are available (**Tab.2.2**). The subset contains about 8-years of available data, from 2007 to 2015. Springs in carbonates represent the outlets of channel networks, and heads in large channels are lower (except at high flow) than in the surrounding bedrock. The statistical properties of spring discharge depend on input system but also by the aquifer geometry and physical properties. The spring flow rate is one of the few water budget elements that can be directly measured. In addition, a thorough analysis of the spring discharge hydrograph provides useful information on the aquifer characteristics, such as the nature of its storage and transmissivity and the types and quantity of its groundwater reserves.

In this study, estimating the "effective infiltration" by using the direct method for each karst springs, and comparison these values with "effective rainfall" estimated in the water balance, allowed to define which subsystems show a mismatch with surface hydrogeological limits within related hydrostructure. For the estimation of effective infiltration with the direct method of Boni et al*ii* (1986), the spring discharge time-series were analysed in the same hydrological year (October 2010 – October 2011) of the meteorological time-series.

2.4.Results and discussions

The Umbria-Marche Apennine ridge show a series of aligned hydrostructures apparently not hydraulically connected from each other. The result is a configuration characterized by different isolated hydrogeological systems that feed one or more karst springs with different discharges and regimes that reflects the hydrostratigraphic characteristics of each catchment basin.

The Umbria-Marche ridge is a mountain range characterized by the presence of extensive outcrops of a thick Mesozoic limestone sequences Minissiale and Vaselli, 2011), where the anticlinal axes divides the Umbria and Marche regions and represents the main watershed of Apennine ridge (Mayer et al., 2003).

The three main carbonatic hydrostructures (MC, MM-MP and MPn) recognized correspond to the anticlines of internal Umbria-Marche ridge morpho-structural province (Bally et al., 1986). In **Tab2.3** has been reported the surface extensions of the hydrostructures considered and their related hydrogeological arrangement of the carbonate complexes (Baq, Maq and Saq).

Tab.2.3. Surface of hydrostructures and estimation of carbonate complexes extension.

Hydrostructure	**Tot. Area (km^2)**	**Baq (km^2)**	**%**	**Maq (km^2)**	**%**	**Saq (km^2)**	**%**
Mt Cucco	113	6.7	5.9	30.8	27.3	32	28.3
Mt Maggio-Mt Penna	146	5	3.4	52	35.6	44.7	30.6
Mt Pennino	43	1.4	3.3	4.1	9.5	25.6	59.5

At the foothills of western portion of these anticlinal carbonatic hydrostructures, at different heights, associated karst springs are mainly located. The geometrical properties of each catchment basin, at a local scale, and the groundwater circulation, at a regional scale, of each karst complex including a spring have been analysed.

Tab.2.4. Estimation of effective infiltration using the direct method (Boni et al., 1986) and comparison with effective rainfall values of water balance.

Year 2010-2011	**Scirca**	**Vaccara**	**Boschetto**	**Capo d'acqua**	**San Giovenale**	**Bagnara**
Average discharge Q (l/s)	211.6	138.3	179.6	100.8	384.9	93.7
Sub-basin area (km^2)	8.0	6.2	11.5	7.4	10.5	4.9
Effective infiltration (l/s per km^2)	**26.5**	**22.3**	**15.6**	**13.6**	**36.7**	**19.1**
Effective rainfall (l/s per km^2)	**26.2**	**12.4**	**12.4**	**12.4**	**13.1**	**13.1**

The comparison of effective infiltration and effective rainfall estimated for each karst sub-basins are shown in **Tab.2.4**. In the Scirca sub-basin (Mt Cucco hydrostructure), the effective infiltration estimated with the direct method is equal to 26.5 l/s per km^2 and is perfectly comparable to 26.2 l/s per km^2 calculated in the hydrological budget. The weather station used (Mt Cucco gauge station) is located within the Scirca sub-basin at an altitude of 1116 m a.s.l. The mean elevation of recharge area is about 1136 m a.s.l. Therefore, the perfect correspondence between the two values imply the reliability of the evaluations.

In the Mt Maggio-Mt Penna hydrostructure two different results are observed. The effective infiltration values of Boschetto and Capo d'acqua sub-basins are slightly higher (15.6 and 13.6 l/s per km^2, respectively) than the 12.4 l/s per km^2 of effective rainfall estimated in the hydrological budget. Also in this case, the good correspondence between the values indicate the correctness of the evaluations parameters used. The weather station used is located an Gualdo Tadino at the altitude of 563 m a.s.l. On the contrary, the recharge area of Vaccara spring show an effective infiltration value (22.3 l/s per km^2) much higher than the same effective rainfall of previous sub-basin analysed (Boschetto and Capo d'acqua).

In the San Giovenale sub-basin, the difference between the effective infiltration estimated with the direct method (36.7 l/s per km^2) and its corresponding effective rainfall (13.1 l/s per km^2) is even more prominent than previous one. This discrepancy can be justified by the presence of groundwater exchanges between the Colfiorito plains and the Mt Maggio-Mt Penna hydrostructure, verified by other authors (Mastrorillo et al., 2009). The southern sector of Mt Maggio-Mt Penna hydrostructure would receive an underground cross-flow of a non-negligible extent.

Finally, the calculation of effective infiltration in the Bagnara sub-basin (Mt Pennino hydrostructure) is 19.1 l/s per km^2 and results rather higher than 13.1 l/s per km^2 of effective rainfall. The non-correspondence can be justified by the underestimation of effective rainfall due to the large difference between the altitude of weather station (542 m a.s.l.) and the mean altitude of recharge area of Bagnara spring (1159 m a.s.l.).

From a hydrogeological point of view, using the mean values of discharge illustrated in **Tab.2.2** the Meinzer's classification of springs can be applied (Meinzer, 1923) to evaluate the magnitude of each karst system. In other words, Meinzer (1923) developed eight discharge classes based on the magnitude of discharge rate from a spring at the time of measurement; however, his numeric scheme is reversed from the intuitive scale (low discharge should have a low value).

Therefore, for evaluating the availability of springwater, it is important to include a measure of spring discharge variability, which should also be based on periods of record longer than one hydrologic year. The simplest measure of variability is the ratio of the maximum and minimum discharge (Iv).

This represents a useful tool for describing the flashiness of an aquifer (White, 2007). Spring with an index of variability greater than 10 are considered highly variable, and those with Iv<2 are sometimes called constant or steady springs. These qualitative evaluations provide an impression of heterogeneity in the studied karst system, but give an important information about water management The elaboration of the statistical parameters previous describes allowed to evaluate the discharge variability of the karst springs studied (**Tab.2.5**) and to classify the magnitude as proposed in literature (Meinzer, 1923).

Tab.2.5. Classification of springs based on average discharge rate proposed by Meinzer, (1923).

Karst springs	Discharge range	Magnitude	Index of var. (I_v)	Stability
Scirca	100-1000 l/s	3rd-third	9.2	Unstable
Vaccara	100-1000 l/s	3rd-third	15.4	Very unstable
Boschetto	100-1000 l/s	3rd-third	37.5	Totally unstable
Capo d'Acqua	10-100 l/s	4th-fourth	4.8	Unstable
San Giovenale	100-1000 l/s	3rd-third	15.8	Very unstable
Bagnara	100-1000 l/s	3rd-third	359.4	Totally unstable

Karst springs analysed shown an average annual discharge range between 100-1000 l/s, classifying them third magnitude. Only *Capo d'Acqua* spring, show a magnitude lower (fourth) with a mean discharge range between 10-100 l/s.

The index of variability (I_v) were used for characterisation of spring's discharge stability (Slovak Hydrometeorological Institute) and show results rather different for the karst subsystem analysed. Scirca and Capo d'Acqua springs manifest a value of I_v range between 2.1-10.0, indicating an *unstable* behaviour. Index of variability ranging between 10.1-30.0 indicates a *very unstable* behaviour for Vaccara and San Giovenale springs, whereas Boschetto and Bagnara show a *totally unstable* behaviour, with a I_v >30.0.

The following hydrostructures analysis with hydrogeological complexes were defined on the basis of the hydrostratigraphy, structural characteristics and the karstification degree of each formation, in order to understand their role in groundwater circulation (Baiocchi et al., 2006; Boni et al., 1986; Capelli et al., 2005). In **Tab.2.6** were estimated the surface outcropping of the hydrogeological complexes in all sub-basins (recharge areas) of the karst springs analysed, using the same criteria previously used for hydrostructures.

Tab.2.6. Surface extensions of sub-basins and estimation of outcropping hydrogeological complexes**.**

Karst spring	**Elev.** (m a.s.l.)	**Sub-basin area** (km^2)	**Baq** (km^2)	**%**	**Maq** (km^2)	**%**	**Saq** (km^2)	**%**
Scirca	575	8	4.5	56	3.5	44	0	0
Vaccara	468	6.2	1	15	4.6	74	0	0
Boschetto	538	11.5	0	0	11.5	100	0	0
Capo d'acqua	570	7.4	0	0	6.9	93	0	0
San Giovenale	480	10.5	0	0	10.5	100	0	0
Bagnara	630	4.9	1.4	29	1.4	28	1.2	24

2.4.1. Mt Cucco hydrostructure

Mt Cucco is an anticline with an extension of about 113 km^2 of which 61.5% (**Tab.2.3**) is represented by carbonate formations.

The hydrostructures is characterized mainly by the outcrop of Maq (27.3%) and Saq (28.3%), whereas Baq outcrops only for the 5.9%. Maiolica complex and Massiccio complex results generally separated by Jurassic aquiclude but, sometimes, are hydraulically connected by faults mostly in the central area where it is present the nucleus of anticline (**Fig.2.2a**).

Mt Cucco presents only one karst spring (Scirca spring) located at 575 m a.s.l in the SW limb of anticline. The ratio between maximum elevation of recharge area (1566 m a.s.l.) and karst spring elevation is about 990 m. The recharge area of this spring it was estimated by geological and hydrological limits and it is about 8 km^2 (**Tab.2.6**) and the aquifer is formed almost entirely on the Baq, that characterize more of the 50% of basin and about 40% by the Maq (**Fig.2.3a**). In fact, the hydrostructure of Mt Cucco is represented by a well-developed underground karst with more than 50 know caves, extending over 30 km and 948 m deep (Menichetti, 1989).

2.4.2. Mt Maggio-Mt Penna hydrostructure

Mt Maggio-Mt Penna is a large anticline (146 km^2) characterized by outcrops of Baq in the northern sector, with an extension of 5 km^2 (3.4 % of surface), Maq widely diffused in the central portion and representing the main hydrological complex outcropping (52 km^2) and Saq along the periclinal termination, bordering the entire hydrostructure, and covering about 30% of the entire area (**Tab.2.3**). Jurassic aquiclude is present and, generally, separates the Massiccio complex from Maiolica complex. The marlstone and clayey-marlstone of Marne a Fucoidi Fm. limits the top of Maiolica complex and inhibits the hydraulic connection with the overlying Scaglia complex (**Fig.2.2b**). Different hydrogeological sub-domains, namely four karst springs (Vaccara, Boschetto, San Giovenale and Capo d'acqua) and their related recharge areas, are present in the hydrostructure.

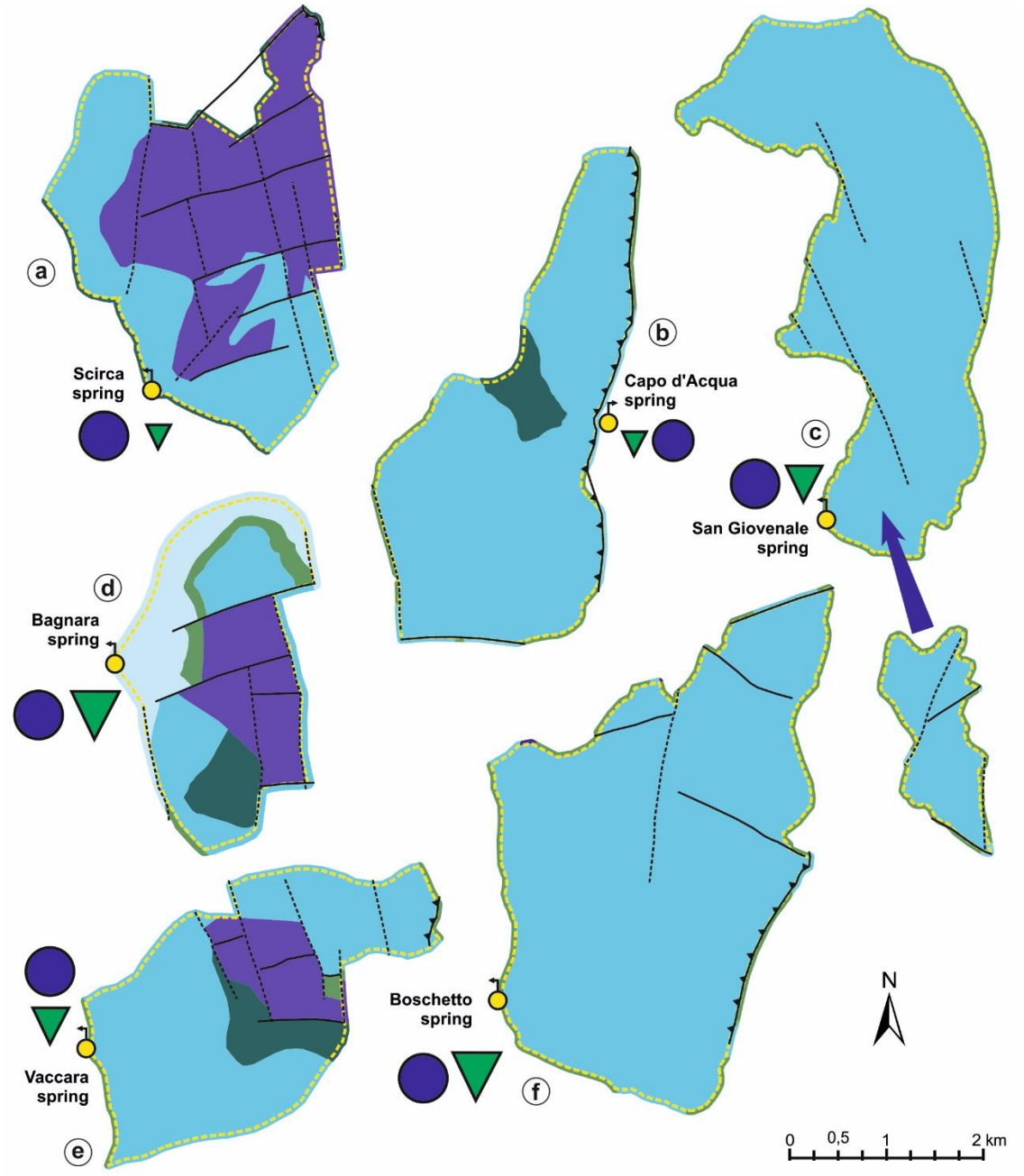

Fig.2.4. Hydrogeological characteristics of recharge areas of karst sub-basins: (a) Scirca spring, (b) Capo d'acqua spring, (c) San Giovenale spring, (d) Bagnara spring, (e) Vaccara springs and (f) Boschetto spring.

Vaccara spring is located in the north sector of Mt Maggio-Mt Penna, at 468 m a.s.l. This spring is fed by a catchment basin of about 6.2 km^2 (**Tab.2.6**), reaching the maximum elevation of 1358 m a.s.l. About 75% of Vaccara sub-basin is represented by Maq and 15% by Baq (**Fig.2.4b**). Southern are present the Boschetto and San Giovenale springs in the western portion and Capo d'acqua spring in the eastern limb of the anticline. This latter is hydrogeologically separated from each other by the Apennine watershed. The surfaces of these sub-basins are represented only by outcrop of Maq (**Fig.2.4c, 2.4d** and **2.4e**), with an extension of 11.5, 10.5 and 7.4 km^2, respectively (this value represents also surface extension of respective recharge area) (**Tab.2.6**). Boschetto spring, situated at 538 m a.s.l., drains both the Maiolica complex and the Massiccio complex, due to the absence in this sector of the Jurassic aquiclude, for an elevation distribution of about 816 m (maximum elevation of recharge area is about 1376 m a.s.l.). San Giovenale (located at 480 m a.s.l.) and Capo d'acqua (at 570 m a.s.l) springs feed two aquifers characterized almost exclusively by Maq because of the outcrop of Jurassic aquiclude inhibits the water exchange with the underling Massiccio complex. These systems are characterized by lower values of elevation ratio between karst springs and the point of maximum elevation: 352 and 513 m, respectively.

2.4.3. Mt Pennino hydrostructures

The southern sector of study area is represented by the anticline of Mt Pennino, having a size extension of 43 km^2 (**Tab.2.3**). The nucleus of anticline and hinge zone are represented by outcrop of Baq and Maq, that characterize the 29% and 28% (respectively) of the recharge area of about 4.9 km^2 (**Tab.2.6**). In this part of anticline are present a set of normal faults that are responsible of hydraulic connection between Maiolica and Massiccio complexes, even though the Jurassic aquiclude outcrops (**Fig.2.2c**). The maximum elevation of recharge area is 1571 m. Bagnara spring is located at 630 m a.s.l. (**Tab.2.6**) in the Saq aquifer and its sub-basin includes all three hydrogeological complexes (Baq, Maq and Saq) (**Fig.2.4f**).

2.5.Conclusions

The map proposed provides a range of hydrogeological information with different details: at a regional scale outlines the distribution of main hydrological structures and karst aquifers in the Umbria-Marche Apennine ridge whilst at a local scale details the recharge areas of sub-basins and their related karst springs.

In particular, this work focused on the delineation of the geological and hydrogeological characteristics that influencing the groundwater circulation in the individual hydrostructures considered (Mt Cucco, Mt Maggio-Mt Penna and Mt Pennino).

The carbonatic lithotypes covered about the 67% of the considered hydrostructures and only the 4.3% is represented by the Massiccio complex (Baq), which is considered the main aquifer of Apennine ridge.

The comparison between the effective infiltration and effective rainfall reveals different results. Some karst systems analysed (Scirca, Boschetto and Capo d'acqua) show a good correspondence between the two values, indicating the correctness of the evaluations parameters used. Hence, these sub-basins can be considered hydrogeologically closed.

On the other hand, the values of effective infiltration in Vaccara and Bagnara karst systems are higher than effective rainfall estimated in the hydrological budget. Probably, this gap is linked to the non-correspondence between the weather stations altitude and the average altitude of sub-basins considered. Furthermore, the effective infiltration of San Giovenale sub-basin (10.5 km^2) is about 23 l/s per km^2 more than effective rainfall estimated in the hydrological budget (13.1 l/s per km^2), implying a not inconsiderable underground feeding from other sectors outside the present hydrostructure. In this case, the groundwater surplus comes from the karst planes of Colfiorito, which is considered as a high infiltration area, since rainwater is collected by the plain, retained at the surface by the low-permeability fluvio-lacustrine complex and channelled by surface runoff towards karst swallow-holes (Mastrorillo et al., 2009).

Therefore, the lack of a rather large network of weather station do not afford a reliable assessment of some recharge area and especially of its effective rainfall estimation. Hence, it is preferable to refer at the effective infiltration values estimated with the direct method of Boni et al*ii* (1986), except of San Giovenale karst basin which does not represent a closed hydrogeological system.

Finally, from a structural point of view, the hinge zones of the anticlines perform a hydrological control, delineating a regional watershed along the Umbria-Marche ridge.

In the hydrostructures at least one basin associated to a karst spring are present. The considered sub-basins showing recharge areas rather small (from 5 km^2 to 11.5 km^2) and the percentage values of outcropping complexes points out as the karst systems in the Umbria-Marche Apennines are controlled by water circulation in the Maq and Baq, which are very often hydraulically connected by faults systems or by the lack of Jurassic aquiclude.

3. Fractures analysis and geometrical arrangement of carbonate aquifers in Umbria-Marche Apennine (central Italy)

Abstract

Fracture networks control the permeability of many reservoirs. Since the fracture patterns in situ are difficult to study in detail, field analogues are very important for understanding their fracture-related permeability and spatial organizations. The modelling of natural fracture in reservoirs requires, as input data, the results of previous detailed and accurate analyses of the 3D fracture network. Here, we report the results of a systematic study carried out on the fracture systems exposed in different outcrops of fractured carbonate formations in the Umbria-Marche Apennines, in the northern Italy, defining a conceptual model of structural and hydraulic properties of the main aquifers of northern Apennine ridge (Calcare Massiccio and Maiolica Formation). We measured the attitude and other structural parameters of 4184 fractures and bedding-planes. There are two main fracture sets: one strikes between SW-NE (dip-direction of N115) and NNE-SSW (dip-direction of N20), that probably the main pathways for the water-circulation from infiltration zone to spring outlet. Structural and statistical analysis of outcrops analysed shown different geometric properties of Calcare Massiccio and Maiolica Formation. Then, Discrete Fracture Network (DFN) models of representative geocellar volumes were built to compute both fracture porosity and correspondent permeability (K_{xx}, K_{yy}, K_{zz}). Results of such a work show that the fracture porosity of Calcare Massiccio Formation is much greater than Maiolica Formation (1.7 and 4.3%, respectively), and the permeability values result well correlated with this trend.

3.1.Introduction

Fractures are widespread structures in rocks, and for practical applications it is imperative to accurately predict fracture attributes that affect fluid flow, including their size and spatial arrangement (Lavenu and Lamarche, 2017). The influence that fractures exert on fluid flow through rocks (Engelder and Scholz, 1981; Sibson, 1996) makes genetic and structural studies of fracturing relevant to geologist from different fields study (Billi, 2005).

In fact, fractures networks can exert a strong control on fluid circulation through water aquifers and hydrocarbon reservoirs (Odling et al., 1999; Berkowitz, 2002; Gillepsie et al., 2001) and influence many geological process such rock alteration and mineral precipitation. In cases of groundwater reservoirs, large fractures provide preferential pathways for regional fluid movement, leading to fast transport. Small fractures as well as low fracture intensity are influential in terms of storage and retardation, as their permeability values are several orders of magnitude smaller (Chen-Chang Lee et al., 2010).

Fractures can introduce highly conductive pathways in case of connected open joints or form barriers to flow in case of cemented veins or fault gauge (Nelson, 2001). Fractures influence flow across

multiple length scales from sub-meter joints to kilometre long fractures and faults (Davy et al., 2010; Gross and Eyal, 2007).

Network connectivity is controlled by fracture orientation and length distributions and in turn influenced by hierarchies and abutment relationships (Barton, 1995; Odling et al., 1999; Sanderson and Nixon, 2015).

Tensile fractures are ubiquitous in rocks, forming a "background" joint network homogeneously distributed within rock volumes (Guerriero et al., 2015). Tensile fractures hosted in well-bedded stratigraphic successions, generally develop orthogonal to bedding (Pollard and Aydin, 1988).

In the geological record, platform carbonates form either massive and/or layered successions depending upon their original depositional environment (Tucker and Wrigtht, 1990). In both cases, these successions show a competing primary (matrix) and secondary (fracture) porosity in the control exerted on fluid flow (Lucia, 1999; Odling et al. 1999).

Fractured and karstified carbonates often form major aquifers and hydrocarbon reservoirs. However, because of the complexity of these systems, significant uncertainties remain in predicting their hydrodynamic behaviour.

Porosity, permeability and groundwater flow characteristics of fractured rocks, particularly their quantitative aspects, are rather poorly understood. Main flow paths in fractured rocks are along joints, fractures, shear zones, faults and other discontinuities.

Burial-related joints, often associated to bed-parallel stylolites (Groshong, 1988; Agosta and Aydin, 2006; Agosta et al., 2009; Gudmundsson et al., 2010; Korneva et al., 2014), in carbonates may show a systematic attitude displaying a spacing distribution somehow proportional to the bed thickness (Price, 1966; Huang and Angelier, 1989; Gross, 1993; Gross and Engelder, 1995; Becker and Gross, 1996; Hanks et al., 1997; Underwood et al., 2003; Gudmundsson, 2011; Rustichelli et al., 2013; Korneva et al., 2014; Panza et al., 2015).

Hence, a careful characterization and knowledge of the in situ structural and geometrical attributes of fractures and fracture networks is still fundamental for understanding the natural variability of fracture networks (McGinnis et al., 2016).

These studies demonstrated that preferential flow paths exist in any discrete networks, and the simplification of a fissured aquifer into an equivalent porous medium model is possible only under certain conditions. Therefore, a valid structural interpretation should simultaneously honour available surface and subsurface data to constrain structural geometry.

In this paper, fracture data collected in outcropping analogues of fractured carbonate reservoirs are used for deriving its hydraulic properties by means of a DFN approach (Long et al., 1996; Wilson et al., 2011). According to his approach, only certain sets of fracture are considered as permeable. The

matrix medium is considered to have zero permeability and it is mainly applicable for fractured aquifers. The modelled rock are carbonates belonging to the Calcare Massiccio and Maiolica Formations (that constitute the main reservoir of Northern Apennines) and are located in a northern sector of Umbria-Marche Apennines in central Italy. Attributes of fractures and fracture networks from vast fold-and-thust belt regions are qualitatively and quantitatively presented. The stochastic modelling of the fracture network was performed by using the MOVE™ software licensed by Midland Valley Exploration Ltd. The structural analysis providing insights on arrangement and distribution of diffuse fractures in the carbonate rock mass in term of geometrical and dimensional properties, in order to define fracture permeability and porosity.

The results of this study may help to gain new insights for a better knowledge of fluid circulation paths in fractured carbonate reservoirs and, possibly, implement predictive modelling tools.

3.2.Geological setting

The Northern Apennines were built by concurrent crustal shortening and extension driven by subduction and rollback of Adria and retreat and extension upper plate (Malinverno and Ryan, 1986; Royden, 1993).

Since the end of the early Miocene, the tectonic evolution of the Northern Apennines is characterized by regional uplifting, accompanied by contemporaneous eastward migration of coupled compression and extension in the foreland and hinterland, respectively (Elter et al., 1975; Lavecchia et al., 1994). At present, extension is affecting the main Apennines ridge, whilst compression is localized along the Adriatic coast.

The brief tectonic evolution just discussed of Umbria–Marche Apennines has characterized a fold-and-thrust belt that is largely described in literature (Decandia and Giannini, 1977; Lavecchia, 1985; Bally et al., 1986; Lavecchia et al., 1994; Barchi et al., 1998). Its consists of asymmetric large anticlines overturned eastward above tight synclines, with prevailing NW-SE trend vergency (Di Naccio et al., 2005) and located between front of the Tuscan Nappe and the relatively undeformed Adriatic foreland, that separates the east-verging Umbria-Marche Apennines from the west-verging Dinarides (Barchi et al., 2012).

In particular, the area can be divided into three tectonic phases (Barchi and Lemmi, 1996): from Lower Jurassic to Lower Miocene, an extensional phase with the deposition of the Umbria-Marche Succession on passive continental margin; between Miocene and Pliocene, a phase of compressional tectonics, which leads to the formation of the fold and thrust belt, associated with thrusts and sub-vertical strike-slip faults; from Pleistocene the area is affected by a constant uplift and extensional deformation, with formation of normal faults systems and their related intramontane basins (Pazzaglia et al., 2015).

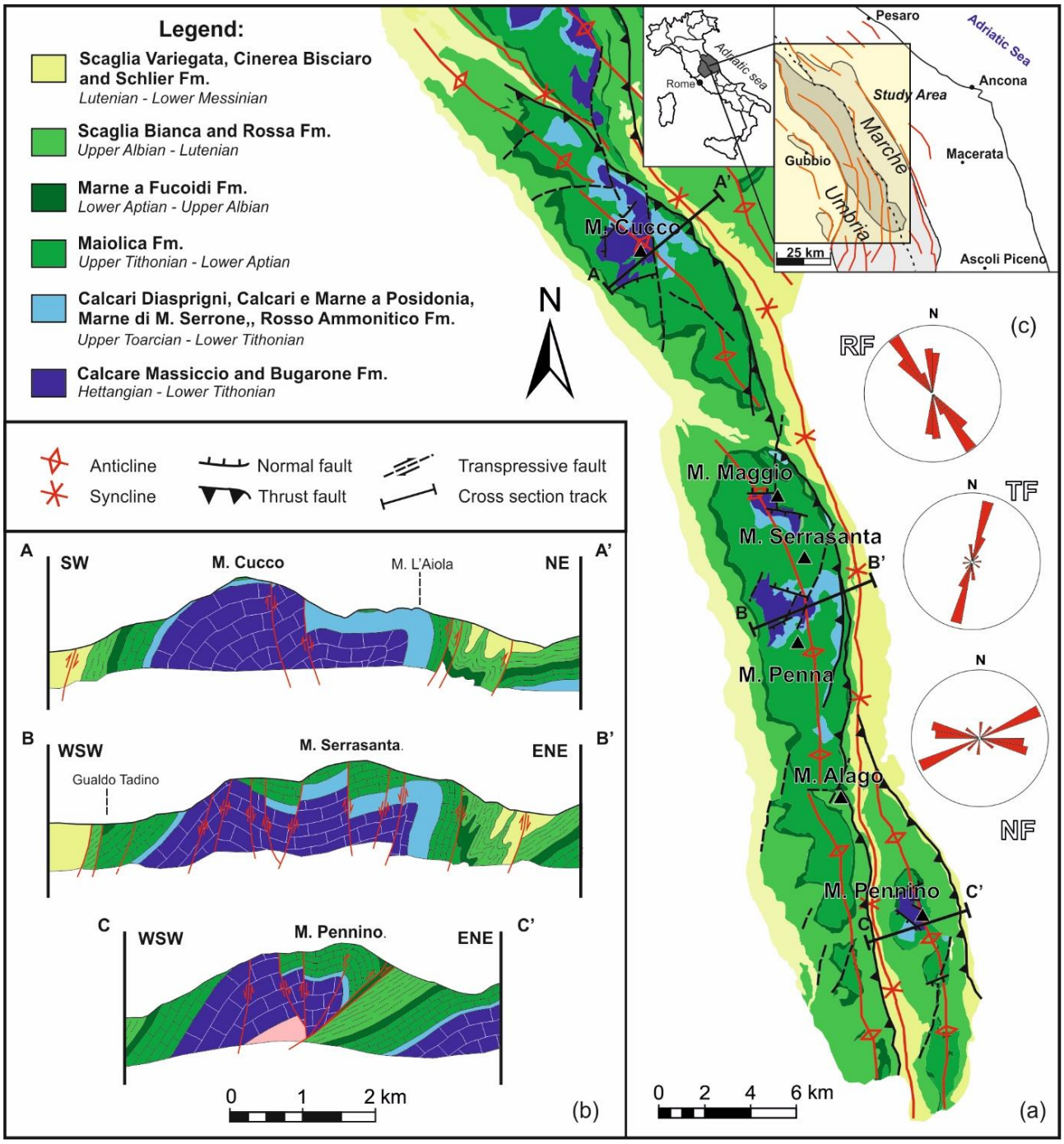

Fig.3.1. Geological map of study area (a); geological cross section of the three anticlines (b); rose diagram of strike-direction of main tectonic lineaments (normal faults, thrust faults and transpressive faults) (c).

The stratigraphic succession in the study area consists of four major mechanical units: (1) a Triassic thick sequence of alternating of dolostones, anhydrites and limestones (Anidridi di Burano Fm. and Calcari a Rhaetavicula Contorta Fm.); (2) lower Jurassic, poorly layered platform limestones (Calcare Massiccio Fm.); (3) a lower Jurassic e Miocene pelagic sequence including mainly well-bedded limestones, marly limestones and marls (from Corniola to Bisciaro Fm.) (e.g. Centamore et al., 1972, 1975; Barchi and Lemmi, 1996).

In this sector of the Apennines, the Anidriti di Burano Fm. provides the most efficient decollement layer (e.g. Bally et al., 1986; De Feyter and Menichetti, 1986; Menichetti et al., 1991; Anelli et al., 1994). Some structures considered are characterised by eteropies and lateral thickness variations (Alvarez, 1989; Galdenzi and Menichetti, 1989). The "condensed" sedimentary sequence (post Calcare Massiccio Fm.), consists of grey stratified limestones, nodular limestones, and marls of Bugarone Fm. (Deiana et al., 2002). The complete Umbria-Marche multilayer sequences are generally exposed in the central folds of each anticline structures (Centamore et al., 1972, 1975), where we performed out structural study.

The study area includes a large sector of northern Apennines that comprises three anticlines structure located in the Umbria-Marche regions with a general axes trend of NW-SE (main map in **Fig.3.1a**): Mt. Cucco anticline, Mt. Serrasanta anticline and Mt. Pennino anticline.

All over the Umbria-Marche region, high-angle right-lateral strike-slip shear zones of various length and displacement are quite common (Lavecchia et al., 1988). The strike-slip shear zones (TF, transpressive faults in rose-diagram in **Fig.3.1c**) mainly trend N-S. Well-developed all over the Umbria-Marche region are also low-angle thrusts, coeval to the strike-slip faults and clearly post-dating the folds. On a regional scale, the high-angle strike-slip faults are expected to merge with these low-angle shearing planes (Lavecchia et al., 1988). In this ridge sector these planes are co-axial to the folds and trends respectively NNW-SSE and locally show a propagation towards N-S (RF, reverse faults in rose-diagram in **Fig.3.1c**).

We detected the structural properties of Calcare Massiccio Fm. and Maiolica Fm. because represents the main aquifers of Apennine ridge.

3.3.Methods and materials

For hydrogeological approach and studies, it is extremely important to understand and describe the structure of the rock-mass and quantify the pattern and nature of its discontinuities (van Golf-Racht, 1982; Sharp, 1993; Lee and Farmer, 1993; de Marsily, 1986).

The main technique used in this study to detect fractures in outcrop involves the single scan line (1D) and areal scanline (2D) methods consisting in measuring fracture spacing and various attributes for each fracture, along one and/or two ideal line oriented parallel and perpendicular to the bedding (Priest and Hudson, 1981; Priest, 1993; Zeeb et al., 2013a). We recorded different genetic characteristics of fractured rock mass analysed: number of sets of discontinuities present in the network, attitude of discontinuities (in term of strike, dip-direction and dip-angle), fracture spacing and bed thickness of each sets, intensity of fracturation and persistence of discontinuities.

In order to evaluate the hydraulic properties of different carbonate reservoirs, a DFN models was built using the "Fracture Modelling" module of the software MOVE™.

The methodology consists on define five geometrical parameters for each fracture set: orientation (dip azimuth, angle of dip), length distribution (persistence), length/height ratio (single value, fracture intensity and hydraulic aperture. In our model we assume that the hydraulic aperture is proportional to fracture length, because the in the study area the karst exert an influence rather relevant on fracture network, especially in depth, making inappropriate the field measure of this parameter. Also fracture intensity has been calculated as the inverse of fracture spacing for each joint sets detected, determing the N parameter, which is the number of fractures per m^3. Such a parameter is equivalent to the geomechanical *Jv* (Joint volumetric count, Palmström, 2001).

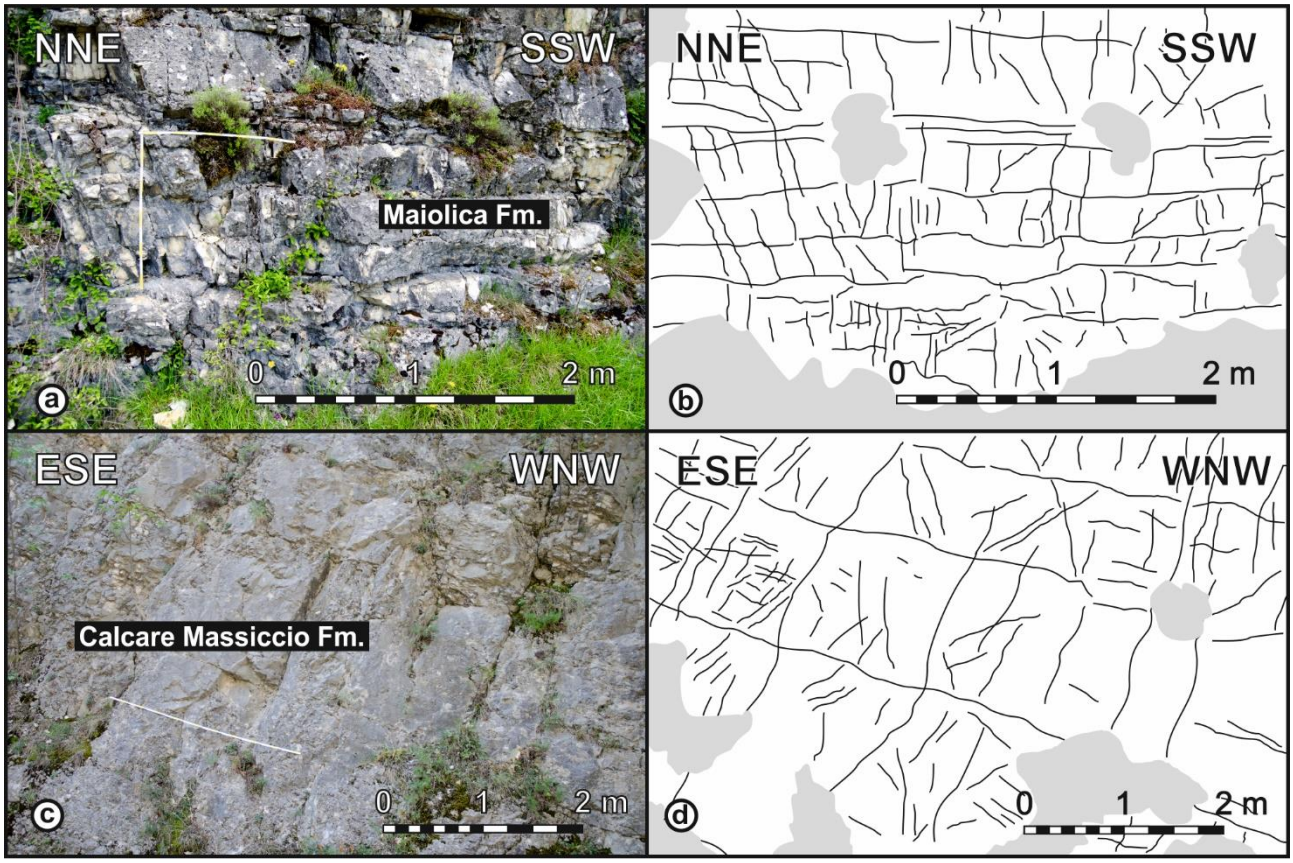

Fig.3.2. Example of Maiolica (a) and Calcare Massiccio Formations (c) outcrops in the Mt Maggio and Mt Serrasanta structures, respectively. The picture (b) and (d) represent the schematic view of discontinuities detected.

The obtained DFNs represents volumes having dimensions similar to outcrops considered. Fractures and their output parameters are associated to a geocellar volume, where the cells are in 0.5x0.5x0.5m. The parameters estimated were computed for each cell of each geocellar volume taking in consideration the discontinuity segments contained in them. In particular, fracture porosity is calculated dividing the total fracture volume contained in each cell, and the volume of the cell, whereas the calculation of the permeability tensor (K_{xx}, K_{yy} and K_{zz}) is based on the Oda's

methodology (Oda, 1985), which derives from both Darcy's law and laminar flow between parallel plates theory (Long et al., 1996):

$$\frac{Q}{A} = \frac{S^3}{12D}\frac{\partial h}{\partial l}\frac{\rho g}{\mu} \qquad \textbf{(Eq.31.)}$$

where Q is the flow rate, A the cross-section area of the modelled volume, S the fracture aperture, D the fracture spacing, h/l the pressure head, ρ the fluid density and μ the fluid dynamic viscosity.

In all models, both matrix porosity and permeability were not considered. Concerning computation of the correspondent permeability, since the flow rate varies as the cube of fracture aperture, the results are profoundly affected by the values inputted into the modelling software.

Therefore, several outcrops of Calcare Massiccio Fm. and Maiolica Fm. in the three anticline structures (Mt Cucco, Mt Maggio-Mt Serrasanta and Mt Pennino) of northern Apennines were carried out.

3.4.Results

Several intersecting intercommunicating fractures create a fracture network which facilities fluid flow. Therefore, a fractured rock mass can be considered to be made by discontinuities having different genetic properties. Structural analysis was performed along along the vertical walls and pavements outcrops to decipher the geometry and the multi-scale properties of background structures.

3.4.1. Number of sets and spatial orientation

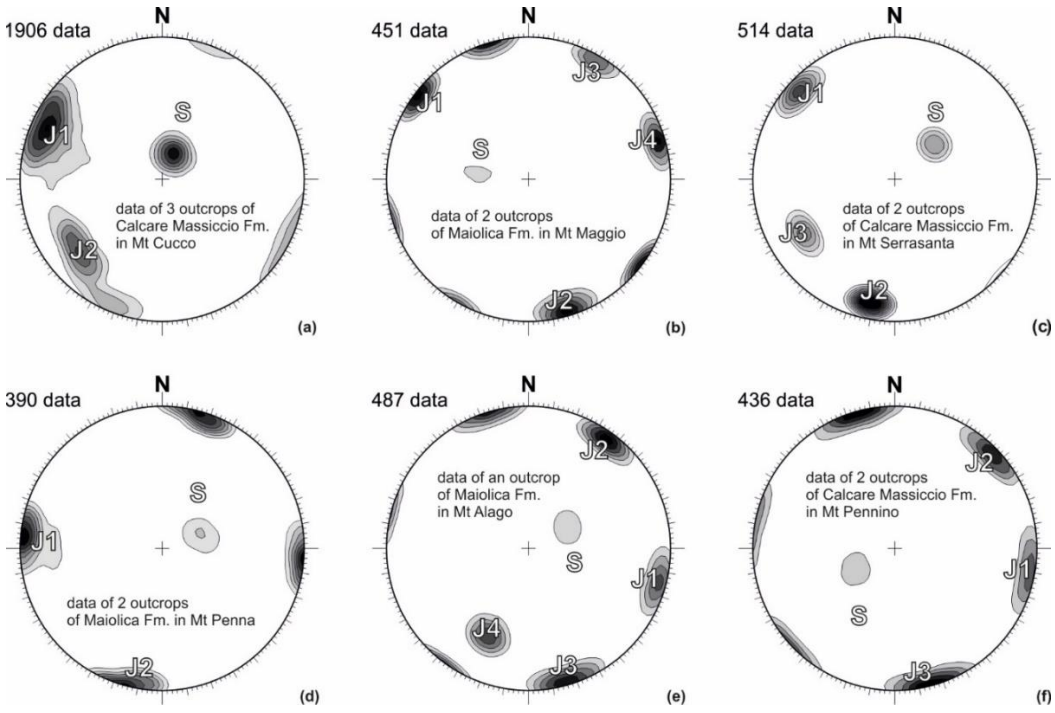

Fig.3.3. Orientations data of discontinuities in the π-pole diagrams of their respective structures analysed from north to south: (a) Mt Cucco, (b) Mt Maggio, (c) Mt Serrasanta, (d) Mt Penna, (e) Mt Burello and (f) Mt Pennino. *J1*, *J2*, *J3* and *J4* represents the respective joint sets; *S* represent the bedding surface.

Several sets of discontinuities are often developed in a rock mass. The spatial orientation represents the attitude of discontinuitis present in the network. Number of sets of discontinuities in a exposure has been determined by statistical analysis and have been defined in terms of dip-direction and dip amount. A total 4184 subvertical fractures and bedding planes were measured at the 12 stations, 7 in the Calcare Massiccio Formation and 5 in the Maiolica Formation, along the three anticline structures considered.

The measurements are represented in contouring poles-plots (**Fig.3.3**) and the results of main fracture sets for each contour-diagrams are reported in **Tab.3.1**. The immense majority of these joints were vertical or nearly so, although other inclinations appeared, wherease bedding planes shows a dip between 10° and 35°.

Tab.3.1. Dip-direction of joints sets and bedding-planes of structures analysed.

Structure	Set 1 (J1)	Set 2 (J2)	Set 3 (J3)	Bedding (S)
Mt Cucco	N115°-85	N50°-75	N22°-85/N202°-85	N210°-
Mt Maggio	N125°-85	N345°-85/N165°-85	N210°-85/N30°-85	N100°-
Mt Serrasanta	N130°-85	N10°-80	N60°-70	N140°-
Mt Penna	N95°-85/N275°-85	N10°-85/200°-85	/	N270°-
Mt Burello	N285°-85/N115°-85	N215°-85/N45°-85	N345°-85/N175°-85	N240°-
Mt Pennino	N280°-85/N100°-85	N228°-85/N45°-85	N345°-85/N175°-85	N60°-

The contour-diagrams of all the joints shows that there are two main sets (*J1* and *J2*) with a clearly marked maximums of SW-NE (N115°-85 or N280°-85) and NNE-SSW (N30°-85 or N280°-85). In addition, secondary joint sets (*J3*) dipping at NNW-SSE (N345°-85 or N165°-85) are relatively abundant, whereas other minor joint sets are observable very rarely (*J4*).

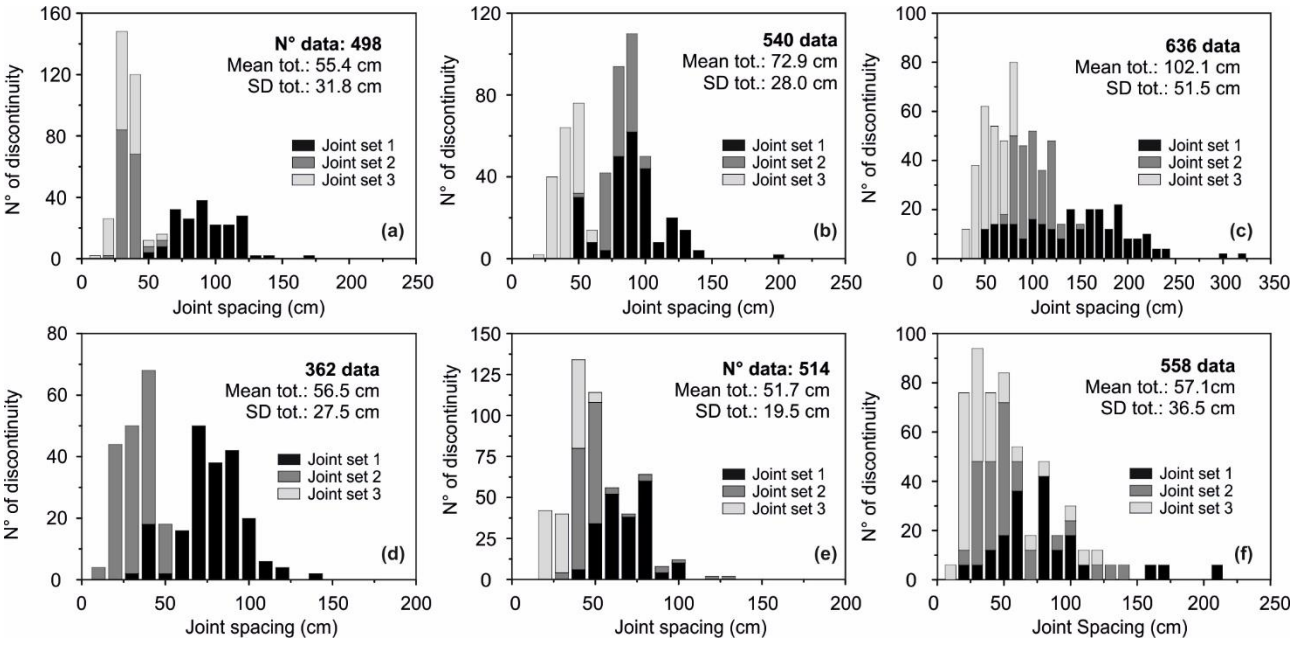

Fig.3.4. Frequency distribution of joint spacing of each structure analysed: (a) Mt Cucco, (b) Mt Maggio, (c) Mt Serrasanta, (d) Mt Penna, (e) Mt Burello and (f) Mt Pennino.

3.4.2. Analysis of fracture spacing and bed thickness

Spacing is defined as the distance between fractures measured along a scnline, while the fracture intensity is the number of fractures per unit length along a scanline (Priest, 1993). Spacing is thus the inverse of fracture intensity. A total number of 3108 spacing measurments made along the 12 outcrops are presented as histograms in **Fig.3.4**, dividing them for individual structures and formations analyzed. The descriptive statistics for each structure, sush as arithmetic mean, median and standard deviation are given in **Tab.3.2**, with their respective value of fracture intensity. Fracture intensity is a pattern characteristic that incorporates both density and size (Dershowitz and Herda, 1992; Mauldon and Dershowitz, 2000). Intensity is defined as number of fractures per unit sample length, fracture length per unit surface area, or fracture area per unit rock volume, in one, two, or three dimensions, respectively.

Fracture spacing in the Calcare Massiccio Fm. (histogram-plots in **Fig.3.4a**, **3.4c** and **3.4f**) have a magnitude generally higher then fracture spacing showed by Maiolica Fm. In particular, the main joint set (*joint set 1*), reach a maximum mean value of 102.1 cm in the Mt Serrasanta outcrops.

Statistically, the main joint sets show higher values of fracture spacing, but the distribution is no-clusterd; this is demostrated by elevated standard deviation see in **Tab.3.2**. On the other hand, the secondary joint sets (*joint set 2* and *joint set 3*) show lower spacing values but with a normal distributions (lower standard deviations), suggesting that the spatial distribution of these fracture is regular (Odling et al., 1999).

Fracture spacing vaiers as a function of bed thickness and of lithology. The linear relationship between fracture spacing and bed thickness is widely documented (Price, 1966; Huang and Angelier, 1989; Narr and Suppe, 1991; Gross, 1993; Mandal et al., 1994; Gross and Engelder, 1995; Wu and Pollard, 1995; Narr, 1996; Pascal et al., 1997; Bai and Pollard, 2000). Therefore, has been analyzed the bed thickness of each structures considered (**Fig.3.5**) in the same way of fracture spacing, differentiating the Calcare Massiccio outcrops (not well-layered sequence) from Maiolica outcrops (well-layererd sequence).

All carbonate facies are arranged into layers at dm-to m scale. The exposed rocks of Maiolica Fm.) correspond to well-layered micritic limestone with bed thickness varying from 19 to 37 cm (**Fig.3.5b**, **3.5d** and **3.5e**). The data are represented by a well clusterd distributions with a low values of standard deviation (see **Tab.3.2**).

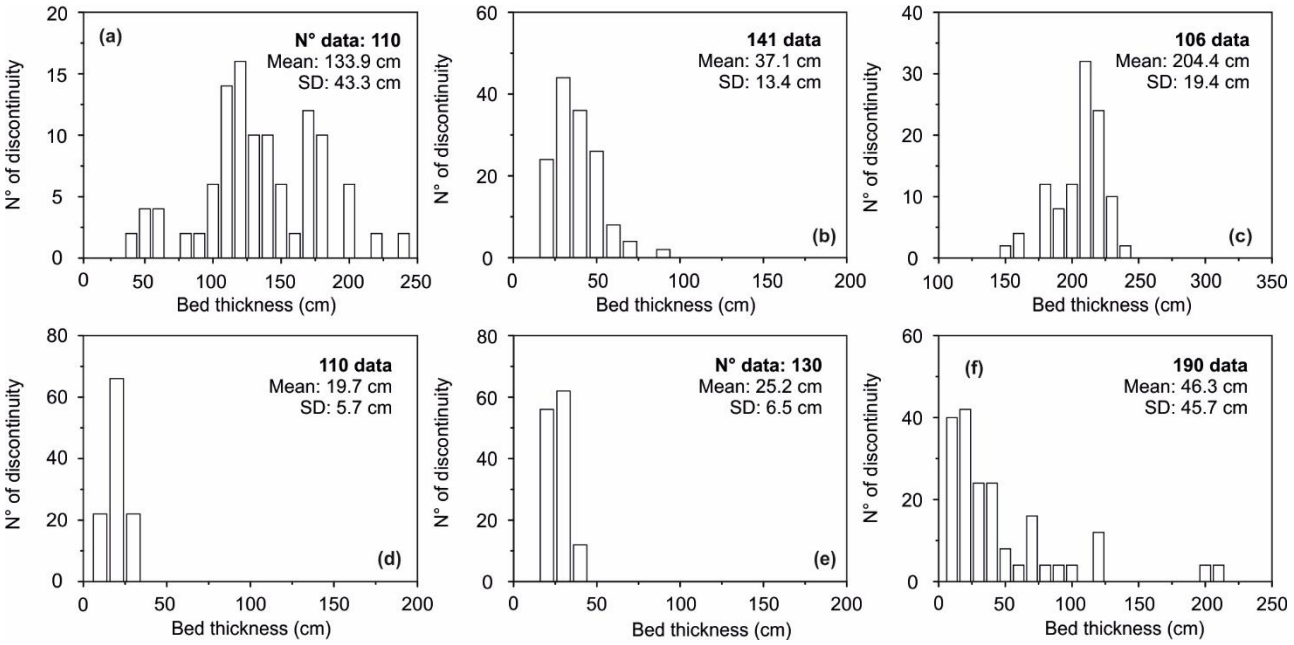

Fig.3.5. Frequency distribution of bed thickness of each structures analysed: (a) Mt Cucco, (b) Mt Maggio, (c) Mt Serrasanta, (d) Mt Penna, (e) Mt Burello and (f) Mt Pennino.

On the contrary, the rock mass of Calcare Massiccio Formation is poorly stratified or massive resulting affected by a distributed deformation by bed-parallel pressure solutions (pseudo-bedding) that disperse the distributions (**Fig. 3.5a**, **3.5c** and **3.5f**). This determine several mechanical units with different thickness. A mechanical unit was defined as an individual bed or a package of beds with common mechanical charateristics.

Bed thickness measured in Calcare Massiccio varying from 46.3 cm (pseudo-bedding) on Mt Pennino outcrops (**Fig.3.5f**) to 204.4 cm (cyclothems surface) on Mt Serrasanta outcrops (**Fig.3.5c**).

Fracture intensity values were estimated as the inverse of the corresponding spacing analysis, which represents the number of joints intersecting a given rock volume. Hence, fracture intensity values (**Tab.3.2.**) follow the same trend of spacing analysis previously discussed.

Tab.3.2. Statistical parameters related to fracture spacing and fracture intensity of each structure analysed.

Structure	No. data	Mean	Median	St. deviation	N, fracture intensity ($1/m^3$)
Mt Cucco					
Set 1	186	92.2	90.0	21.3	1.1111
Set 2	162	34.2	34.0	6.9	2.9412
Set 3	150	32.7	31.0	8.2	3.2258
Bed thickness	110	133.9	130.0	43.3	0.7692
Mt Maggio					
Set 1	246	89.9	90.0	24.5	1.1111
Set 2	138	80.3	82.0	9.8	1.2195
Set 3	156	39.7	40.0	8.9	2.5000
Bed thickness	144	37.1	35.5	13.4	2.1869
Mt Serrasanta					
Set 1	256	140.1	141.0	55.8	0.7092
Set 2	180	99.5	97.0	16.9	1.0309
Set 3	200	55.9	54.0	14.5	1.8349
Bed thickness	106	204.4	208.0	19.4	0.4848
Mt Penna					
Set 1	200	76.9	75.5	19.5	1.3245
Set 2	162	31.3	30.0	9.4	3.3333
Bed thickness	110	19.7	19.0	5.6	5.2632
Mt Burello					
Set 1	204	67.1	66.5	13.9	1.5038
Set 2	172	49.1	46.5	16.0	2.1505
Set 3	138	32.2	33.0	8.1	3.0303
Bed thickness	130	25.2	25.0	6.5	4.0000
Mt Pennino					
Set 1	174	79.9	76.0	40.7	1.3158
Set 2	192	54.1	45.5	28.3	2.1978
Set 3	192	39.5	30.5	28.2	3.2787
Bed thickness	190	46.3	31.0	45.7	3.2258

3.4.3. Analysis of fracture persistence

Like fracture spacing, vertical persistence is also controlled by the geometric and mechanical properties of the individual mechanical units (Gross et al., 1995; Cooke et al., 2006; Gudmundsson et al., 2010; Rustichelli et al., 2013).

In **Tab.3.3** have been reported the statistical data of this parameter, as data number, mean, standard deviation and variability range (min and max) of each sets.

Fracture length analysis confirm the results of the spacing analysis. Joint set 1 show the high mean length of joints, varying from 1.14 to 4.47 m in the Calcare Massiccio outcrops and from 0.6 to 1.83 m in the Maiolica outcrops. The mean correspondent persistence of Joint set 2 varies from 0.65 to 2.43 m in the Calcare Massiccio Formation and from 0.32 to 1.17 m in the Maiolica Formation. Joint set 3 show the lowest mean values of fracture persistence, vaying from 0.44 to 1.22 m in Calcare Massiccio Formation and from 0.25 to 0.41 m in Maiolica Formation.

The aspect ratio was estimated by the ratio between the maximum and the minimum value of persistence. In consequence, the aspect ratio will be variable for each sets analyzed.

Generally, the aspect ratio estimated results about 2 (ratio of 1:2), varying from a minimum of 1.4 at Maiolica of Mt Maggio outcrops to 3.1 at Maiolica of Mt Penna. Hence, the field observation shows as the fractures of Calcare Massiccio Formation are most persistent than fractures of Maiolica Formation.

Tab.3.3. Statistical parameters related to fracture persistence and aspect ratio of each structure analysed.

Structure	No. data	Mean	St. dev.	Min	Max	Aspect Ratio
Mt Cucco						
Set 1	128	148.4	46.6	101.8	195.1	1.9
Set 2	83	104.5	39.1	65.3	143.6	2.2
Set 3	96	66.2	26.3	39.9	92.6	2.3
Mt Maggio						
Set 1	96	183.1	32.1	151.0	215.2	1.4
Set 2	70	117.9	24.4	93.5	142.4	1.5
Set 3	77	39.4	11.1	48.3	81.3	1.7
Mt Serrasanta						
Set 1	38	447.2	153.5	293.7	458.7	1.6
Set 2	44	243.3	54.5	188.9	297.8	1.6
Set 3	60	122.1	22.3	99.8	144.4	1.4
Mt Penna						
Set 1	104	59.0	17.4	48.6	148.3	3.1
Set 2	93	40.8	15.3	39.5	98.3	2.5
Mt Burello						
Set 1	101	66.3	12.0	78.3	143.3	1.8
Set 2	104	32.2	9.9	42.2	82.1	1.9
Set 3	83	25	9.8	15.2	34.8	2.3
Mt Pennino						
Set 1	186	114.5	25.0	89.5	139.5	1.6
Set 2	162	64.5	15.7	48.8	80.2	1.6
Set 3	88	44.4	12.6	31.8	57.0	1.8

3.4.4. DFN modelling and hydraulic properties

As reported above, a multi-scale fracture distribution was documented after fieldwork. Discrete Fracture Network (DFN) are generated stochastically based on user-defined input parameters for each fracture set. Fracture are generated in each cell based on the specific length distribution until the intensity values are reached. Once the individual DFN are constructed using the MOVE^{TM}, fracture porosity, N and correspondent permeability tensors and porosity were computed.

The numerical results of fracture modelling computer for such a configuration are illustrated in **Fig.3.6** and reported in **Tab.3.4**. The field observations indicate conceptual DFN models made of three joint sets, which oriented perpendicular to bedding plane. A number of 18745 is generated and fracture set 1 (N115°-85) results the most developed in all the DFNs, in agreement with the contour-plot shown in **Fig.3.3**.

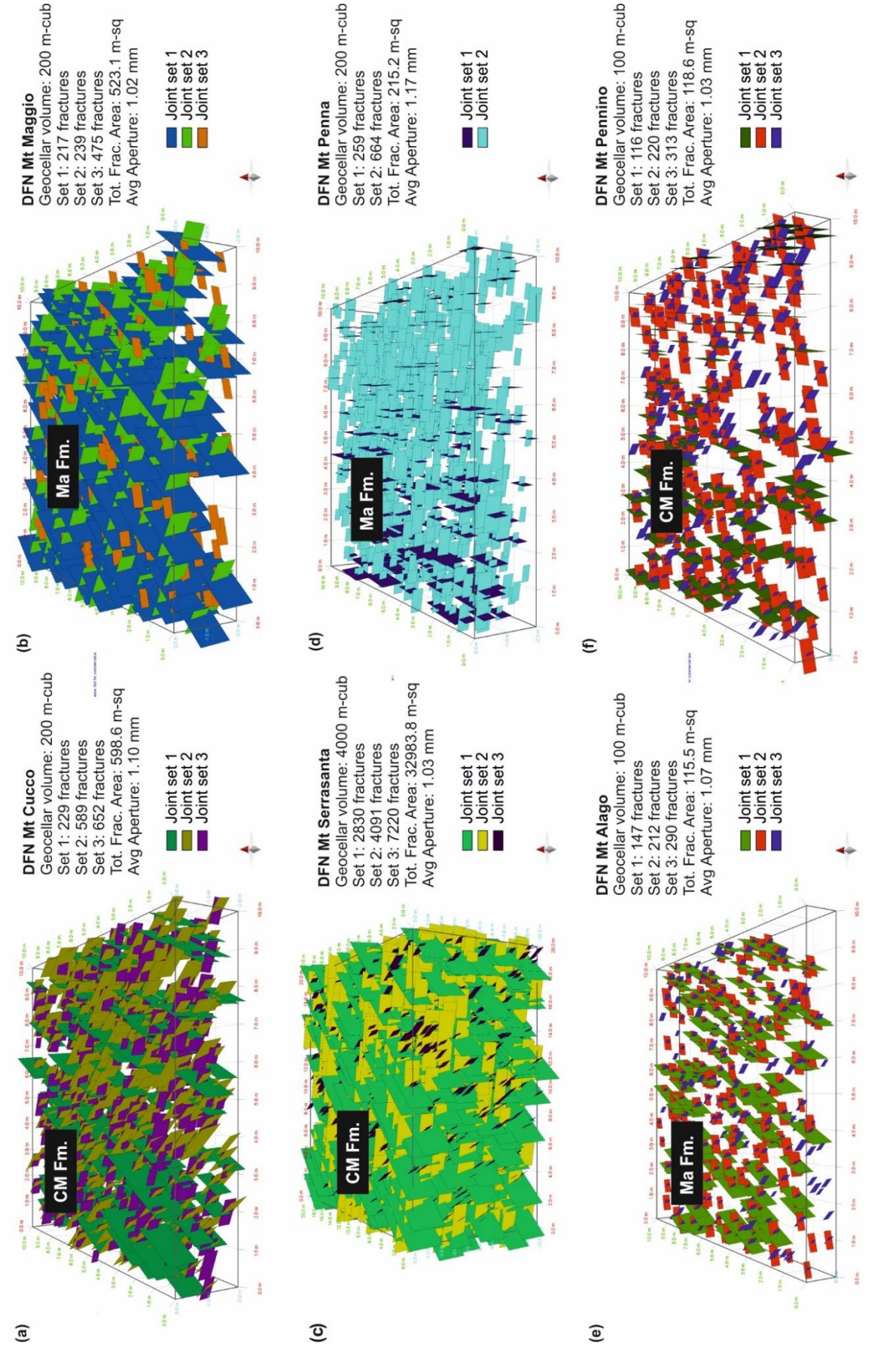

Fig.3.6. Fracture modelling results of joint sets obtained for the geocellar volumes builded for each structure analysed: (a) Mt Cucco, (b) (Mt Maggio, (c) Mt Serrasanta, (d) Mt Penna, (e) Mt Burello and (f) Mt Pennino.

It can be shown that the fracture networks are largely influenced by lithological layering (bed thickness), since many fractures are mostly confined to single layers. Fractures of set 1 can be more continuous and frequently penetrate many layers, whereas those of the other set are mostly confined to single layers, especially in the Maiolica outcrops. Odling et al*ii* (1999) suggest a classification of fracture systems that describes its behaviour at bedding interfaces. Two end-members, stratabound and non-stratabound are defined.

In this study, the joints of set 1 can be considered a non-stratabound fractures, except for the Mt Pennino outcrops (**Fig.3.6f**) where the bed presso-solution discontinuities exert a strong control on fracture propagation.

Several geocellar model volumes are 10x10 m-wide and 2 m-thick (Mt Cucco, Mt Maggio and Mt Penna), whereas Mt Burello and Mt Pennino are modelled with a geocellar volume of 10x10 m-wide and 1 m-thick. Only Mt Serrasanta were computed on volume of 20x20x10 m. The individual cell size adopted is 0.5x0.5x0.5 m.

DFN of Mt Cucco (**Fig.3.6a**) show a low P32 (2.99 m^2/m^3), in agreement with high values of fracture spacing, determining a fracture volume of 0.659 m^3 on 200 m^3, while the average fracture porosity computed is 3.29%. The mean correspondent permeability along the x-direction, *Kxx*, is about 1225 Darcy, about 1329 Darcy along the y-direction, *Kyy*, and about 2213 Darcy along the vertical direction, *Kzz* (**Tab.3.4**).

Tab.3.4. Results obtained after DFN modelling of Calcare Massiccio and Maiolica Fm. outcrops in northern Apennines.

Parameters	**Mt Cucco**	**Mt Maggio**	**Mt Serrasanta**	**Mt Penna**	**Mt Burello**	**Mt Pennino**
Fracture number	1443	931	14141	923	649	658
Fractured Area (m^2)	598.64	523.08	32983.80	215.25	115.48	118.61
Fractured Volume (m^3)	0.6589	0.5347	34.0218	0.2509	0.1230	0.1221
Model Volume (m^3)	200	200	4000	200	100	100
Avg Fracture Porosity (%)	3.2944	2.6734	8.5054	1.2544	1.2302	1.2207
Avg Fracture Aperture (mm)	1.1006	1.0222	1.0314	1.1656	1.0652	1.0292
Avg DFN P32 (1/m)	2.9931	2.6154	8.2459	1.0762	1.1548	1.1861
Max Perm_Kxx (Darcy)	1225.5	713.8	1815.3	955.5	565.1	356.8
Max Perm_Kyy (Darcy)	1329.7	626.3	1492.9	1273.8	519.3	553.8
Max Perm_Kzz (Darcy)	2213.3	1210.1	2883.9	1678.9	960.7	690.2

Average P32 value of Mt Maggio structure (**Fig.3.6b**) is 2.67 m^2/m^3 and average computed porosity is 2.67%. Also in this case, the structural properties of rock mass reflect rather well the field data. The mean correspondent permeability along the x-direction, *Kxx*, is about 713 Darcy, about 626 Darcy along the y-direction, *Kyy*, and about 1210 Darcy along vertical direction, *Kzz* (**Tab.3.4**).

The generated DFN model of Mt Serrasanta outcrops (**Fig.3.6c**) made up of 14141 fractures computing about 34 m^3 of fracture volume on 4000 m^3. The average fracture porosity estimated is 8.5% (higher recorded value), probably linked to the strong persistence of joint sets. The mean permeability computed by this DFN show the highest recorded values: about 1815 Darcy along the x-direction, *Kxx*, about 1492 Darcy along y-direction, *Kyy* and about 2884 Darcy along vertical direction, *Kzz* (**Tab.3.4**).

Mt Penna, Mt Burello and Mt Pennino DFN models (**Fig.3.6d**, **3.6e** and **3.6f**) show the lower value of P32 (1.07, 1.15 and 1.18 m^2/m^3, respectively) and fracture porosity (1.25, 1.23, and 1.22%).

Mt Penna model (**Tab.3.4**) show a mean correspondent permeability of about 955 Darcy along x-direction (*Kxx*), 1273 Darcy along y-direction (*Kyy*) and 1679 Darcy along vertical direction (*Kzz*).

The mean permeability compute by Mt Burello DFN is about 565 Darcy along x-direction (*Kxx*), about 519 Darcy along y-direction (*Kyy*) and about 961 Darcy along vertical direction (*Kzz*) (**Tab.3.4**).

3.5.Discussion

The study of several outcrops of Calcare Massiccio and Maiolica Formations in Umbria-Marche Apennines has indicated two principal fracturing directions: NW-SE (N115°) and NNE-SSW (N20°) (Mayer et al., 2003). Other maximums, although less marked, are N220°, N345° and N70° (see rose-diagram in **Fig.3.7b**).

The structural configurations is characterized by a different anticlines having a NW-SE trend and exhibits a concentric geometry, where no discrete hing znes ca be traced between the crest and the fold limbs (Tavani et al., 2008). Bedding dip across the fold strike, SW-NE (see cumulative contouring of poles to bedding in **Fig.3.7c**) progressively passes from 40° toward the SW in the southwestern sectors and up to 75° in the northeastern sector, in proximity of thrust faults.

The faults, as well as folding, clearly affect the structural asset of the units. In fact, in the study area can be distiguished three different fault systems (rose-diagram in **Fig.3.7e**): a normal fault system (NF), transtensive system (TF) and thrust system (RF).

The NE and NW-striking normal faults, which developed during early Jurassic extensional tectonics (rifting), are responsible for the contacts between the Calcare Massiccio Fm. and younger pelagic formations (Colacicchi et al., 1970; Centamore et al., 1971; Galdenzi and Menichetti, 1999). This kinematics seems to be not correlated with fracturation sets.

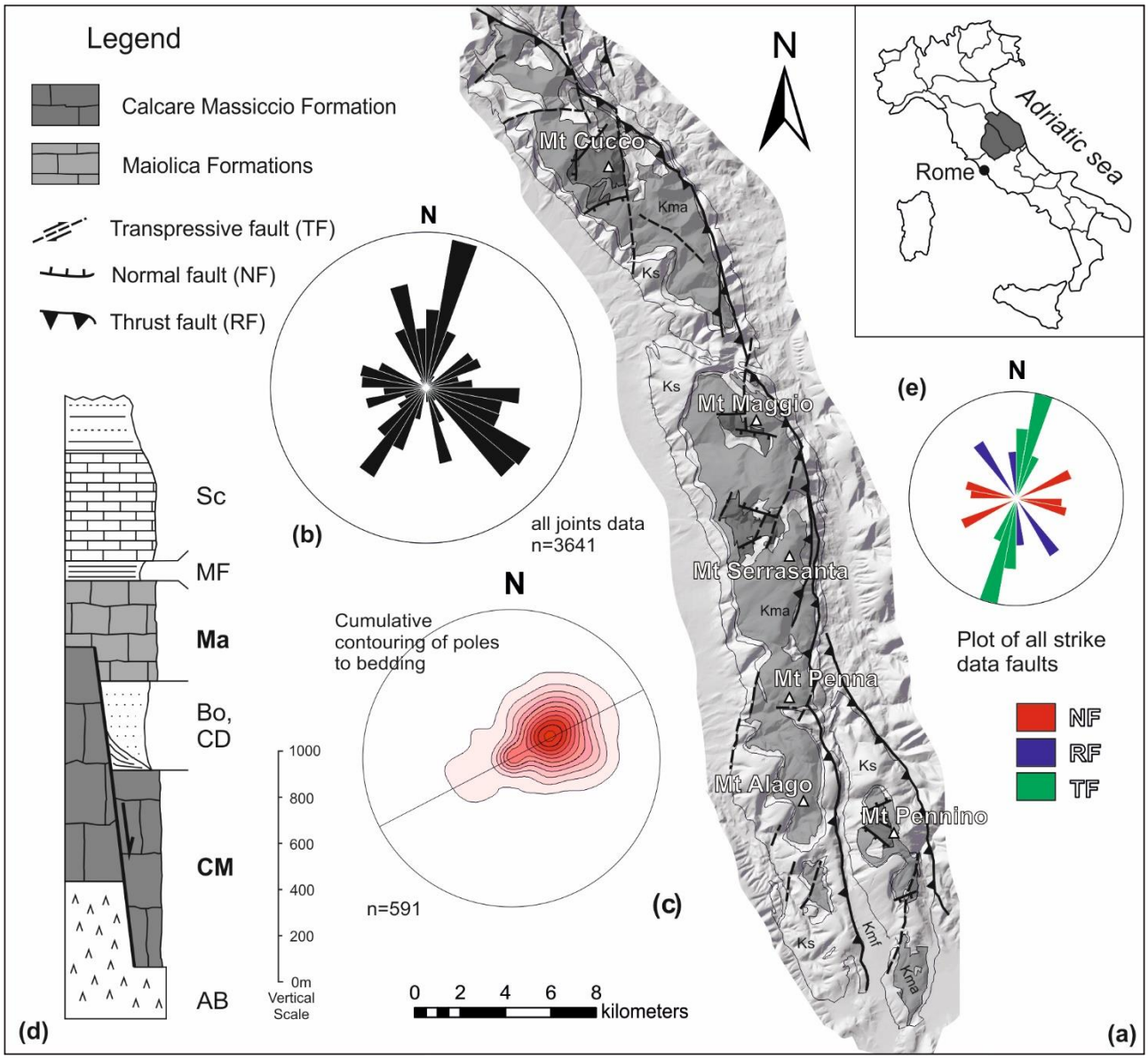

Fig.3.7. Simplified hydrogeological scheme of Calcare Massiccio and Maiolica Formations in the study area (a) and the relative stratigraphic column of Umbria-Marche succession (d). The structural properties of discontinuities analysed are also indicated: (b) rose-diagram of the all joints measured, (c) contour-plot of bedding-planes and (e) rose-diagram of different faults systems.

The main sets, N115° (SE-NW) and N20° (NNE-SSW), are about parallel and perpendicular at σ^1 of Negogenic deformation direction (about N75°). These joint sets probably forming the major discontinuities where flow circulation appens into the carbonate reservoir of Umbria-Marche Apennine ridge (Calcare Massiccio and Maiolica Formations).

DFN models built by field structural-data highligthed the role played by fractured arrengement of rock mass. In fact, the joint sets SE-NW and NNE-SSW control the connectivity between them and other fracture sets present, incuding bedding planes and bed-parallel presso-solution (pseudobedding). This is achieved thanks both high fracture spacing (0.6-1.4 m for Joint Set 1 and

0.35-0.97 m for Joint Set 2) and high fracture persistence (0.6-4.4 m for Joint Set 1 and 0.32-2.45 m for Joint Set 2).

Despite this, the computed results of DFN models highilight a marked difference in terms of hydraulic properties of the fractured rock mass between the two formations analzyed (Calcare Massiccio and Maiolica Formations), considered the main aquifers of Umbria-Marche Apennine ridge (**Fig.3.8**).

The mean fracture porosity estimated from DFNs of Maiolica outcrops is about 1.7%, ranging from 1.23 to 2.67% (**Fig.3.8a**). On the other hand, DFN models of Calcare Massiccio outcrops show a mean fracture porosity of 4.3%, ranging from 1.23% to 8.5% (**Fig.3.8a**).

The same result has been observed by permeability tensor trend (*Kxx*, *Kyy* and *Kzz*). The "*xx*" direction corresponds to the East direction, "*yy*" to the North direction, and "*zz*" is to the vertical one. Generally, the permeability is assumed to be positively correlated to the fracture porosity and, in this study, the DFN models show a great correlation between them (**Fig.3.8**).

The Maiolica Formation show a mean permeability of about 745 along x-direction, *Kxx*, about 807 Darcy along y-direction, *Kyy*, and about 1283 Darcy along vertical direction, *Kzz*. On the other hand, the mean permeability shown by the Calcare Massiccio Formation is about 1133 Darcy along x-direction, *Kxx*, about 1226 Darcy along y-direction, *Kyy*, and about 1929 Darcy along vertical direction, *Kzz*.

Furthermore, the greatest of permeability component correspond to the vertical one, *kzz*, for both formations analysed (**Fig.3.7b**). This is probably correlated with the greater vertical connectivity of facture networks than the horizontal one, guaranteed by the high fracture intensity (fracture per meter) and by a generally high dip of joint sets (on average about 85°).

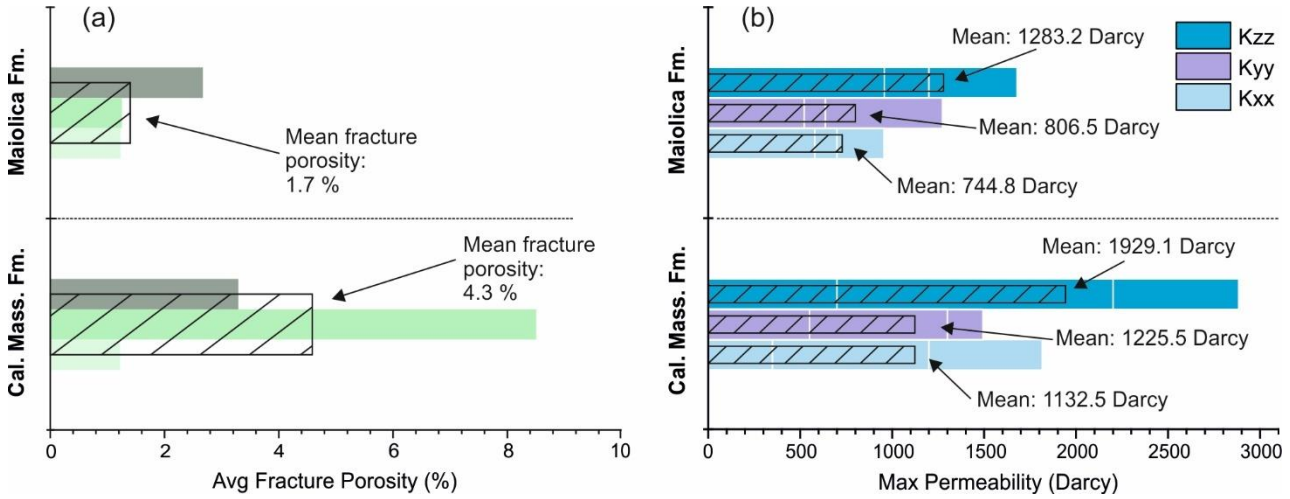

Fig.3.8. Mean trend of fracture porosity (a) and max permeability (b) deriving from computed DFN models; the values represented were subdivided based on Calcare Massiccio and Maiolica Formations.

3.6.Conclusion

With this study, has been investigated the fracture network of two carbonate formation (Calcare Massiccio and Maiolica Formations), in order to define the mechanisms through the fluids circulation occurs within the two-main reservoir of Umbria-Marche Apennines.

The structural analysis basis on field-data show the existent of two main joint sets, oriented at NW-SE and NE-SW. They have a key role for ground fluid circulation, providing the main pathways that water make from its entry into the aquifer-system (infiltration), reaching the outlet (spring). Probably, this is guaranteed by the high persistence values, penetrating both bedding planes that other secondary sets present in the rock mass.

On the other hand, the secondary joint sets detected have a low mean fracture length but a great fracture intensity (low fracture spacing); this is an important characteristic for water-storage of an aquifer system.

The control exerted by the fracture network on hydraulic properties, as well as porosity and correspondent permeability, of outcropping carbonates was computed, by means of Discrete Fracture Network (DFN) modelling of representative rock volumes.

The results of DFN models corroborate this interpretation, showing as the fracture systems are made of two main orthogonal fracture sets and other secondary sets, having different structural and hydraulic properties. So, the principal direction of fracture flow is mainly controlled by the dominant systematic joints.

As a whole, the modelling performed indicates that fracture networks enhance the porosity and the permeability of the aquifers.

Furthermore, the DFN models have pointed out a difference of hydraulic properties between the rock mass of two carbonate formations analysed. In fact, Calcare Massiccio Formation show a fracture porosity much greater respect to Maiolica Formation (4.3 and 1.7%, respectively), and the permeability values result well correlated with this trend.

Finally, results of this study therefore define a conceptual model to assess the fluid circulation and water-storage of fractured carbonate aquifers of Umbria-Marche Apennines. In fact, data reported in the present work document the role played by fractures on the structural and hydraulic reservoir properties.

4. Functioning of groundwater circulation in karst aquifers of umbria-marche Apennines

Abstract

The umbria-marche Apennine has a large number of karst springs that drainage the water stored by the carbonatic formations. The aim of this study is to understand the hydrological mechanism of groundwater circulation and their relation between structural and stratigraphic setting of each aquifer considered.

Recession analysis (Master Recession Curve method) and time series analysis (auto- and cross-correlation functions) were applied at daily discharge to six karst springs monitored for eight years (from 2007 to 2015). Both the analysis highlighted the presence of two type of karst aquifers: aquifer with unimodal behavior and aquifers with bimodal behavior. Scirca, Vaccara, Boschetto and Bagnara springs are characterized by two hydrodynamic sub-regimes, where the fracture networks control the baseflow with recession coefficients of about 10^{-3} day $^{-1}$ and the conduit networks control the quickflow with recession coefficients of one order of magnitude lower. On the contrary, San Giovenale and Capo d'acqua springs present only one hydrodynamic sub-regime associated to fracture networks drainage, with recession coefficients ranging from 10^{-3} to 10^{-2}.

Time series analysis confirm the results of recession analysis, showing a large memory effect (over 80 days) and a large response time (over 100 days), implying the dominance of the baseflow sub-regime.

These results indicate that Maiolica Formation is characterized by high fracturation degree and a slightly karstification, controlling the infiltration and percolation processes, whereas Calcare Massiccio Formation regulate the groundwater circulation in the deeper zones of aquifer characterized by a high karstification degree through a rather developed conduit networks.

4.1.Introduction

To understand a distributive models of groundwater circulation in the karst aquifers, the definition of realistic hydraulic and geometric parameters is essential (Király and Morel, 1976; Király, 1998a, 2002). Karst aquifers differ from other types of hydrogeological systems in their complex behavior originating from strong spatial heterogeneity and temporal variation (Kovács and Perrochet, 2008). These heterogeneity is linked at the hydraulic properties of through media, as low-permeability of rock matrix or high-permeability of conduit networks. However, in most cases spring discharge time series data are possible to obtain and the analysis of hydrograph recession curves is an often-used method in hydrological practice, providing interpretation of the characteristics and flow attributes of the aquifer (Bonacci, 1993; Brodie and Hostetler, 2009; Kresic and Bonacci, 2010).

Some hydrograph analytical techniques are based on the analysis of slow hydrograph recession segments with use of the Maillet and Boussinesq equations (Boussinesq, 1904; Maillet, 1905). The deviation from the exponential trend may indicate the presence of hydraulic anisotropies and, therefore, highlight the close relationship between spring hydrographs and hydrostructure geometries (Mangin, 1975; Amit et al., 2002; Kovács et al., 2005; Fiorillo, 2014).

Other authors proposed to describe the recession process by employing different mathematical functions. Drogue (1972) describe the whole recession process by using one single hyperbolic formula, where the recession coefficient, α, is note equivalent to the coefficient used by Maillet (1905). In contrast, Mangin (1975) distinguished two processes that influence recession curves. The discharge from the non-saturated zone with a non-linear flood recession and the discharge from the saturated zone with a linear baseflow recession.

Kovács et al. (2005) showed that recession coefficient allows to obtain important information about aquifer hydraulic parameters and conduit network characteristics. One main advantage of recession-curve analysis is that a set of empirical, quantitative parameters attributed to drainage mechanisms can be calculated (Malík, 2007).

Analysis of individual recession periods, sometimes, generates inconsistences related to the complexity of groundwater circulation and to the processes acting on the system (Giacopetti et al. 2017). Therefore, for analyzing a set of hydrograph recessions at a particular catchment simultaneously, a master recession curve (MRC) is commonly used (Nathan and McMahon, 1990; Tallaksen, 1995; Posevac et al., 2006, 2010; Gregor and Malík, 2012; Fiorotto and Caroni, 2013).

Malík and Vojtková (2012) performed recession curve analysis in order to evaluate the karstification degree and the hydrodynamic behavior of the aquifer. With given recession coefficients and initial discharge values, both runoff and partial runoff segments (sub-regime) can be completely described. In karst hydrogeology, the term "sub-regime" refers to the changing conditions of groundwater phenomenon, its characteristics behavior or prevailing system of natural processes which are usually observed in regular pattern of occurrence (Malík, 2015).

Apart from recession analysis univariate and bivariate analyses can also be applied to analyze spring hydrographs. Indeed, valuable indirect information regarding karst systems can be obtained as a result of the time series analysis (Box and Jenkins, 1970; Yevjevich, 1972). Mangin (1984) developed a special methodology of study of the input-output relations in the karst aquifers, as well as auto-correlation (univariate analysis) and cross-correlation (bivariate analysis). This methodology was based on the systemic approach, and it was applied and further developed by a number of authors (Padilla and Pulido-Bosch, 1995; Larocque et al., 1998; Panagopoulos and Lambrakis, 2006; Jemcov and Petric, 2009). In karst hydrogeology, auto-correlation function (ACF) of the spring discharge (Q) are generally used to assess the interdependence of spring discharge to evaluate the "*memory effect*" (Mangin, 1981; 1984).

Kresić and Stevanović (2010), whereas the cross-correlation function (CCF) methodologies is widely used to analyze the linear relationship between input (rainfall or snowmelt, P) and output (Q).

The present work aims to characterize the behavior and the groundwater circulation of the Umbria-Marche karst aquifers (northern Apennines) at a regional scale. The construction of MRCs has been used (1) to define the mechanisms of flow path that occur within carbonate hydro-structures, (2) to discretize the possible sub-regimes and (3) to define the karstified degree of each karst complex analyzed. The statistical methods applied to time series gave information about the characterization of the karst systems under study, giving more emphasis to the hydro-geological interpretation of the functions and their relationship with the structural setting of this portion of the Apennine ridge.

4.2.Study area

The Apenninic chain of Central Italy is a mountain range characterized by the presence of extensive outcrops of thick Mesozoic limestone sequences. The study area includes a large sector that starts from the M. Cucco anticline and terminates with the M. Pennino anticline.

The outcropping geological formations are mainly composed of calcareous and marly lithotypes (from Trias to Cretaceous in age) belonging to the Umbria-Marche Succession (Centamore and Deiana, 1986; Ciarapica and Passeri, 2002).

From structural point of view, the Umbria-Marche Apennines can be considered a typical thin-skinned thrust belt in which a hierarchy of multiple, superimposed detachments occurred over a main, basal detachment at the level of Triassic evaporites that acting as aquiclude. The Apenninic arch show a vergency towards ENE (Menichetti et al., 1991; Barchi et al., 1998) and it's characterize by fault systems with N-S and E-W orientation.

Above the evaporitic level lies the Mesozoic carbonatic sequence, where can be recognize three superimposed aquifers (see the hydrogeological map in **Fig.4.1**), having different permeabilities due mainly to fissures, joints and karst conduits (Boni et al., 1986; Capaccioni et al., 2001; Nanni and Vivalda, 2005; Boni and Petitta, 2007, 2008, 2010). Starting from the bottom can be found the basal aquifer of Massiccio complex, the middle aquifer of Maiolica complex and the upper aquifer of Scaglia complex. The "Calcare Massiccio" aquifer, with a thickness ranging between 700 and 900 m, represents the most important hydrogeological complex in the Umbria-Marche limestone ridge, where occurs the regional flow through very well-developed fissures and karst conduits.

The Maiolica aquifer is separated from basal aquifer by a sequence (thickness ranging between 100 and 350 m) of marls and calcareous marls of Upper Jurassic (Calcari ad Aptici, Diasprini, Posidonia, Rosso Ammonitico Fms.) that represents an aquiclude. This sequence locally can be substituted by the very thin (20-100 m) Bugarone calcareous Fm. becoming an aquitard from hydrological point of view. Maiolica complex has a rather thickness (200-400 m) with a karstification more limited but its characterized by high fracturation degree. This aquifer is overlied by the Marne a Fucoidi Fm., a low permeable formation that represents a regional aquiclude (Boni et al., 1986).

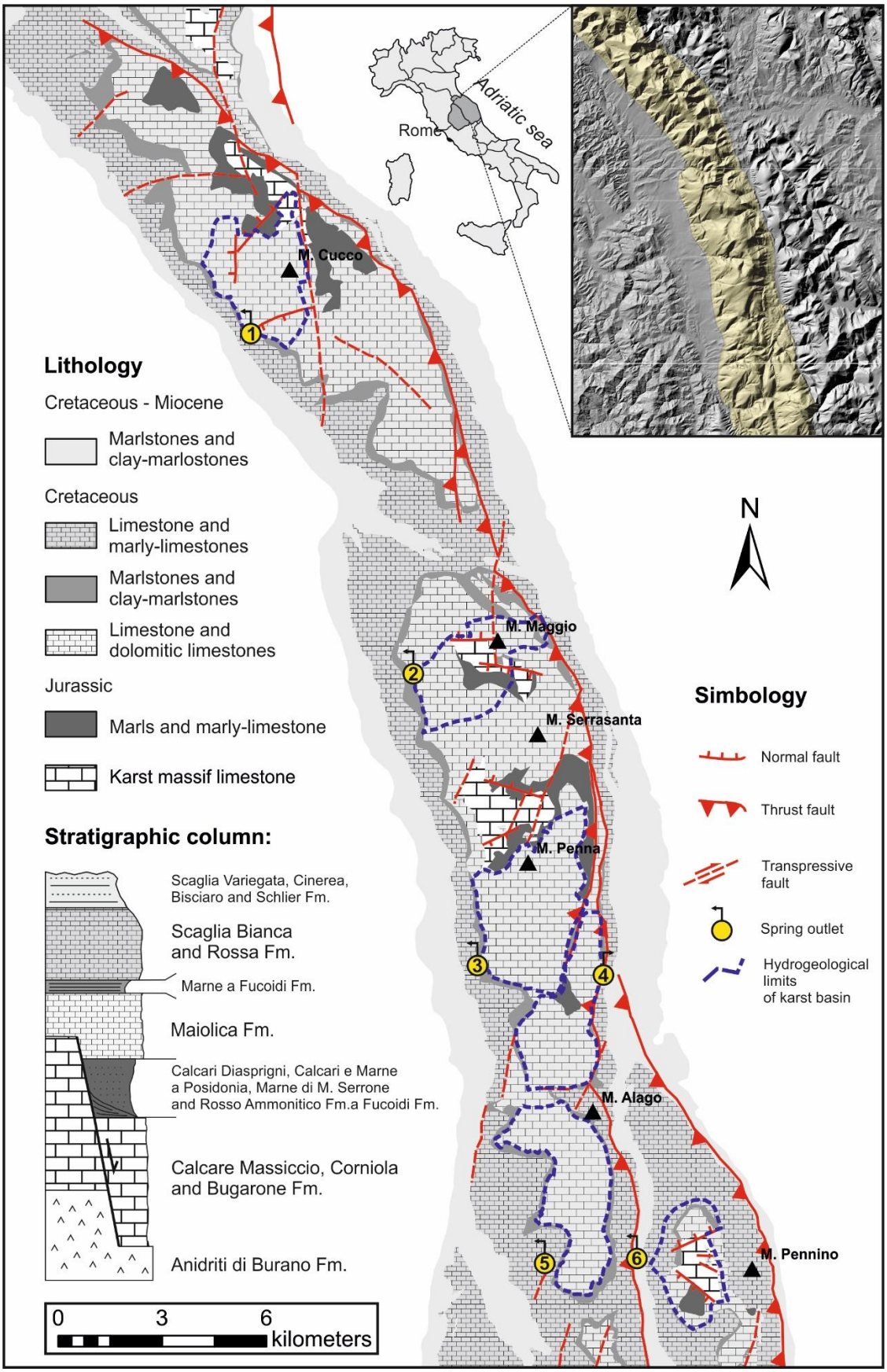

Fig.4.1. Simplified hydrogeological map of the study area at a regional scale (Northern Apennines). There are displayed different geological and hydrogeological elements: a stratigraphic column of a part of Umbria-Marche stratigraphic succession from Upper Triassic to Upper Miocene; the localization of karst springs studied and their hydrogeological limits of recharge area.

Finally, above the Marne a Fucoidi Fm. there is a Scaglia aquifer complex, made up by alternances of limestones and marly limestones with chert nodules and ribbons (Giacopetti et al., 2017). This complex is characterized by a high fracturation degree and an important thickness (200-400 m) showing, consequently, a high storage of infiltration water. Upward the aquifer is bounded by low permeable clayey-marly-calcareous sequence (Scaglia Variegata, Scaglia Cinerea, Bisciaro and Schlier Fms), usually revealing an independent aquifer (Mastrorillo, 2001).

80% of the groundwater resource of the Umbria-Marche hydrogeological domain surfaces from liner springs (Boni et al., 1986).

Tab.4.1. General characteristics of the karst complexes and their related catchment areas.

Karst complex	Spring related	Spring elev. (m a.s.l.)	Recharge area (km^2)
M. Cucco	Scirca	575	8.0
M. Maggio	Vaccara	468	6.2
M. Penna	Boschetto	538	11.5
M. Penna	Capo d'acqua	570	7.4
M. Burella	San Giovenale	480	10.5
M. Pennino	Bagnara	630	4.9

The area under study, about 220 km^2, includes the following main reliefs: M. Cucco (1566 m a.s.l.), M. Maggio (1362 m a.s.l.), M. Serrasanta (1423 m a.s.l.), M. Penna (1432 m a.s.l.), M. Burella (1095 m a.s.l.) and M. Pennino (1572 m a.s.l.). These hydrostructure show internal karst systems connected to one or more spring and that own an its recharge area (**Tab.4.1**).

4.3.Materials and methods

4.3.1. Data acquisition

It was analyzed the discharge of 6 karst springs (Scirca, Vaccara, Boschetto, Capo d'acqua, San Giovenale and Bagnara) monitored by ARPA Umbria (www.arpa.umbria.it) localized in umbria-marche Apennines, with an acquisition time interval of one day. **Fig.4.2** show about 8-years subset of the available data, that are not continuously recorded. Indeed, some gaps are present into the time series and the statistical analysis on the quality of datasets are represented in **Tab.4.2**.

Tab.4.2. General characteristics of the time-series of the karst springs analysed.

Karst springs	Monitored period	No. of all data	No. miss data	Time-series lag (%)
Scirca	2007-2015	3186	107	3.4
Vaccara	2007-2015	3097	754	24.3
Boschetto	2007-2015	3194	246	7.7
Capo d'acqua	2007-2015	3232	55	1.7
San Giovenale	2007-2015	2107	180	5.8
Bagnara	2007-2015	3240	47	1.5

4.3.2. Recession analysis

Recession analysis focuses on the recession curve which is the specific part of hydrograph following the stream peak (and rainfall event) when flow diminishes. In this study we used the Maillet exponential equation (**Eq.4.1**) as generates good fits for analyzing hydrograph recession curves and accurately describes recession over long time periods (Dewandel et al., 2003; Kovács et al., 2005; Fiorillo, 2014):

$$Q_t = Q_0 \times e^{-\alpha_i t} \quad \textbf{(Eq.4.1)}$$

Where Q_t is the discharge at time t, Q_0 is the discharge at time $t=0$, and the term $e^{-\alpha_i}$ in this equation ca ben replaced by k, called the depletion constant or recession coefficient. In particular, we used the modified Maillet equation that it can be expressed by a sum of several exponential components that represent the presence of possible sub-regimes (Eisenlhor et al., 1997; Fiorillo, 2014; Forkasiewicz and Paloc, 1967; Ghasemizadeh et al., 2012; Tallaksen, 1995):

$$Q_t = \sum_{i=1}^{n} Q_{0i} \times e^{-\alpha_i t} \quad \textbf{(Eq.4.2)}$$

Where i represents the media i in the aquifer, Q_{0i} represents the discharge of media i at $t=0$, and n represents the number of sub-regimes or flow components. Karst aquifer can always be divided into different sub-regimes, based on the different hydraulic conductivities of media (White 2003; Ghasemizadeh et al., 2012; Katsanou et al., 2015). Therefore, the modified Maillet equation can be written as:

$$Q_t = Q_q \times e^{-\alpha_q t} + Q_b \times e^{-\alpha_b t} \quad \textbf{(Eq.4.3)}$$

Where Q_q and Q_b are the initial discharges, and α_q and α_b are the recession coefficients of the quickflow and baseflow, respectively.

Analyzing the hydrographs of each karst system (**Fig.4.2**) can be showed as the recession curves not exhibit the same trend within the time series analyzed, making impossible to use a single interpolating curve for understand each karst system. Therefore, a separation technique to divide the curve into multiple segments with different slopes is needed. The *Master Recession Curve* methodology enables to work simultaneously with numerous recession periods, making negligible the influence exerted by precipitation and obtaining realistic parameters of each karst system.

The MRCs were calculated using the open source software *RC 4.0* of the *HydroOffice* (Gregor and Malík, 2012), applying the manual method tool to create the graphical analysis and to divide into different segments having homogeneous trends, thereby enabling separate analysis. The conceptual model applied is that of a linear reservoir (Boussinesq, 1877; Maillet, 1905) that follow the exponential recession function of Maillet showed above.

4.3.3. Time series analysis

ACF evaluates of a time series quantifies the linear dependency of successive values over a specified time period (lag time) (Mayaud et al., 2014) and can be written as follow (Eisenlohr et al., 1997; Laroque et al., 1998):

For $k > 0$,

$$C(k) = \frac{1}{n}\sum_{t=1}^{n-k}(x_t - \bar{x})\,(x_{t+k} - \bar{x}) \quad \textbf{(Eq.4.4)}$$

$$r(k) = \frac{C(k)}{C(0)} \quad \textbf{(Eq.4.5)}$$

where $r(k)$ is the auto-correlation function, $C(k)$ is the correlogram, k is the time lag ($k = 0$ to m), n is the length of the time series, x_t is the value of the studied variable at time t, and m is the cutting point (Box et al., 1994). The cutting point determines the interval within which the analysis is conducted. The correlogram outlines the "memory effect" of a system (Mangin, 1981, 1984; Mangin and Pulido-Bosch, 1983; Eisenlohr et al., 1997), i.e. the time needed for the system to "forget" its initial conditions and corresponds at the lag time required for the ACF to reach 0.2 (Katsanou et al., 2015; Lo Russo et al., 2014; Mayaud et al., 2014).

The CCF is used to examine the dependence of output series y (discharge) on the input series x (precipitation) and can be calculated by follow equation (Padilla and Pulido-Bosch, 1995):

For $k > 0$,

$$C_{xy}(k) = \frac{1}{n}\sum_{t=1}^{n-k}(x_t - \bar{x})\,(y_{t+k} - \bar{y}) \quad \textbf{(Eq.4.6)}$$

$$r_{xy}(k) = \frac{C_{xy(k)}}{\sigma_x \sigma_y} \quad \textbf{(Eq.4.7)}$$

where the k is the time lag; n is the length of time series; x_t and y_t are input and output time series, respectively; $r_{xy}(k)$ is the cross-correlation function; σ_x and σ_y are the standard deviations of the time series and $C_{xy}(k)$ is the cross-correlogram (Box et al., 1994).

Both of ACF and CCF are analyzed in correlograms. The steep slope in the correlogram means a fast response of the aquifer to the rainfall and indicates a higher karstification degree. The results can be compared with the recession coefficients estimated by hydrograph analysis.

4.4.Results

4.4.1. Discharge time series description

The monitoring in the fields provides the time series of daily average discharge of six springs for about eight years, from 2007 to 2015. The hydrographs in **Fig.4.2** show as the springs are reactive, i.e., that the discharges vary after a rainfall event throughout the year, but the response of each springs reflects the spatial distribution permeability of each aquifer and their hydrogeological characteristics

(Delbart et al., 2016). The amplitude of the discharge variations depends both by the recharge areas size that by the porosity and heterogeneity characteristics of karst reservoir.

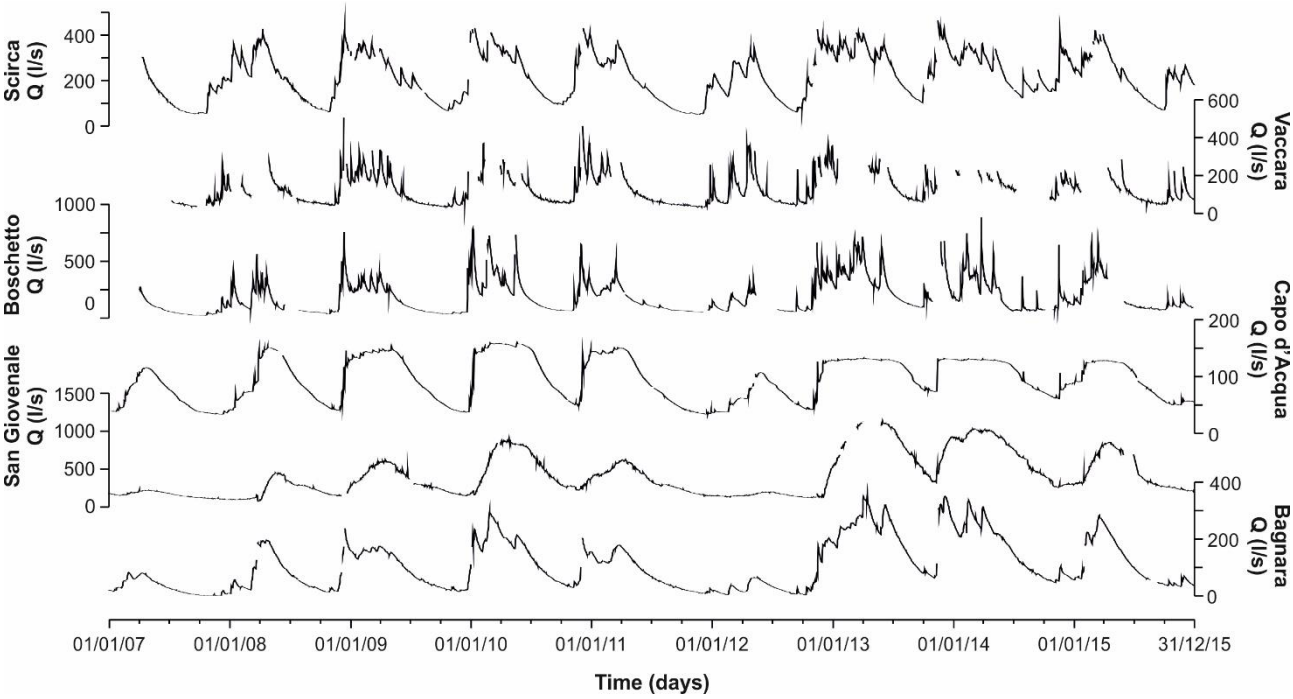

Fig.4.2. Discharge time series of the umbria-marche karst springs (data from ARPA Umbria).

Scirca spring is located in SW limb of the M. Cucco anticline, at 575 m a.s.l. The catchment area of spring is about 8 km^2 and discharge an average of 214.9 l/s, in accord with Menichetti et al*ii* (1988). Time-series of Scirca karst spring is rather continuous and the hydrograph pass from quick- to base-flow conditions generally during the early summer period with a corresponding fast decreasing of water level.

The SW limb of M. Maggio drains the water of Vaccara spring at an elevation of 468 m a.s.l. The spring discharge meaning about 119 l/s and has a larger recharge area of 6.2 km^2. The time-series is not rather complete (24% of miss data), the lack of data acquisitions was due to instrumental errors. Spring hydrograph show a very fast response to recharge events and the passages from quick- to base-flow during dry periods is rather clear.

The hydrograph for Boschetto spring was very similar to that for Vaccara spring, with a clear distinction between the base-flow and quick-flow regimes. This karst spring is located on M. Penna at 538 m a.s.l. and discharge a mean of about 185 l/s, that is about 65 l/s more than Vaccara spring but is justified by the largest recharge area of Boschetto spring (about 11.5 km^2).

Capo d'acqua spring is located on the same hydrostructures of Boschetto spring but drains the water on the other side (NE limb of M. Penna). This karst spring has an average discharge of 94.2 l/s and its doesn't show a clear passage from quickflow to baseflow regime because the discharge response after infiltration input is very delayed. The catchment area estimated is about 7.4 km^2.

San Giovenale spring drains the higher amount of water than all other karst systems of this study, with an average of 394.7 l/s. The recharge area estimate is about 10.5 km^2 and the karst system show the same behavior of Capo d'acqua spring. Differences between quick- and base-flow regime are not observed and the decrease of water level is very slow and delayed. The high average discharge of San Giovenale spring is not justified by the recharge area. Probably, this karst system is supplied by groundwater flows of a non-negligible extent coming from Colfiorito plain (Mastrorillo et al., 2009)
The hydrograph of Bagnara spring show intermediate characteristics between those of Scirca, Vaccara and Boschetto, and those of San Giovenale and Capo d'acqua. Indeed, this karst aquifer show about fast response to the infiltration input through the quickflow regime and a slow decrease of discharge during the baseflow regime. This behavior indicates a very marked spatial heterogeneity of porosity distribution along the aquifer.
Thus, Scirca, Vaccara, Boschetto and Bagnara springs show a quick response to a rainfall event showing steep peaks followed by rapid decrease of water level. This behavior is characteristics for all the karst systems that have a well-developed network of fractures and conduits. On the other hand, San Giovenale and Capo d'acqua springs show a delayed response after rainfall events, with a slow decrease of discharge on time. This behavior is showed by poorly-developed karst systems, where groundwater circulation occurs through matrix and fractures networks.

4.4.2. MRCs analysis

Recession-curve analysis was performed on hydrographs from six karstic springs located in the umbria-marche Apennines. Different shapes of the spring's recession are attributed to drainage from different components of the groundwater system, reflecting karstification degree (Malík, 2007).
It was used the *Master Recession Curve* methodology that enables to work simultaneously with numerous recession periods (**Fig.4.3**), making negligible the influence exerted by precipitation and obtaining an average value representative of the recharge area (Giacopetti et al., 2017).
The change in the slope of the recession curve has been attributed to the heterogeneity of the aquifer (Riggs, 1964; Petras, 1986), whereas recession curves that can be expressed by one exponent represent homogeneous conductivity and storage properties. Therefore, recession analysis using MRC methodology has allowed to identify two groups with a different hydraulic behavior, distinguishing the karst aquifers having a unimodal behavior (observation of one sub-regime) from the karst aquifers having a bimodal behavior (observation of two sub-regime). All the karst springs analyzed show a good fit with exponential equation of Maillet (1905), indicating how the conceptual model more appropriate is that of a linear reservoir (Boussinesq, 1877; Maillet,1905).

Recession-curve analysis was conducted on records of 8 years, resulting about 7 intervals (individual recessional discharge sets). This partial recession-curves records were assembled to create a master recession curve of each spring (**Fig.4.3** and **Fig.4.4**).

Tab.4.3 and **Tab.4.4** present the recession coefficients, discharge range, duration of sub-regime of measured recession curves and the number of assembled individual recessional discharge successions for creation of a MRC of each spring.

attributed to drainage from different sub-regimes of the groundwater systems (Malìk and Vojtková, 2012).

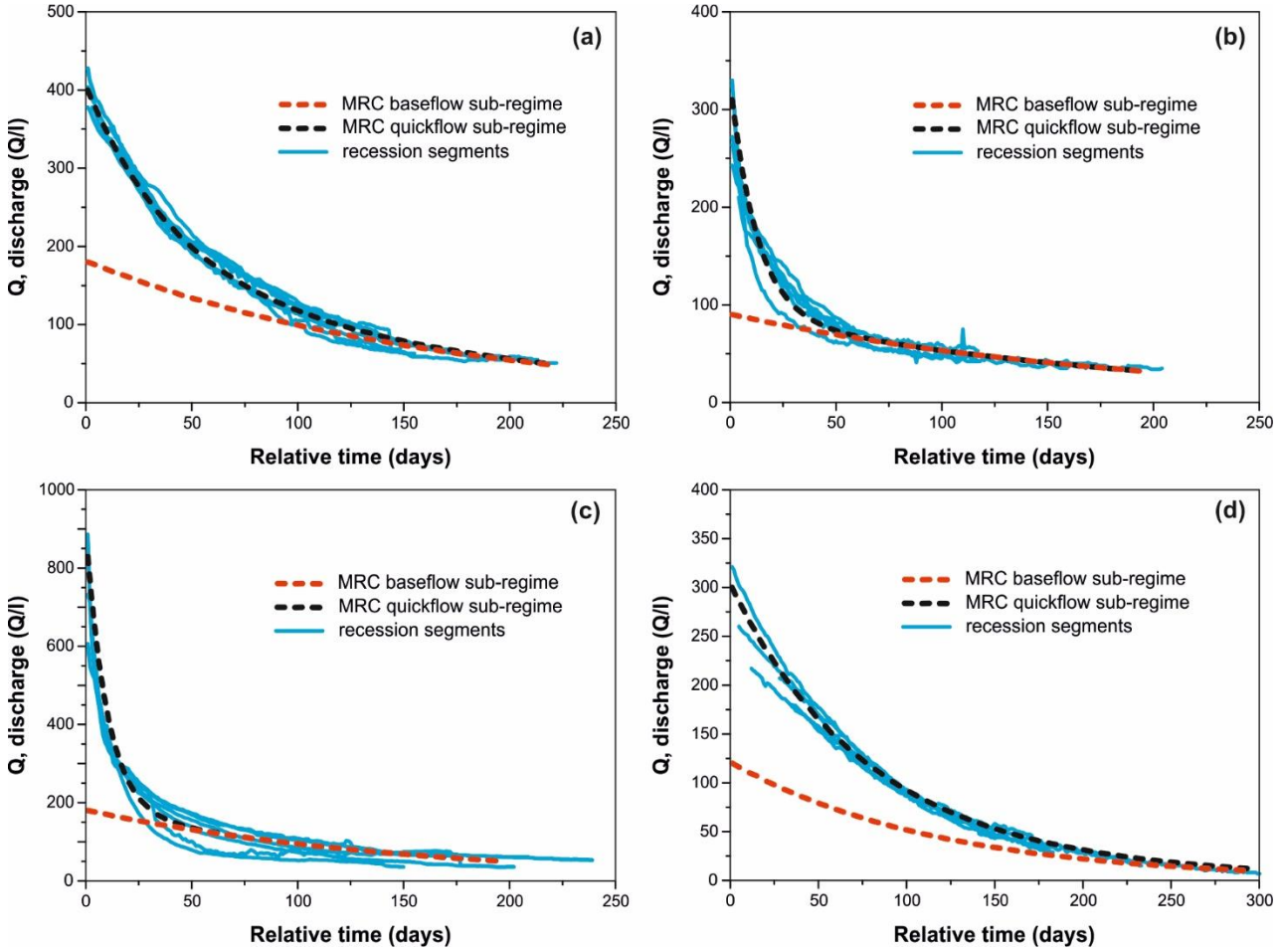

Fig.4.3. Master Recession Curves of karst springs with bimodal behaviour. (a) Scirca spring; (b) Vaccara spring; (c) Boschetto spring and (d) Bagnara spring.

For the Scirca, Vaccara, Boschetto and Bagnara springs, the results showed significant values for curve separation in two segments characterized by a different recession constant values (**Fig.4.3**), Indeed, the values of recession coefficients of quickflow sub-regimes (α_q) are rather high coming up from 0.015 d^{-1} (Bagnara spring) to 0.1 d^{-1} (Boschetto spring). Accord to Amit et al*ii* (2002) the exponential term with the largest slope represents the rapid depletion of flow channels with highest hydraulic conductivity.

Tab.4.3. Characteristics of recession curve of karst springs with bimodal behaviour and their related sub-regime (baseflow and quickflow); (a) Scirca spring, (b) Vaccara spring, (c) Boschetto spring and (d) Bagnara spring.

Spring	No. of recession segments	Q_b (l/s)	α_b (d^{-1})	t_b (day)	Q_q (l/s)	α_q (d^{-1})	t_q (day)
Scirca	8	180	0.0060	225	220	0.025	150
Vaccara	7	90	0.0053	200	220	0.080	60
Boschetto	7	180	0.0065	200	650	0.100	50
Bagnara	6	120	0.0085	300	180	0.015	200

The transition to quickflow to baseflow occurs after 150 and 180 days in Scirca and Bagnara (**Fig.4.3a** and **4.3.d**) springs respectively, indicating as the fast drainage is the dominant component for most of the years. On the contrary, baseflow sub-regime is the dominant component of Vaccara and Boschetto springs, with a sub-regime transition that happens about 30 and 50 days in Boschetto and Vaccara springs (**Fig.4.3b** and **c**), respectively. The parameters of these springs reflect the structural properties of its karst aquifer, as karstification degree, fracture networks and conduit networks.

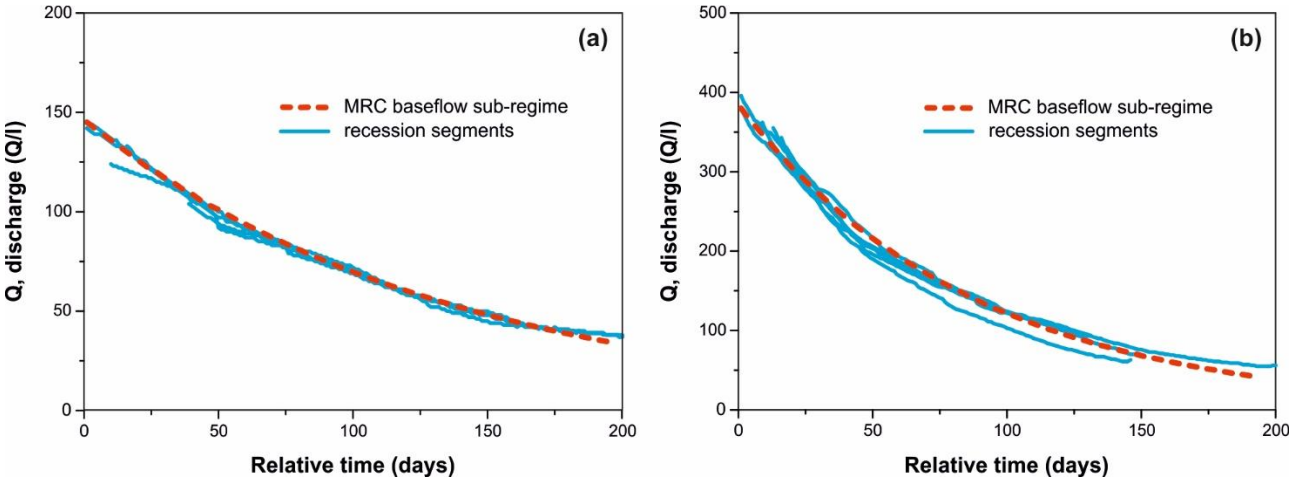

Fig.4.4. Master Recession Curves of karst springs with unimodal behaviour. (a) Capo d'acqua spring and (b) San Giovenale spring.

Capo d'acqua and San Giovenale springs presents a unimodal behavior because their MRCs are expressed by one exponent (**Fig.4.4**). This means that the karst systems are characterized by homogeneous conductivity and storage properties.

The recession coefficients point out the difference between the two springs considered. In fact, Capo d'acqua spring has a recession coefficient of 0.0074 d^{-1}, a value having the same order of magnitude of baseflow recession coefficients of karst springs with bimodal behavior previously shown. The exponential term with a small slope corresponds to the slow depletion of the flow network with low hydraulic conductivity (Amit et al., 2002).

On the contrary, the recession coefficient of San Giovenale springs (0.0115 d^{-1}) is very similar to values of quickflow components of karst springs with a bimodal behavior.

Recession period estimated by MRC method is 200 days for both karst systems (**Tab.4.5**). The difference between two aquifers is represented by dominant component (quickflow and baseflow sub-regime); indeed, Capo d'acqua spring is dominated by baseflow sub-regime, where the drainage is linked to matrix and fracture networks porosity. San Giovenale spring is a quickflow dominated sub-regime, characterized by a fast decrease of water level through fracture and conduit networks.

Tab.4.4. Characteristics of recession curve of karst springs with unimodal behaviour.

Spring	No. of recession segments	Q (l/s)	α (d^{-1})	t_r (day)
Capo d'acqua	4	145	0.0074	200
San Giovenale	6	380	0.0115	200

4.4.3. Time-series analysis: autocorrelation and cross-correlation

a. Autocorrelation function (ACF)

The autocorrelation functions treatment quantifies the linear dependency of successive values over a time period and outlines the memory of the system (Delbart et al., 2016) and the values estimated are shown in **Tab.4.5**. The correlogram of each spring for daily time series are shown in **Fig.4.5**.

The correlogram of Scirca spring shows a rapidly and regular slope of ACF, reaching r_k=0.2 after 80 days. The shape of autocorrelation functions and the high memory effect imply a significant storage capacity, probably linked to well-developed fractures network.

ACF of Vaccara spring underline the bimodal behaviour, with a rapidly decrease in the first days (10 days), associated at the quickflow sub-regime, followed by a slope much more slowly that reach a r_k value after 90 days, linked to a baseflow sub-regime.

In the case of Boschetto spring, the decrease of the autocorrelation function is uneven and two discrete components can be distinguished. The first one drops quickly within about 20 days while the second decrease more slowly and reaches the r_k=0.2 after 89 days, indicating a strong duality of this karst systems. Bagnara spring show a very slowly decrease of ACF with no step. The memory effect estimated is high value of about 121 days, showing a higher storage capacity and high potential filtering of this karst systems.

The correlogram of the discharge of Capo d'acqua spring display a regular decrease of slope of ACF that reach the r_k=0.2 at the same time lag of other system seen so far (90 days), showing a prevalence of baseflow component probably linked to fractured matrix.

ACF for the flow rates at San Giovenale spring diminish very slowly when the time lag increases. This karst system shows a memory effect of 150 days, presenting a great inertia and indicating as the aquifer and the part of drainage by the systems have a large storage capacity which is emptied over a long period of time.

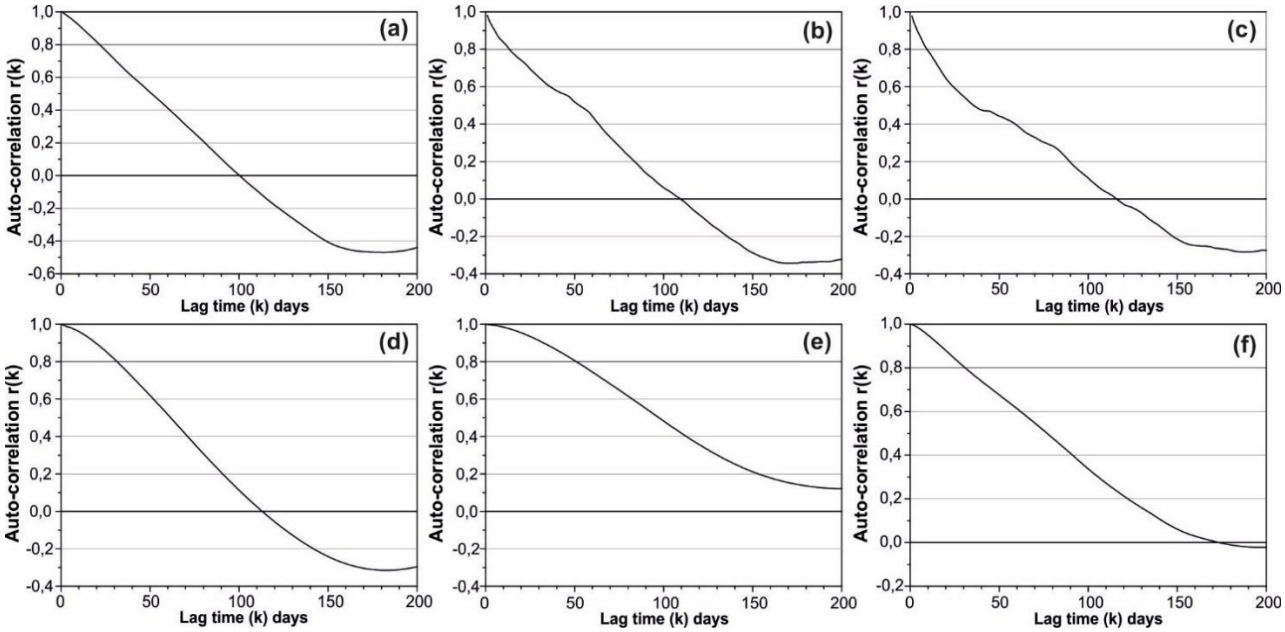

Fig.4.5. Auto-correlation functions of karst springs analysed; (a) Scirca spring, (b) Vaccara spring, (c) Boschetto spring, (d) Capo d'acqua spring, (e) San Giovenale spring and (f) Bagnara spring.

b. Cross-correlation functions (CCF)

The delays between inputs and outputs are useful in the regional study of a karst aquifer because they give an estimation of the variation of the pressure pulse transfer times and of the particle travel times through the aquifer (Panagopoulos and Lambrakis, 2006). The delays constitute an important information for the modelling of the aquifer and indicate the karstification degree of a karst system.

The CCF between rainfall and discharge time series for each spring are shown in **Fig.4.6**. and the relative parameters (maximum cross-correlation coefficients and their related time lag) of time-series analysis are indicated in **Tab.4.5**. The cross-correlograms show a $r_{xy}(k)$ values rather low (between 0.18 to 0.27). This indicate that the precipitation signal is significantly reduced between its entry in the system and the time when it reaches the water table through the unsaturated zone (Panagopoulos and Lambrakis, 2006).

Cross-correlograms of Boschetto, Scirca and Vaccara springs are composed by a sharp peak (0.27, 0.24 and 0.18, respectively), that diminishes rather rapidly in the first days, showing a response times very short (2 days for Boschetto and Vaccara springs and 13 days for Scirca spring). Subsequently, the CCF gradually decrease with a gentle slope for about 50 days. This shape indicates a duality of the karst aquifers with a transmissive function described by the sharp peak and a capacitive function distinguished by a slow decrease (Delbart et al., 2016).

Cross-correlation functions of Capo d'acqua, San Giovenale and Bagnara springs show a unimodal trend much more regular then springs previously seen. In fact, CCF decrease rather slowly with a gentle slope where the mean delay of the response is hardly appreciable with cross-correlation

coefficients ranging between 0.18 to 0.20; this case would correspond to that of a very slightly karstified system, similar to a porous medium, in which there is no quickflow.

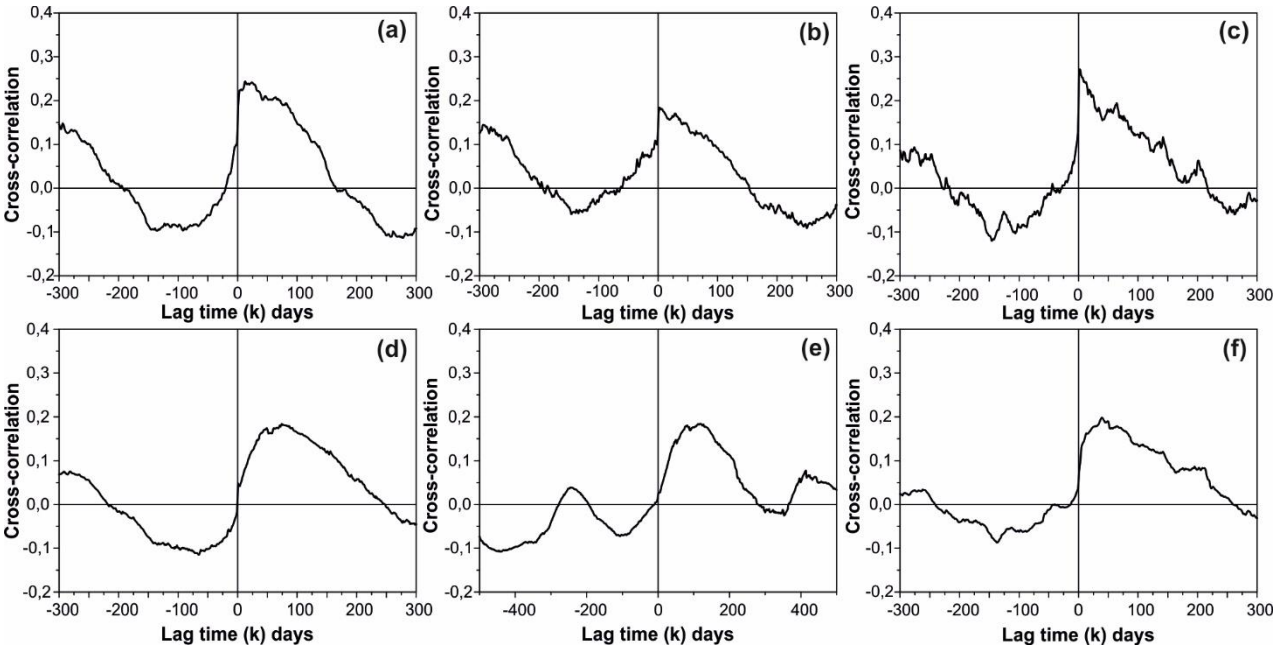

Fig.4.6. Cross-correlation functions of karst springs analysed; (a) Scirca spring, (b) Vaccara spring, (c) Boschetto spring, Capo d'acqua spring, (d) San Giovenale spring and (e) Bagnara spring.

The response times of these karst systems result of 39 days for Bagnara spring, 74 days for Capo d'acqua spring and 119 days for San Giovenale spring. These results indicate a gradational emptying of hydric system to which correspond a large storage capacity that regulates the input flow (baseflow sub-regime).

Finally, at both Boschetto and Bagnara springs a series of peaks in the CCF were observed after the first peak (64, 142 and 201 days for Boschetto spring, 68, 145 and 232 days for Bagnara spring). It might appear that these were caused by one or more other flow components within the same aquifers. The response to this behaviour must be sought in the slight control exercised by the system on the input function.

Tab.4.5. Time series analysis parameters: system memory effect, maximum discharge/rainfall cross-correlation coefficient and time lag for maximum cross-correlation coefficient (Q discharge).

Karst springs	Memory effect (days)	Cross-correlation coef.	Time lag (days)
Scirca	80	0.24	13
Vaccara	90	0.18	2
Boschetto	89	0.27	2
Capo d'acqua	90	0.18	74
San Giovenale	150	0.18	119
Bagnara	121	0.20	39

4.5.Discussion

Recession coefficient is one of the most important parameter that reflect the aquifer characteristics. In this study it was applied the Master Recession Curve method on the recession periods which are mainly controlled by the rate of decline in water table (Mohammadi and Shoja, 2014). Different recession coefficients reflect the flow regimes with different hydraulic conductivities (Bonacci, 1993). Therefore, the recession coefficient was always used to identify the structural properties (matrix, fractures and conduit networks) and the karstification degree of a karst aquifer (Bailly-Comte et al., 2010; Ghasemizadeh et al., 2012; Katsanou et al., 2015; Malík and Vojtková, 2012; Padilla et al., 1994; White, 2003).

Applying the MRC methods on the six springs it allowed to define two main structural types of karst systems (heterogeneity of aquifers): systems with a unimodal behavior (characterized by a single flow component, α_b) and systems with a bimodal behavior (characterized by two flow components, α_q and α_b). The number of the flow phases mainly depends on the degree of karstification (Fu et al. 2016).

The recession analysis (illustrated in the equation of **Fig.4.7**) show different groups of karst system. The bimodal aquifers have a mean value of recession coefficients during the quickflow sub-regime of about an order of magnitude higher then recession coefficients estimated during the baseflow condition. The MRCs displaying values between $5.3 \cdot 10^{-3}$ (α_b of Vaccara spring) to 0.1 day^{-1} (α_q of Boschetto spring). This, in agreement with Mangin (1975) and Amit et al*ii* (2002), confirm the presence of two types of flow (fast and slow) verified by the two main slopes of the recession curve. The exponential term with the largest slope, α_q, represents the fast depletion (quickflow sub-regime) of flow channels with the high transferring capacity. The largest α-value is probably a measure of the degree of fracturing and intrakarst connectivity (Amit et al., 2002).

Capo d'acqua and San Giovenale springs (unimodal karst systems) present only one type of flow having very different values. In fact, Capo d'acqua was characterized by an exponential term with small slope, about $7.4 \cdot 10^{-3}$ day^{-1} (analogue value of the bimodal aquifers during the baseflow conditions), whereas San Giovenale shows a depletion coefficient of $1.15 \cdot 10^{-2}$ day^{-1}, that is a lowest value but with the same magnitude of bimodal aquifers under quickflow sub-regime. Therefore, the drainage of Capo d'acqua spring happens as diffusive flow in low hydraulic conductivity conditions, probably controlled by a dense fracture networks in the rock matrix. On the other hand, the discharge of San Giovenale spring occurs in intermediate flow conditions (diffusive-turbulent) through a well-developed fracture networks with possible presence of karst conduit of limited extent.

The analysis emphasizes the role the role of structural geological setting, revealing a net demarcation between the dominantly calcareous cores of anticlines, surrounded by the impermeable Marne a

Fucoidi belt and containing more or less extensive basal aquifers in accord with Mastrorillo and Pettita (2014).

In according to Malìk and Vojtková (2012), a summary of the equations describing discharge and the relative karstification degree estimated using a 10-degree scale, from the six springs analyzed is shown in **Tab.4.6**.

Boschetto and Bagnara springs show a karstification degree of 4.0, a value little higher of Scirca and Vaccara springs with a karstification degree of 3.7. These karst springs are characterised by aquifers with irregularly developed fissure network, with majority of open microfissures, probably associated to shallow infiltration zones (upper portion of aquifer) mainly characterized by drainage of Maiolica complex. Also, it's very likely the presence of karst conduits of limited extent in the basal portion of aquifer linked to drainage of the Massiccio complex, where the karstic processes are very common. In extreme cases, even short-term turbulent flow might occur in this type of rock environment. From geological point of view, these aquifers are characterized by a hydraulic connection between the Massiccio complex and overlying Maiolica complex (**Fig.4.7**).

Tab.4.6. Characteristics of karstification degree in recharge area of springs according to recession curves parameters (after Kullmann, 2000; Malík, 2007; Malík and Vojtkova, 2012).

Spring	Characteristics of recession curve parameters	Karstification degree
Scirca	α_b>0.0043 and α_c<0.060	3.7
Vaccara	α_b=0.0041 to 0.018 and α_c=0.055 to 0.16	4.0
Boschetto	α_b=0.0041 to 0.018 and α_c=0.055 to 0.16	4.0
Bagnara	α_b>0.0043 and α_c<0.060	3.7
Capo d'acqua	α>0.007	2.3
San Giovenale	α>0.007	2.3

Capo d'acqua and San Giovenale springs show a single exponential flow component with a values of recession coefficient (α>0.007) to which is associated a karstification degree of 2.3 (much lower than karst aquifers with duality of discharge). Based on this value of karstification degree, Malík and Vojtková (2012) describe the karst systems characterized by a recharge area with tectonics faults filled with crushed material with higher permeability and lower buffering capability in relation to discharge. As shown in **Fig.4.7**, the water discharged by Capo d'acqua and San Giovenale springs it is drained by only Maiolica complex. These aquifers are inferiorly confined by Upper Jurassic marls and calcareous marls that represent an aquiclude. Maiolica complex, as well as the basal aquifer, can be characterized by a karst network, even though less developed. Moreover, the Capo d'acqua and San Giovenale systems are characterized by shallow aquifers, where the drainage is controlled almost exclusively by fractures networks.

Hence, in terms of regional hydrogeology, the Umbria-Marche carbonate domain has a generally deeper groundwater flowing through the hydrogeological complexes consisting of the Calcare

Massiccio, Corniola and Maiolica Formations (Boni et al., 2005). Furthermore, the structural geological and geomorphological conditions favoured the emplacement of a drainage network transversal to the axes of the carbonate ridges (Centamore and Micarelli, 1991).

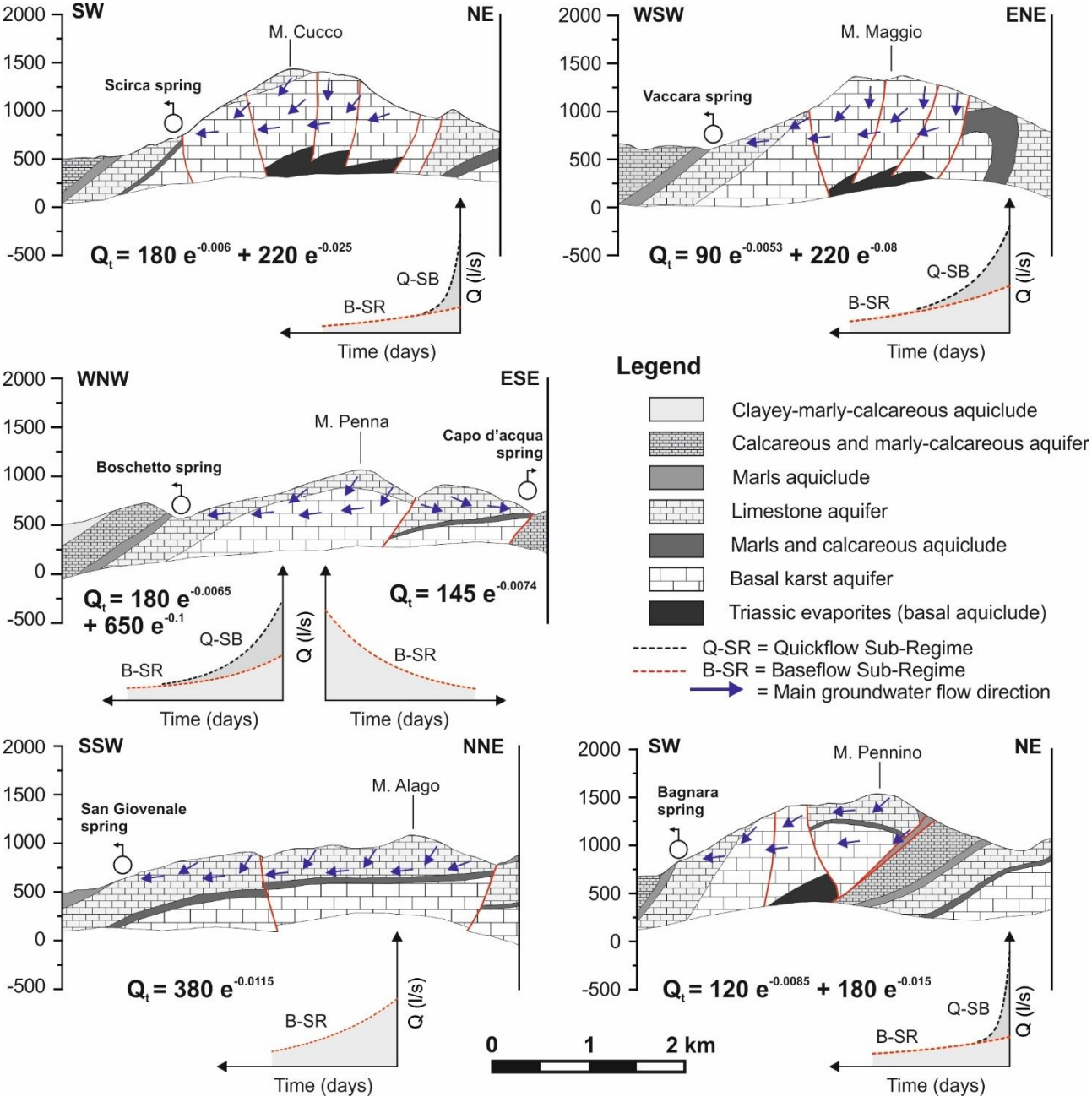

Fig.4.7. Geological sketch of flow dynamic into carbonate hydrostructures: geological cross-section, graphics of recession curves (MRC analysis) and their relative equations that describe the discharges of karst springs.

Employing the daily time series data of each springs, the interpretation of auto-correlation and cross-correlation functions supplied a valuable tool in the study of these karst systems, although the respectively analysis have not shown the same results, because the two hydrodynamic systems (bimodal and unimodal behaviour) have not been recognized in some cases.

The shape of auto-correlation functions (**Fig.4.5**) shows a regular correlograms in most cases. Only Vaccara and Boschetto spring present a sharp drop of the ACF in the first 10-20 days and a second component with much gentler slopes, showing a decorrelation time of about 90 days, confirming the bimodal behaviour in accord with results of recession analysis.

This suggesting the existence of an appreciable quickflow component in the first days, linked to karst conduits that quickly drain the aquifer after a rainfall event, and the dominant baseflow sub-regime in the next days, controlled by emptying of fracture networks.

On contrary, the univariate analysis of Scirca and Bagnara springs do not reflect the duality of karst systems point outed by recession analysis. The auto-correlation functions shown a regular and very gentle slope with a decorrelation time of 80 days for Scirca spring and 121 days for Bagnara spring. The memory effect is therefore rather high for both systems in which the baseflow component should prevail greatly (Pulido-Bosch et al., 1995).

On the other hand, also the correlograms of San Giovenale and Capo d'acqua springs are in agreement with the recession analysis, presenting one flow hydrodynamic component (unimodal behaviour).

The time lag of Capo d'acqua spring shows a similar value to those seen so far and it's about 90 days. Considering the small recharge area and the limited thickness of Capo d'acqua aquifer, the karst system is characterized by only flow component under baseflow condition and it is associated with a low karstification degree.

The auto-correlation function of San Giovenale spring presents the higher memory effect of all karst systems analysed, reaching r_k=0.2 after about 150 days. The great inertia indicates a low karstification degree and, consequently, a large storage capacity of the system. From hydrogeological point of view, the aquifer is characterized by a large recharge area (6.6 km^2) and a thickness rather limited (**Fig.4.7d**) due to drainage that occurs only into Maiolica complex.

Analysis of cross-correlation functions reflect approximately the same results obtained by recession analysis and partially by the auto-correlation analysis, though the coefficients estimated between spring discharges and rainfall events are rather low (0.18-0.27). In fact, the CCF of Scirca, Vaccara and Boschetto springs demonstrate a bimodal character, showing a discrete peak appears with a delay of few days. This can be interpreted as a rapid response of the aquifer to a rainfall occurrence.

On the contrary, the CCF of Capo d'acqua, San Giovenale and Bagnara springs show a long impulsional response, which exceed 200 days, and with a delay rather highs ranging from 39 days (Bagnara spring) to 119 days (San Giovenale spring). This indicates the powerful memory of the systems and the dominance of baseflow at the expense of quickflow.

4.6.Conclusion

In order to define the characteristics of groundwater circulation into carbonate hydrostructures of Umbria-Marche Apennine were analysed the discharge time-series of six karst springs, from 1 January of 2007 to 31 December of 2015 (8 years), using different methodological techniques (MRC "master recession curve" analysis, ACF "auto-correlation function" analysis and CCF "cross-correlation analysis").

The karst aquifers analysed simulate the drainage as a linear reservoir conditions where the discharge follow the exponential form of modified equation of Maillet, though not all systems show the same structural properties. In fact, can be observe two types of aquifers: karst aquifer having a bimodal behaviour and karst aquifer having unimodal behaviour. These substantial differences can be attributed to structural and geological settings of a single hydrostructures that reflects the different components of groundwater systems (Bonacci, 1993).

More in detail, the discharges of Scirca, Vaccara, Boschetto and Bagnara springs are characterized by two hydrodynamic sub-regimes (bimodal behaviour), where the fracture networks and microfissures (rock matrix) control the slow drainage (baseflow sub-regime) with a α_b of about 10^{-3}, and the conduits networks control the fast drainage (quickflow sub-regime) with a α_q of one order of magnitudes lower than that of the matrix. This indicate a certain karstification degree (3.7-4 in accord to classification of Malík and Vojtková, 2012), in which a conduit networks of limited extent characterized by few interconnected systems and surrounded by a fractured rock mass irregularly developed with fissures rather opened. These karst aquifers are characterized by the hydrostratigraphic contact between Maiolica complex and Massiccio complex.

On the contrary, Capo d'acqua and San Giovenale present a unimodal behaviour, showing a single exponential flow component with values of recession coefficients lower than other karst systems previously seen. This is easily understandable because the groundwater circulation happens only within the Maiolica complex, where the karst is scarcely developed and the water moves through a fracture networks (Angelini and Dragoni, 1997).

Both auto-correlation and cross-correlation functions show approximately the same results of recession analysis. Indeed, bimodal aquifers show a steep slope in short lag time (2-13 days) followed by a gentle slope, whereas the unimodal aquifers show a quite uniform decrease with high values of delay times. Besides, the CCF and ACF highlighting large memory effect (over 80 days) and a large response time (over 100 days), implying the dominance of the baseflow sub-regime. This indicate a great inertia showing how the aquifers filters the information contained in the rainfall event very well. Consequently, the karst systems analysed underline the large storage capacity (very important from the water management) and the character of attenuation.

Taking into consideration the above results, we conclude that the structural and hydrogeological setting influence the structural properties of aquifers and, consequently, the groundwater circulation within the Apenninic carbonate sequence.

The hydrostructures characterized by the Maiolica complex present a high fracturation degree and a rock mass slightly karstified, controlling mostly the infiltration and percolation processes. Here, groundwater circulation happens within fracture network and the discharge is dominated by baseflow sub-regime, probably with a Darcian flow, making hiring a unimodal behaviour at the reservoir.

On the other hand, the aquifers that involving Massiccio complex present a higher karstification degree, through which regulate the water circulation with different flow components. This complex is interested by a conduits networks rather developed, especially in the deeper zones of aquifers, that are responsible of quickflow sub-regime and, therefore, the dual behaviour.

5. Hydrological and geometrical characterization of a karst aquifer using relationship between fractured rocks and spring discharge: an example of karst basin in Umbria-Marche Apennine (central Italy)

Abstract

Karst aquifer are characterized by a strong heterogeneity in their physical properties. The purpose of the study is to understand the relationship between spring discharge and structural setting of a karst aquifer located in the umbria-marche Apennine (central Italy) in order to define the geometrical and hydrological properties. It was investigated recession curve of a karst spring on about 3 years (from January 2013 to October 2015) using the modified equation of Maillet. The variability of recession coefficients during dry periods seems to be linked at variation of porous media, where the quickflow is controlled by conduits with a recession coefficient of one order of magnitude higher than baseflow (controlled by fracture networks). The conduits drain 31,6% of total volume discharged during recession period in about 25 days. Besides, the η_{eff} calculated for the total aquifer is 1,65%, of which 90,3% was attributed at fracture networks and the 9,7% remaining was attributed at conduits. This suggest that the conduits network is poorly branched and there are a few systems, but with large sizes and well interconnected, localized in the basal portion of aquifer. Saturated water storage estimated is 7425 mm for the total aquifer. Therefore, the maximum water that aquifer can store is about two times of the average effective infiltration estimated on the whole karst basin (of about 3859 mm/y), indicating that karst aquifer has a high potential for water supply. Structural survey shows main sets of discontinuities are oriented at NW-SE and SW-NE. This indicate that the directions of main development karst conduits network, in the basal aquifer, follow the same orientations of main sets of discontinuities. The geometrical setting gives an echelon shapes, with sub-vertical wells connected at sub-horizontal planes.

5.1.Introduction

Karst systems are characterized by a highly heterogeneous structures, leading to complex underground stream flows that are neither fully observable nor accurately measurable. Furthermore, the insufficient data on conduit network geometry entails difficulties in the characterization and modelling of groundwater dynamic.

Therefore, an aquifer drainage system can be characterized by an impulse function that transforms the input (e.g. rainfall or snowmelt) into variations in spring hydrograph responses.

Karst aquifers and springs have been extensively studied by hydrographs analysis, which are often used to providing an interpretation of the characteristics and flow attributes of the aquifer obtaining some hydraulic parameters (Mangin, 1975; Bonacci, 1993; Padilla et al., 1994; Fiorillo, 2011; Kresic and Bonacci, 2010).

Numerous equations were used to calculate this parameter (Boussinesq, 1877; Maillet, 1905). In general, the recession coefficient varies directly with the hydraulic conductivity but inversely with the aquifer storativity (Bonacci, 1993; Fiorillo, 2014; Katsanou et al., 2015).

For the aquifer structure, the karst aquifer behaves as a dual-flow system consisting of highly conductive conduits and a relative low permeability fractured rock matrix with high significant storage (Ford and Williams, 2007; White, 2003). Groundwater flow in such aquifer types differentiates from the respective one in porous media due to the fact that the flow velocity is related to a network of high-velocity drains (quickflow) within a slow-velocity matrix (baseflow, Atkinsson, 1977). This is represented by different recession coefficients, which reflect the flow regimes with different hydraulic conductivities (Bonacci, 1993).

The conduit network is an important part of the karst aquifer and has very different characteristics with the surrounding matrix. It is always the main drainage passage and connects to the spring directly in the karst aquifer for its high hydraulic conductivity (Chang et al., 2015).

Therefore, the recession coefficient was always used to describe the development of the conduit network with high hydraulic conductivity, and also to identify the karstification degree of an aquifer (Bailly-Comte et al., 2010; Ghasemizadeh et al., 2012; Katsanou et al., 2015; Malìk and Vojtkovà, 2012; Padilla et al., 1994).

Kovàcs et al*ii* (2005) provided two main flow regime. Stevanovic et al*ii* (2010) outlined how, despite the prevalence of conduits, some large reservoir systems, due to large saturated karstified volumes, may have slow reaction and drainage.

Most of the descriptions were qualitative. However, the quantification of the effective porosity (n_{eff}) and water storage capacity for each hydraulic conductivity media may be more valuable in understanding the aquifer characteristics (Amit et al., 2002; Li, 2009).

It has been found that the recession coefficient has positive a high correlation with discharge at the beginning of the recession period.

In the study of functioning of a karst system is essential to consider the structural and geological setting of rock mass constituent the reservoir, as spatial orientation of main discontinuities, fracture degree and main structure linked to local tectonic.

The influence that fractures exert on fluid flow through rocks (Engelder and Scholz, 1981; Sibson, 1996; Eichbul et al., 2004) makes genetic and structural studies of fracturing relevant to geologist. Fracture networks can control the infiltration, percolation of groundwater and the karstification degree of rock mass.

Permeability of shallow aquifer can be considered relatively low and it is mainly linked to primary and secondary porosity of rock mass, i.e. at syngenetic voids and, specially, to the discontinuities

(joints, faults and bedding planes). Primary porosity of matrix media can be neglected because syngenetic voids are poorly connected together. Therefore, fractures and bedding planes are considered the main flow pathway of fluids, which they are conveyed from upper portion of aquifer (infiltration domain) to basal portion (conduit domain) until the spring outlet.

The purposes of this study were to define the geometry and hydrogeology of a karst aquifer located in northern Apennines, through:

(1) interpretation of the spring hydrographs using the Maillet modified equation;

(2) characterization of the structural properties of fractured rock in order to define their effective porosity and the associated main direction of karst conduits in the basal aquifer;

(3) estimation of the proportion of water storage capacities of aquifer components (conduits and fractures) using the quantitative relationship between recession coefficients and effective porosity proposed by Fiorillo (2011, 2014).

5.2.Study area

5.2.1. Geographic, morphologic and climatic context

The studied area (43°32'53.97"- 43°31'58.11"N, 12°31'21.60"- 12°32'32.90"E) is located in a SW limb of M. Nerone anticline, in the northern sector of the Umbria-Marche Apennines (Central Italy). The studied system consists in a small karst basin with an area of about 3,9 km^2 and its characterized by a fractured carbonatic sequence. From a morphologic point of view, the karst basin is characterized by steep slopes, of which the altitude varies between 660 m asl. and 1450 m asl, where a tight valley is interposed by several topographic hill (**Fig.5.1**).

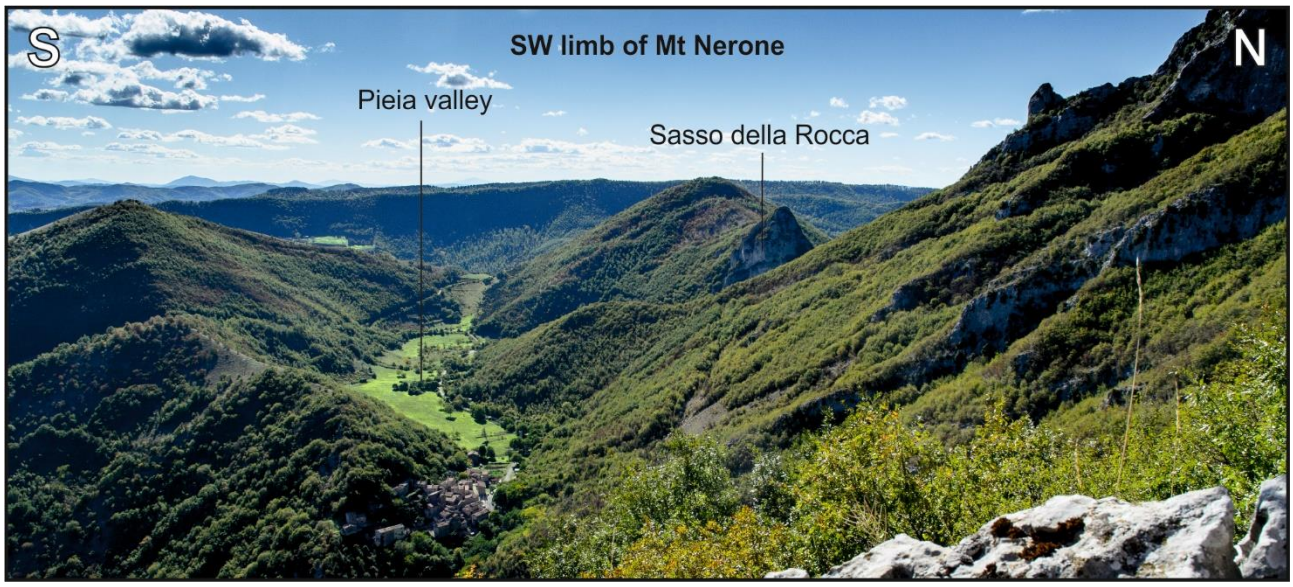

Fig.5.1. Panoramic view of a part of the Giordano karst basin in the SW limb of Mt Nerone anticline.

This area has a typical subcontinental climate, characterized by a dry and warm summers, and wet and cold periods occurring during winter. Monthly rainfall reaches its highest annual peaks during November and March, while the minimum annual values are recorder during June-August. In the high-elevation zones (above 1000 m a.s.l.) snow can accumulate for several weeks during winter, providing a time-shift of the infiltration processes.

Fig.5.3a shows the rainfall and temperature distribution in the studied area with the related values of evapotranspiration and runoff. The annual rainfall ranges from 1266,8 mm/y to 1710,2 mm/y, with an average of 1534 mm/y and with annual atmospheric temperatures from 11,1 °C to 11,9 °C, with an average of 11,5 °C. The average evapotranspiration, calculated with a Thornthwaite's method (Thornthwaite, 1957), resulting about 680 mm/y while the mean runoff estimated is about 854 mm/y.

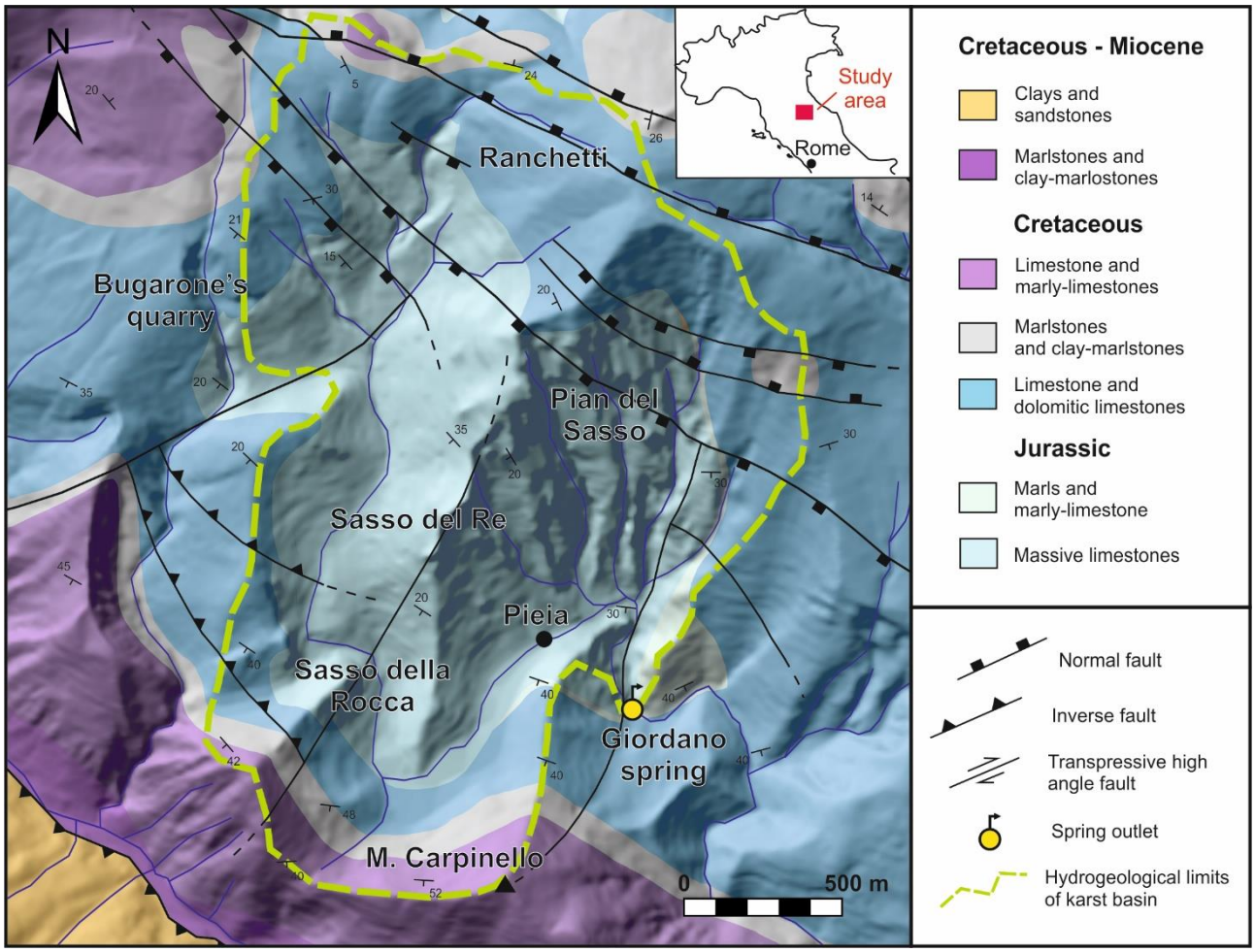

Fig.5.2. Geographic location and geological-hydrogeological map of the Giordano karst basin.

5.2.2. Geologic, hydrogeologic and hydrologic context

The study area is located in the SW flank of M. Nerone anticline, an antiformal structure with an axis elongated NW-SE (Northern Apennines). The karst system investigated is constituted by a carbonate sequence of three superimposed geological formations: Calcare Massiccio Fm. (Lower to Upper Jurassic), Bugarone Fm. (Upper Jurassic) and Maiolica Fm. (Upper Jurassic-Lower Cretaceous), which is heavily fractured and faulted. The anticline is developed over a main basal detachment level located in the Triassic evaportites.

The axial sector of anticline is tectonically characterized by a main set of normal faults oriented NW-SE, which displace the carbonate sequence with offset of some tens of meters, and secondary set of transtensive faults oriented NE-SW. The spatial distribution of shear zones and beddings orientation of carbonate sequence define a tectonic scheme characterized by monoclinal blocks of limited extension (Menichetti, 1995). The present karst basin seems to be limited to the topographic and structural depression of the small Pieia valley and the fractures and beddings discontinuities constitute a fundamental phenomenon in controlling fluid motion at depth. The hydrostructural setting of the Umbria-Marche carbonate domain consists of an alternation of complex with different hydrogeological characters, combined with a regional tectonic style (Mastrorillo et al., 2009). In this domain, the cores of anticlines accommodate thick basal aquifers. The deep groundwater runs inside the regional basal aquifer, which is embedded in the Maiolica and Corniola-Calcare Massiccio complexes. In this study, the partially lack of Jurassic marls and marly-limestone complex does not affect significantly the flowpaths of this groundwater, except for the karst spring. In fact, this is located in proximity of the Jurassic carbonate paleo-escarpment where a localized stratigraphic contact with the Jurassic marls and marly-limestone act as aquiclude. The structural and permeability limits of recharge area are represented by outcropping of regional aquiclude of Marne a Fucoidi Formation, which on the surface closes hydrogeologically the whole hydrostructure.

As mentioned above, the Calcare Massiccio Fm., outcropping with a thickness of about 800 m, represents the main reservoir of northern Apennines and forms a continuous hydrostructure with to overlying Formations Bugarone Fm. and Maiolica Fm., with thickness of about 30 m and 50 m, respectively.

This stratigraphic and structural setting forces a parallel-to-the-ridge circulation of groundwater, and the ridge itself has been considered as an isolated hydrogeological system (Bison et al., 1995).

In this study area can be found all the end-members of karst processes, from solution caves to carbonate travertine deposits. Moreover, the main cave-forming processes are related to deep-seated hydrogeological recharge where limestone corrosion is drive by endogenic agents (Menichetti, 2009).

The most significant karst evidence is represented by Fondarca cave, a sinkhole generated by the collapse of rocks whose diameter estimated to be around 50 meters and characterized by the typical bell shape and its wall are counter sloping. Moreover, this sinkhole presents an arch (Fondarca arch) on the southern side and a smaller arch on the south-eastern side which represent all that remains of the original karst cave's great vault.

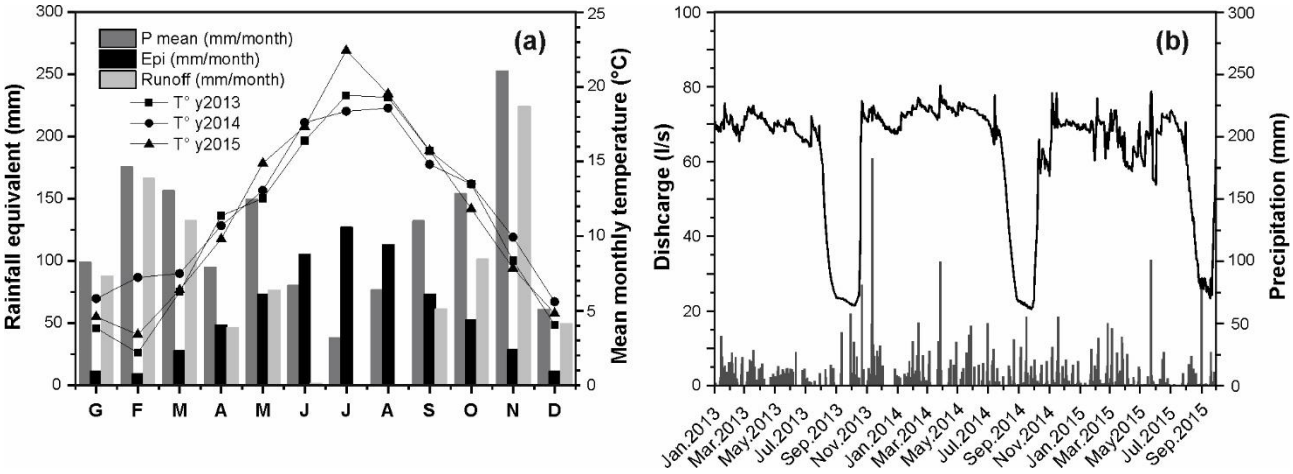

Fig.5.3. Hydrological balance of Giordano karst basin: by rainfall and temperature data (provided by www.geometeo.it) were calculated the Epi (by Thornthwaite's method) and the runoff values; Spring discharge (solid line) and precipitation (grey bars) of Giordano karst basin (a).

5.3.Materials and methods

5.3.1. Data acquisition

The discharge of the Giordano karst spring (560 m a.s.l.) at the Pieia has been daily acquired in the collection system of *Marche-Multiservizi* for about 3 years. Spring flow is intercepted through different systems: a perforated well driven directly into the basal aquifer and a trench that intercepts discharge of an intermittent spring located about 70 m upstream. Discharge rate is recorded continuously in both capture systems and the water intercepted is directly conveyed in a single tank. Gaps are not present. The entire dataset used in this study ranges between 01/01/2013 to 30/09/2015. The rainfall and temperature time series is recorded daily by *Meteo-Regione-Marche* (http://www.protezionecivile.marche.it) at Pianello gauge station, located 2.2 km south-east of the study site center.

5.3.2. Recession analysis

The recession coefficient is one of the most important parameter that reflect the aquifer characteristics and in this work we used the exponential equation of Maillet (1905) to simulate the recession process with the following formula:

$$Q_t = Q_0 \times e^{-\alpha_i t} \qquad \textbf{(Eq.5.1)}$$

Where Q_t is the discharge at time t, Q_0 is the discharge at time $t=0$, and α is the recession coefficient. In particular, we used the modified Maillet equation that it can be expressed by a sum of several exponential components (Eisenlhor et al., 1997; Fiorillo, 2014; Ghasemizadeh et al., 2012):

$$Q_t = \sum_{i=1}^{n} Q_{0i} \times e^{-\alpha_i t} \quad \textbf{(Eq.5.2)}$$

Where i represents the media i in the aquifer, Q_{0i} represents the discharge of media i at $t=0$, and n represents the number of flow components. Karst aquifer can always be divided into conduit, fracture, and matrix systems based on the different hydraulic conductivities (Ghasemizadeh et al., 2012; Katsanou et al., 2015; White, 2003). Therefore, the modified Maillet equation can be written as:

$$Q_t = Q_c \times e^{-\alpha_c t} + Q_f \times e^{-\alpha_f t} + Q_m \times e^{-\alpha_m t} \quad \textbf{(Eq.5.3)}$$

Where Q_c, Q_f and Q_m are the initial discharges, and α_c, α_f and α_m are the recession coefficients of the conduit, fracture and matrix, respectively.

Since in this work the primary porosity, linked to the syngenetic voids of the rock, the matrix component can be neglected and the recession is given by hydraulic conductivities of the conduits and fractures components. Hence, the **Eq.5.3** became:

$$Q_t = Q_c \times e^{-\alpha_c t} + Q_f \times e^{-\alpha_f t} \quad \textbf{(Eq.5.4)}$$

To understand the drainage of the studied karst system, we can approximate the aquifer to the composite reservoir proposed by Fiorillo (2011, 2014). The model is represented by an aquifer of cylindrical shape, with constant area, and characterized by two distinct zones superimposed effective porosity zone, with $n_{eff\text{-}2} > n_{eff\text{-}1}$. For basal spring, the author has found how the ratio between two different values of the recession coefficient obtained by semi-logarithmic plot can be approximated to the inverse ratio of the effective porosity computed along the surface of the water table:

$$\frac{\alpha_1}{\alpha_2} \approx \frac{n_{eff-2}}{n_{eff-1}} \quad \textbf{(Eq.5.5)}$$

Following the modified equation of Maillet (**Eq.5.4**), the **Eq.5.5** can be rewritten:

$$\frac{\alpha_f}{\alpha_c} \approx \frac{n_{eff-c}}{n_{eff-f}} \quad \textbf{(Eq.5.6)}$$

Where α_f and α_c are the recession coefficients, and $n_{eff\text{-}c}$ and $n_{eff\text{-}f}$ are the effective porosity of the conduits and fractures, respectively.

Following the same approach used by Fu et al*ii* (2016), it possible estimate the n_{eff} of the conduits and fractures starting from recession coefficients of two components (α_c and α_f) and the related effective porosity of one these:

$$n_{eff-c} \approx \frac{\alpha_f \times n_{eff-f}}{\alpha_c} \quad \textbf{(Eq.5.7)}$$

$$n_{eff-f} \approx \frac{\alpha_c \times n_{eff-c}}{\alpha_f} \quad \textbf{(Eq.5.8)}$$

Then the total effective porosity ($n_{eff\text{-}t}$) of the aquifer can be calculated by:

$$n_{eff\text{-}t} = n_{eff\text{-}c} + n_{eff\text{-}f} \quad \textbf{(Eq.5.9)}$$

Finally, integrating the segments of recession curve, related at quickflow (V_c, conduits drainage) and baseflow (V_f, fractures drainage) over the time, it was provided the water storage capacity of each components:

$$V_c = \int_0^{t_c} Q_c dt \quad \textbf{(Eq.10)}$$

$$V_f = \int_0^{t_f} Q_f dt \quad \textbf{(Eq.11)}$$

The sums of this terms (**Eq.5.10** and **Eq.5.11**) represents the water storage capacity, i.e. the maximum water drained by the aquifer (Amit et al., 2002; Farlin and Maloszewski, 2013; Tallaksen, 1995):

$$V_t = V_c + V_f \quad \textbf{(Eq.12)}$$

5.3.3. Structural analysis and measurement of effective porosity of fractures

Fractures in carbonate rocks have long been recognized as major features controlling fluid circulation and related karstic processes, particularly in the early phases of karstification (Fetter, 1980; Ford and Ewers, 1978; Palmer, 1991).

In general, when a fracture network forms the principal reservoir permeability and porosity, fluid flow patterns are largely controlled by fracture orientation, connectivity and aperture (Odling et al., 1999). In a carbonate rocks, it is knowing that secondary porosity, due to fractures, can also be strongly modified after diagenetic processes and karst phenomena (Agosta and Aydin, 2006; Aydin et al., 2010).

A network may have a hierarchical structure, with fractures confined within individual beds (Strata-Bound, SB), fractures crosscutting several beds (Non Strata-Bound, NSB) and other vertically persistent fractures dominating within given scale ranges (Strijker et al., 2012) (**Fig.5.4**).

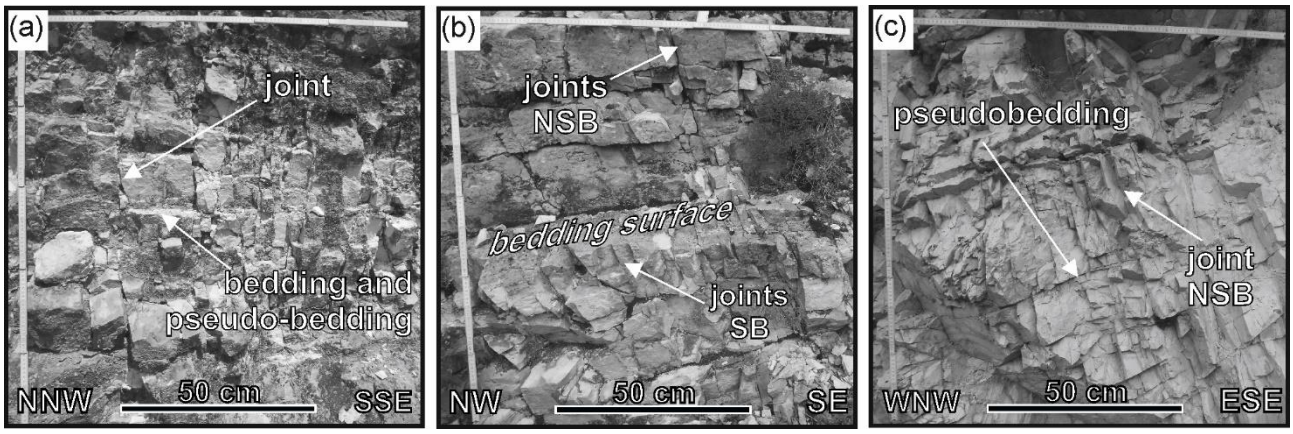

Fig.5.4. Example of 3 structural windows of Calcare Massiccio Fm. The area of each windows is 1 m^2. (a) W1 is located at north Sasso del Re; (b) W3 is located at north-west Sasso della Rocca; (c) W4 is located at Giordano basal spring. The joints marked with SB=stratabound and NSB=non-stratabound.

In order to define the development main directions of karst conduits and the geometrical properties of fractured rock mass, it was identified 8 structural windows at the studied area, having the same area of about 1 m^2 (**Fig.5.4**). In each window were analyzed all discontinuities present (sub-vertical joints and bedding/pseudobedding) from structural and geomechanics point of view. The parameters detected are as follow:

- number of set discontinuities and their orientations;
- number of fractures of each sets;
- average persistence of each sets;
- average aperture of each windows.

The spatial distribution of the main set of discontinuities gives important information on the probably development orientation of conduits network in basal aquifer.

The structural parameters as number of fractures, persistence and aperture give some information on fracturation degree and the associated karstified degree of entire rock mass.

Therefore, by combining these geometrical parameters can be calculated the ratio between the present voids on the surface and the surface area itself, i.e. “secondary porosity” of rock mass:

$$n_{eff-f} = \frac{\sum_{i=n}^{n}(N_i \times \overline{a_i} \times \overline{L_i})}{A} \quad \textbf{(Eq.5.13)}$$

Where N is the number of fractures of i-set, $\bar{a}$, average aperture of i-set, $\bar{L}$, average length of i-set and A, surface area of window outcrop.

5.4.Results

5.4.1. Characteristics of the hydrographs during the recession limbs using modified Maillet model

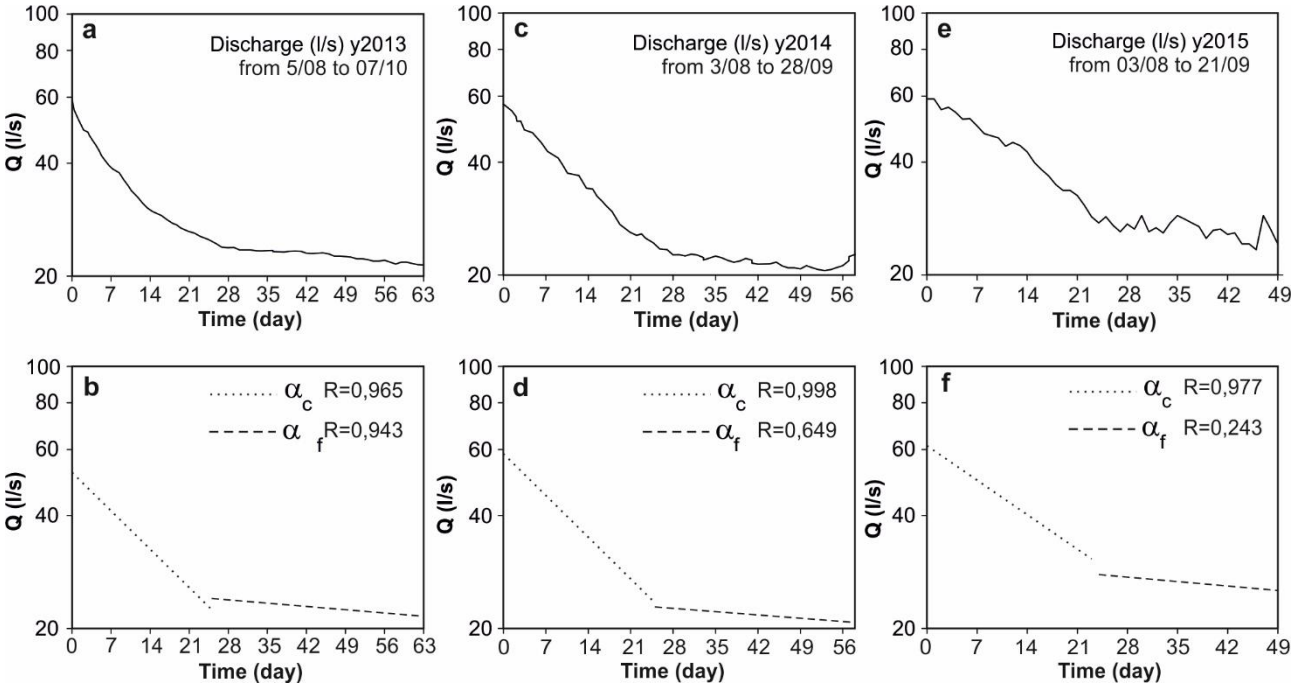

Fig.5.5. The daily discharge (solid line) in the recession limb on years 2013 (a), 2014 (c), 2015 (e) and their fitting recession curve (dashed lines) for quickflow (conduits) and baseflow (fractures) on years 2013 (b), 2014 (d) and 2015 (f), respectively.

Recession-curve analysis was conducted on records ranging from 3 years (from 2012 to 2015) of daily average discharge of Giordano karst spring (**Fig.5.5**).

Different shapes of the spring recession are attributed to drainage from different components of the groundwater system, reflecting karstification degree.

Base on **Eq.5.4**, have been identified two exponential term that represents the conduits flow (quickflow) and the fractures flow (baseflow).

The sum of exponents represents the depletion of a specific reservoir, where the hydraulic conductivity of the reservoir is proportional to α_i (Amit et al., 2002).

Accordingly, the exponential term with the largest slope, α_c, represents the rapid depletion of flow channels with the highest hydraulic conductivity.

The exponential term with the smallest slope, α_f, corresponds to the baseflow, i.e., to the slow depletion of the flow network with low hydraulic conductivity. In this case, the slope of baseflow may reflect a fractures network porosity.

The initial discharge of each components is $Q_{in\text{-}c}$ for the quickflow and $Q_{in\text{-}f}$ for the baseflow. Together with the exponential coefficients, α_c for the quickflow and α_f for the baseflow, these parameters provide a complete quantitative description of the discharge decay (**Tab.5.1**).

For the modified Maillet model, the α_f values derived from recession curves of fractures network range from 0,00314 (day^{-1}) to 0,00385 (day^{-1}), whereas the recession time of baseflow ranged from 26 to 37 days. The α_c values are an order of magnitude higher than depletion constant of baseflow; indeed, the exponential coefficients of conduits range from 0,0302 (day^{-1}) to 0,0344 (day^{-1}), during a recession time of about 25 days.

These observations imply that the geological environment and structural geometry are the decisive factors dictating the values of α_c and α_f, whereas the initial discharges, $Q_{in\text{-}c}$ and $Q_{in\text{-}f}$ depend on the amount of precipitation.

Tab.5.1. Parameters of the modified Maillet equation provided by recession analysis in the years 2013, 2014 and 2015.

Year	**$Q_{in\text{-}c}$ (l/s)**	**t_c (day)**	**α_c (day^{-1})**	**$Q_{in\text{-}f}$ (l/s)**	**t_f (day)**	**α_f (day^{-1})**
2013	59.04	27	3,33E-02	24.02	37	3,10E-03
2014	57.14	26	3,44E-02	23.91	33	3,85E-03
2015	61.24	23	3,02E-02	27.62	26	3,54E-03
Mean	**59.14**	**25**	**0,03263**	**25.18**	**32**	**0,00349**

The integrating of the recession curve allows calculating the amount of water drained through of Giordano from the beginning of the dry period. This it was estimated through the application of **Eq.5.10** at recession curves of conduits and fractures (**Tab.5.2**) to distinguish the water drained by the two components.

The volume discharged by Giordano karst spring during recession periods range from 161876 m^3 (in 2013) to 182624 m^3 (in 2012) in about 57 days. Volume discharged by conduits range from 50893 m^3 to 60007 m^3 during an average interval time of 25 days, whereas the volume discharged by fractures range from 110983 m^3 to 128678 m^3 in about 32 days.

The observed variations of total volume discharged during the time series can be related to amount of rainfall and temperature (that affect evapotranspiration), because they influence initial discharge (Q_{in}) at the beginning of recession curves.

Tab.5.2. The characteristic volume discharged by the conduits and fractures and their related percentage.

Types	Volume (m^3)	Percentage (%)
Conduit	53946	70,5
Fracture	128678	29,5
Total y2013	**182624**	**100**
Conduit	50893	68,6
Fracture	110983	31,4
Total y2014	**161876**	**100**
Conduit	60007	66,2
Fracture	117433	33,8
Total y2015	**177440**	**100**

5.4.2. Structural analysis of fractures

It was examined 8 structural stations to understand the relationship between the main sets of fracture and that of probably associated karst conduits in the same carbonate sequence, where we measured their orientation.

The collected data consist of a total of 280 joints and bedding/pseudobbedding planes in the Calcare Massiccio Formation. The contour-plot in **Fig.5.4a** show three main sets of joints oriented to N30, N130 and N290, and other secondary sets oriented to N180 and N330.

The bedding and pseudobedding planes are oriented to N225 and follow the cyclotems trend of carbonate sequence.

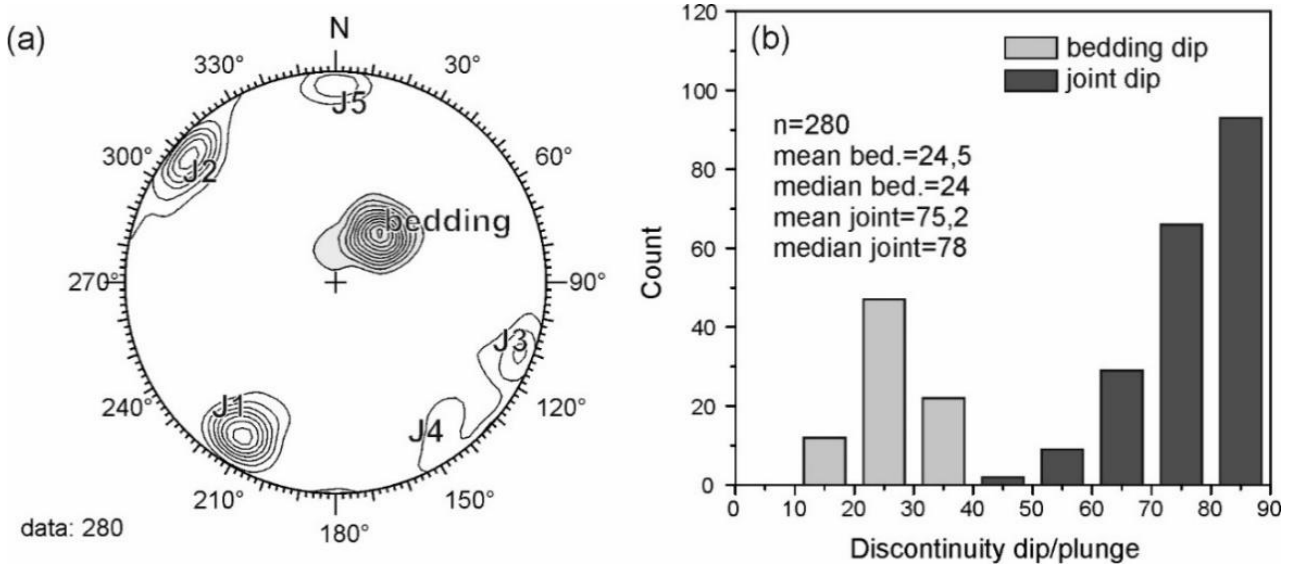

Fig.5.6. Structural characterization of all data collected in the 8 windows: (a) contour-plot of dip-direction of the 280 measured discontinuities in the all 8 structural windows (J1, J2 and J3 are the main sets, J4 and J5 are the secondary sets and the grey distribution represents the bedding planes); (b) histogram-plot of dip/plunge distribution. The color code refers to the following discontinuity sets: dark grey – bedding and pseudobedding, light gray – joints.

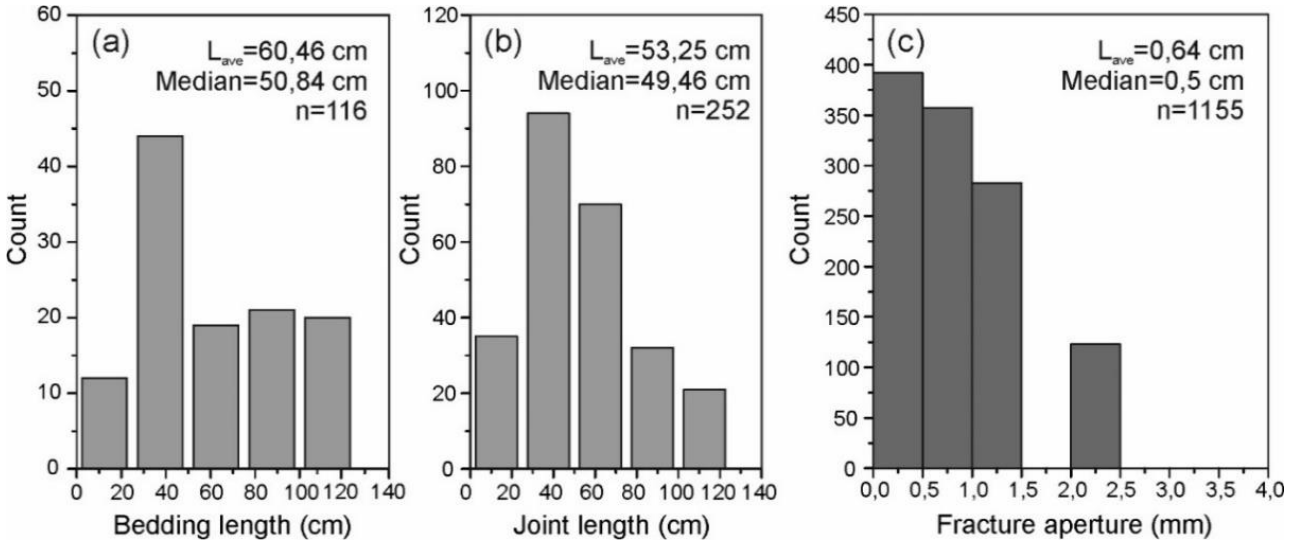

Fig.5.7. (a) Hisogram-plot of length distribution from all 8 structural windows; (b) histogram-plot of length distribution of joints; (c) histogram-plot of aperture sizes distribution of all discontinuities (bedding and joints).

The joint sets show a one trend with high values of dip (of about 85°), while the bedding and pseudobedding planes show a weak inclination with a main trend of 25° (see histogram-plot in **Fig.5.6b**). Therefore, sub-vertical joints and bedding and pseudobbedding planes occur approximately perpendicular each other.

The joints are characterized by their own spacing distribution, connectivity, aperture and, thus, hydraulic properties (Aydin, 2000).

The statistical analysis of fractures length shows a uniform distribution of entire data population (n=252); indeed, the mean value is 53,25 cm and the median value is 49,46 cm (**Fig.5.7b**).

The distribution of bedding length shows more open range of data (n=116), with an average value of 60,46 cm and a median value of 50,84 cm (**Fig.5.7a**).

The distribution of aperture sizes shows mean value of 0,64 mm, calculated on the statistical population of 1155 data (**Fig.5.7c**).

This statistical representation gives an idea on structural characteristics of discontinuities present in the rock mass analyzed in the whole karst basin.

In more detail, we analyzed the structural parameters distinguishing each joint sets and bedding/pseudobedding planes of each windows in order to define the secondary porosity of fractured rock mass (**Tab.5.3**).

Tab.5.3. Statistical results of geomechanic analysis of structural windows; are indicated the average length, no. of fractures and average aperture for each joint sets and bedding-planes.

Structural Windows	Length avg-Bed	Length avg-J1	Length avg-J2	n° fracture Bed	n° fracture J2	n° fracture J2	Aperture avg (cm)
W1	53,22	41,03	41,30	14	18	16	0,0878
W2	50,64	51	64,33	21	17	13	0,0502
W3	71,14	46,34	50,26	15	24	11	0,0733
W4	63,96	53,17	65,84	20	28	12	0,0291
W5	83,51	64,4	68,63	9	11	11	0,0504
W6	35,66	46,82	42,28	15	13	11	0,1181
W7	47,69	30,04	37,03	15	20	18	0,0726
W8	59,59	59,82	48,95	7	10	10	0,0758

5.4.3. The effective porosity of fracture and conduit using Fiorillo (2011) quantitative equation

The application of **Eq.5.13** using the geomechanics parameters detected has allowed to define the effective porosity at each structural windows (**Tab.5.4**).

The $\eta_{eff\text{-}bed}$ calculated range from 0,32% to 0,79%, (average value of 0,51%), whereas the $\eta_{eff\text{-}joint}$ range from a minimum of 0,66% to a maximum of 1,27% (average value of 0,96%), i.e. about twice the highest value of the bedding porosity. As a consequence, the total porosity of fractures ($\eta_{eff\text{-}f}$) was calculated by the sum of the two components ($\eta_{eff\text{-}bed}$ and $\eta_{eff\text{-}joint}$) and range from 1,04% to 2,01%, with a mean value of 1,49%.

Tab.5.4. Effective porosity of fractures calculated in each structural window.

Structural window	Bedding porosity (%)	Joint porosity (%)	Total porosity (%)
W1	0,52	0,92	1,44
W2	0,37	0,66	1,04
W3	0,38	0,74	1,12
W4	0,32	0,82	1,14
W5	0,63	1,27	1,90
W6	0,65	1,23	1,88
W7	0,53	0,86	1,39
W8	0,79	1,22	2,01

Base on quantitative relationship provide by Fiorillo (2011, 2014) between recession coefficient (α_i) and the effective porosity (η_{eff}) (**Eq.5.6** and **Eq.5.7**) we used the mean values of fracture porosity ($\eta_{eff\text{-}f}$ =1,49%) to estimate the effective porosity of conduit ($\eta_{eff\text{-}c}$) and the total porosity, $\eta_{eff\text{-}tot}$ (**Tab.5.4**).

Then, the $\eta_{eff\text{-}c}$ calculated give a constant value in the years of about 0,16% respect to 1,49% of fractures, for a total of 1,65%.

Tab.5.5. Effective porosity of conduits and total.

Year	n_{eff-f} (%)	n_{eff-c} (%)	$n_{eff-tot}$ (%)
2013	1,49	0,14	1,63
2014	1,49	0,17	1,66
2015	1,49	0,17	1,65

5.5.Discussion

Applying the modified equation of Maillet (**Eq.5.4**) at recession curves of Giordano karst spring (Northern Apennine) from data set January 2012 to 30 September 2015, it was possible obtain a structural characterization of aquifer; in fact, the depletion coefficients in quickflow sub-regime condition represent the conduits network drainage, whereas the depletion coefficients estimated in baseflow sub-regime condition are related to fractures network and matrix drainage.

Each exponential term, in a recession curve that comprises a sum of exponents, represents the depletion of a specific reservoir, where the hydraulic conductivity of the reservoir is proportional to α_i (Tallaksen, 1995).

Analysis of recession limbs show how the conduits coefficient are an order higher than fractures coefficient. Indeed, during the first segment it has been recorded an average value (α_c) of 0,03263 day^{-1} for an interval time of about 25 days, whereas during the second segment it has been recorded an average value (α_c) of 0,00349 day^{-1} that's remains constant for about 32 days.

Accordingly, the exponential term with the largest slope, α_2, represents the rapid depletion of flow channels or conduits with the highest hydraulic conductivity. The largest α-value is probably a measure of the degree of fracturing and intrakarst connectivity. The exponential term with the smallest slope, α_1, corresponds to the baseflow, i.e., to the slow depletion of the flow in fracture network with low hydraulic conductivity (Amit et al., 2002).

In the **Tab.5.1** it is shown as the characteristic parameters of the system remain fairly constant over the years. In fact, the recession coefficients related at different sub-regimes preserve about the same magnitudes independently from hydrological annual trends variations. These values depend by clear hierarchical geometry, connectivity and sizes of conduits and fractures networks, confirming as the karst system is well defined from a structural point of view and hydrogeologically closed.

To estimate of total spring storage volumes and individual contribution of the quickflow (conduits) and baseflow (fractures) components has been applied the **Eq.5.12** in order to define a quantitative description of recession curves. During the recession periods, the Giordano karst spring discharge by conduits and fractures a mean annual volume of 55 10^3 m^3 and 120 10^3 m^3 of water, respectively.

Tab.5.6. Average values of characteristics parameters of the karst aquifer.

Types	**Avg volume (m^3)**	**Percentage (%)**	**Avg porosity η_{eff} (%)**	**Percentage (%)**	**Saturated water storage (mm)**
Conduits	54948	31,6	0,16	9,7	680,2
Fractures	119032	68,4	1,49	90,3	6332,3
Total	**173980**	**100**	**1,65**	**100**	**7012,5**

In order to define the geometry of fracture networks and the probably structure and organization of conduits of karst aquifer was conduced a structural-geological survey. The results show that the fractured rock masses is characterized by three main sets of joints oriented to N130, N30 and N290, whereas the bedding planes and the associated pseudobedding is oriented about to N225.

Structural analysis of dip discontinuities shows high values of inclination of joint sets (75°-85°) and weak values associated at bedding planes (about 20°). This suggest that the joints and fractures can quickly conveyed the infiltration water toward the deeper areas of aquifer, whereas the bedding planes forces parallel-to-the-ridge circulation, slowing down and stratifying the flow at various levels. This mechanism can lead an increase of karstification degree from top to bottom of the fracture surfaces related at the increase of hydraulic head, until reaching to their evolution in real conduits in the basal aquifer.

Plotting all data of the dip-direction as strike directions in a rose diagram (**Fig.5.8a**), the main lineations are oriented to NW-SE and SW-NE. These directions represent the main development orientations of karst conduits in the basal aquifer. In particular, the direction NW-SE includes one of the main set of joints and the stratification toward the Giordano spring.

Total porosity calculated in the studied area measure about 1,65% and suggest a general low karstification degree of entire rock mass. This value represents the sum of two components related at fractures effective porosity (η_{eff-f}) and conduits effective porosity (η_{eff-c}), which measure 1,49% and 0,16% respectively. Therefore, the 90,3% of total porosity is attributed at fractured rock mass and the remaining 9,7% is gives at the conduits, with a ratio between two components of about 0,1.

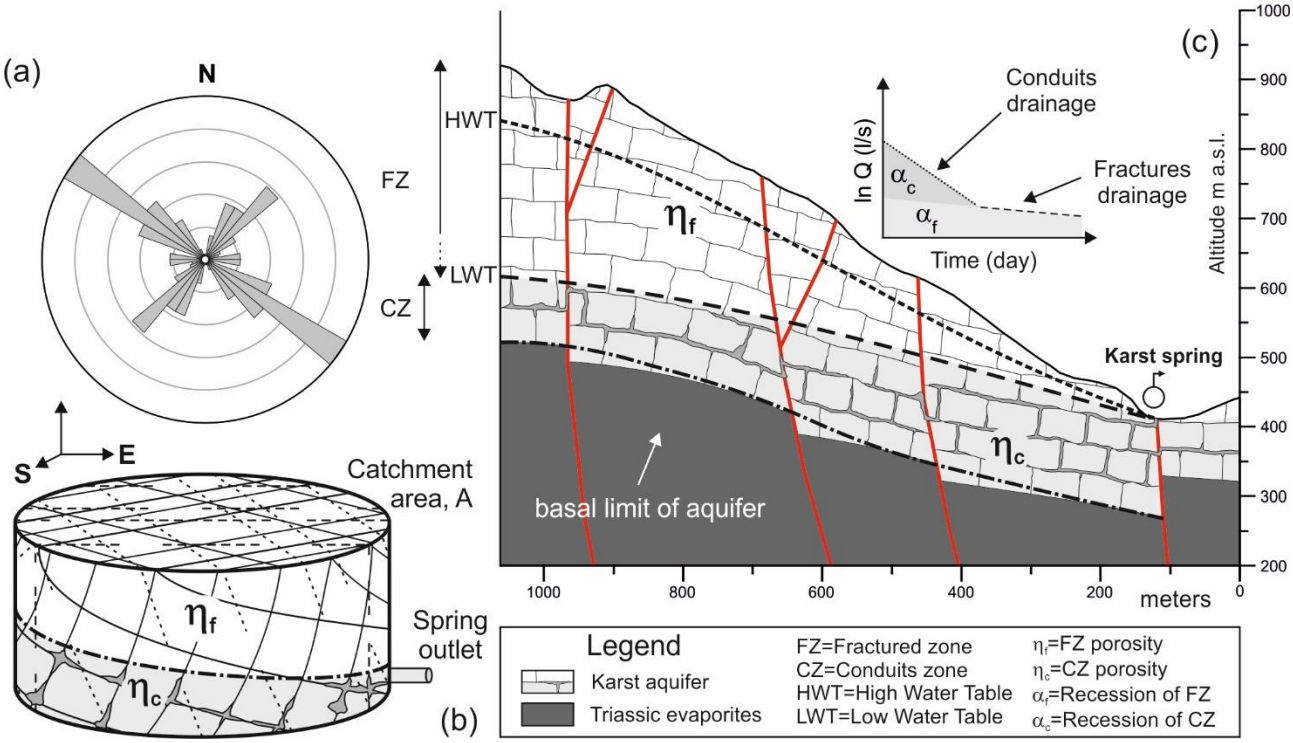

Fig.5.8. Conceptual model of karst aquifer: (a) rose diagram of strike-direction of the 280 measured fractures in the all 8 structural windows; (b) cylindrical model of reservoir with different effective porosity (FZ porosity and CZ porosity); (c) hydrogeological cross-section of a karst aquifer with the associated recession coefficients which reflects the hydraulic characteristics of the FZ and CZ, respectively. The different stages of the water table (HWT and LWT) were reported with exaggerated slopes.

From the point of view of quantitative volume discharged, the ratio between two components, calculated in time series, shows that the 68,4% of total water volume (average of 170 10^3 m^3) is discharged by fractures and the remaining 31,6% is discharged by conduits (**Tab.5.6**).

To define a water storage model associated at fractures and conduits system, we considered the aquifer as a tank-reservoir similar to that proposed by Fiorillo (2011); the model is characterized by a cylinder with an equal area (A) of the karst basin (3,9 km^2) and a height (h) equal at the T_a (average thickness of aquifer).

When the aquifer is completely saturated, i.e. all the effective porosities are filled with water, the water storage of the aquifer can be estimated by multiplying aquifer thickness and the total effective porosity, $\eta_{eff\text{-}tot}$ (Fu et al., 2015). In present work, there is not found any aquifuge in the aquifer above the outlet (**Fig.5.8c**); thus, the assumption is made that the discharge from the outlet reflects the characteristics of the aquifer above the spring outlet.

The thickness of aquifer (T_{aq}) can be calculated by mathematical difference between average topographic elevation measured along the cross-section showed in **Fig.5.8c** and the elevation of Giordano spring outlet. The average topographic elevation is about 1075 m and the elevation of spring outlet is 650 m. Then, the average thickness (T_{aq}) is about 425 m and the total porosity ($\eta_{eff\text{-}tot}$)

measure 1,65%. Therefore, the saturated water storage estimated is 680,2 mm for the conduits, 6332,3 mm for the fractures and 7012,5 mm for the total aquifer (**Tab.5.6**).

The average effective infiltration calculated in the interval time (from January 2013 to 30 September 2015) is 989,5 mm/y (about 30 l/s for km^2) according to Bison et al*ii* (1995). This means that the maximum water that aquifer can store is about two times of the average effective infiltration of about 3859 mm/y estimated on the entire karst basin.

5.6.Conclusion

The present paper describes a quantitative methodology to characterize and combine the ological properties and internal structure of a karst aquifer from hydrograph analysis and structural survey.

In this study, to evaluate a spring discharge it was used the modified equation of Maillet, because the aquifer can be clearly divided into two hydraulic conductivity components (the matrix component can be neglected), each of which drained water followed an exponential formula: quickflow linked to conduit discharge and baseflow linked to fractures discharge. The first term is a one order of magnitude higher than the fractures components, and discharge 31,6% of total volume in about 25 days, during the recession period. Therefore, fractures component controls the flow mechanism with remaining 68,4% of volume discharged during a mean value of 32 days. This indicate that fractures are well developed and well interconnected to accommodate about 40% of volume discharged by conduits domain.

For basal spring, the hydraulic behavior has been explained by the model of Fiorillo (2011), who point out how the ratio between two different values of the recession coefficient obtained by the semi-logarithmic plot can be approximated to the inverse ratio of the effective porosity computed along the surface of the water table ($\alpha^I/\alpha^{II} \approx n_{eff}^{II}/n_{eff}^{I}$).

The combination of spring hydrograph analysis and structural characterization of discontinuities provide information on hydraulic properties of karst system and conduit network geometry.).

The effective porosity of fractures, resulting 1.49%, whereas the effective porosity of conduits is about 0,16%, for a total value of a 1.65%. This value is included between range values estimated by Bonacci (1993), of 0,1-1%, and range values estimated by Delbart et al*ii* (2014), of about 2-7%. Thus, 90,3% of total porosity is attributed at fractures and 9,7% remaining is gives at conduits. This percentage value attributed at conduit porosity results much higher than literature values; indeed, Fu et al*ii* (2016) estimated about 2%. This suggest that the conduits are large enough and well interconnected each other, but with poorly branched network and arranged in a few systems. Therefore, it is supposed that the conduits domain is probably localized at more basal portions of the aquifer (approximately at the same height of spring outlet).

The main directions of discontinuities (joints and bedding planes) are oriented at NW-SE and SW-NE. These directions represent the main development orientations of karst conduits in the basal aquifer. In particular, the direction NW-SE includes one of the main set of joints and the stratification planes. Therefore, it is very likely that the conduits have developed in the points where the joints and beddings, with the same strike-direction, were crossed against. In addition, the structure of the basal aquifer can give an echelon shapes, with sub-vertical wells (dip 75°-85°) associated to main joint sets connect at sub-horizontal plans (20°) associated to bedding dips.

Finally, the saturated water storage estimated indicate that the karst system has a high potential for water supply and it is attributed at storage capacity of fractures and at their slowly release on time.

Fig.5.9. Panoramic view of Giordano karst basin in the SW limb of Mt Nerone anticline.

6. Groundwater temperature as natural tracers to characterize hydraulic behaviour and geometry of a carbonate aquifers: M. Nerone karst system, central Italy

Abstract

Temperature variations in groundwater discharge from the Giordano karst system (northern Apennines) have been observed continuously for six months (from January 2016 to July 2016), in order to determine the flow patterns and geometrical properties of aquifer. The karst system discharge about 32.2 L/s on average during over the hydrological year and it's characterized by two outlets: a basal-continuous spring (BCS) with a mean discharge of 8.9 L/s and an upper-intermittent spring (UIS) with a mean discharge of 23.3 L/s, located about 60 m above the previous one.

Results show significant difference in the two spring outlets between the time lags as well as non-simultaneous and not analogue responses of temperature (T) to the same recharge events: temperature of UIS range from 9.7 to 10.7°C whereas temperature of BCS remain rather stable, ranging from 9.8 to 9.9°C. This data suggests a stratification of the water along the aquifer probably associated by different residence times and linked to the structural organisation of karst aquifer (conduit and fracture networks): deeper and oldest water in the basal-continuous springs and youngest water in the upper-intermittent spring.

6.1. Introduction

Groundwater physical and geochemical parameters are widely used as natural tracer in hydrogeological investigations. Seasonal and daily water temperature variations of karst springs permit to characterize different flow types and the structural organization of drainage patterns (Roy and Benderitter, 1986; Birk et al., 2004).

Several processes may affect water temperature during seepage, such as heat exchange, mainly by conduction, with the reservoir host rock mass; advection exchange into or out the groundwater mass and heating and cooling in the undergrounds karst conduits where the convective exchanges with air are important (Martin and Dean, 1999; Convington et al., 2011).

The discharge of a karst spring generally responds much quicker to recharge events than the physicochemical properties of the discharged water, such as temperature. The increase in hydraulic pressure due to recharge is almost instantaneously transmitted through phreatic (water-filled) conduits to the spring, while the fluid properties change only after the actual recharge water reaches the spring (Birk et al., 2004). In this way, the lag between the hydraulic and physico-chemical responses time corresponds to the physical path of the infiltrating water through the conduit system can be estimated when the spring discharge is known (Sauter, 1992; Rayn and Meiman, 1996).

Time-series analysis is a robust method to investigate in karst hydrogeology and cross-correlation functions (CCF) are widely used to analyse the linear relationship between input (rainfall or snowmelt

- P) and output (discharge or temperature variations). This relationship can be analysed with the equation (Padilla and Pulido-Bosch, 1995).

For $k > 0$,

$$C_{xy}(k) = \frac{1}{n}\sum_{t=1}^{n-k}(x_t - \bar{x})\,(y_{t+k} - \bar{y}) \qquad \textbf{(Eq.6.1)}$$

$$r_{xy}(k) = \frac{C_{xy(k)}}{\sigma_x \sigma_y} \qquad \textbf{(Eq.6.2)}$$

where the k is the time lag; n is the length of time series; x_t and y_t are input and output time series, respectively; $r_{xy}(k)$ is the cross-correlation function; σ_x and σ_y are the standard deviations of the time series and $C_{xy}(k)$ is the cross-correlogram (Box et al., 1994). The delay, which is the time lag between lag 0 and the lag of the maximum value of the cross-correlation coefficient ($r_{xy}(k)$), gives an estimation of the pressure pulse transfer times thorough the aquifer (Panagopoulos and Lambrakis, 2006).

The objectives of this study are: (1) to investigate temporal relationships between karst spring discharge and water temperature; (2) to compare the different residence time of two spring outlets belonging to the same karst system; and (3) to define the structural organisation of karst aquifer.

6.2. Geological and hydrogeological setting

The study area is located in the norther sector of Umbria-Marche Apennines in the SW flank of Mt. Nerone (1525 a.s.l.) an asymmetric NE verging anticline with the axe strike NW-SE, part of a fold-and-thrust belt. The investigated karst system developed in a carbonate massif of Ceno-Mesozoic Formations from the Calcare Massiccio Fm. (Hettangian-Carixian), Bugarone Fm. (Upper Toarcian-Lower Tithonian) to the Maiolica Fm. (Upper Tithonian-Lower Aptian), which is heavily fractured and faulted. This carbonate reservoir is confined by a basal level of Triassic evaportites and Fucoidi Marls on the top. The total thickness of the karst reservoir is about 1000 m where about 800 m pertains to the Calcare Massiccio Fm., which represents the regional basal aquifer of the Umbria Marche Apennines with an average discharge of about 30 L/sec/km^2 (Boni et al., 1986).

The karst block seems to be limited by a structural depression of the Pieia valley where the fractures and beddings discontinuities constitute the structures that control the drainage.

The Giordano karst system drains a basin of about 3.8 km^2 (Tamburini, 2016) where a discharge of about 40 L/sec are collected and diverted by Marche Multiservizi to supply villages and town. The karst system is characterized by two main spring outlet: a basal-continuous spring (BCS) located at 535 m a.s.l. and an upper-intermittent spring (UIS) located about 65 m above the previous one

(**Fig.6.3**). Several linear springs are located along the stream as linear spring partially intercepted by shallows wells.

6.3. Data collection

Discharges and groundwater temperature were monitored simultaneously at basal-continuous spring (BCS) and upper-intermittent spring (UIS). Discharges data are provided by an automatic collecting system that records continuously the daily values of the hydrographic level in a discharge gauge. Groundwater temperature is measured automatically using waterproof commercial temperature loggers manufactured by Onset Computer Corporation installed within both of outlets. The loggers have temperature and response time accuracies of 0.1°C and 0.01% respectively. Between January and July 2016, the temperature loggers measured temperature every 15 minutes, in order to identify also the rapid response to rainfall events. Daily mean values of precipitation were monitored by a gauge station located near to study area.

6.4. Results and discussion

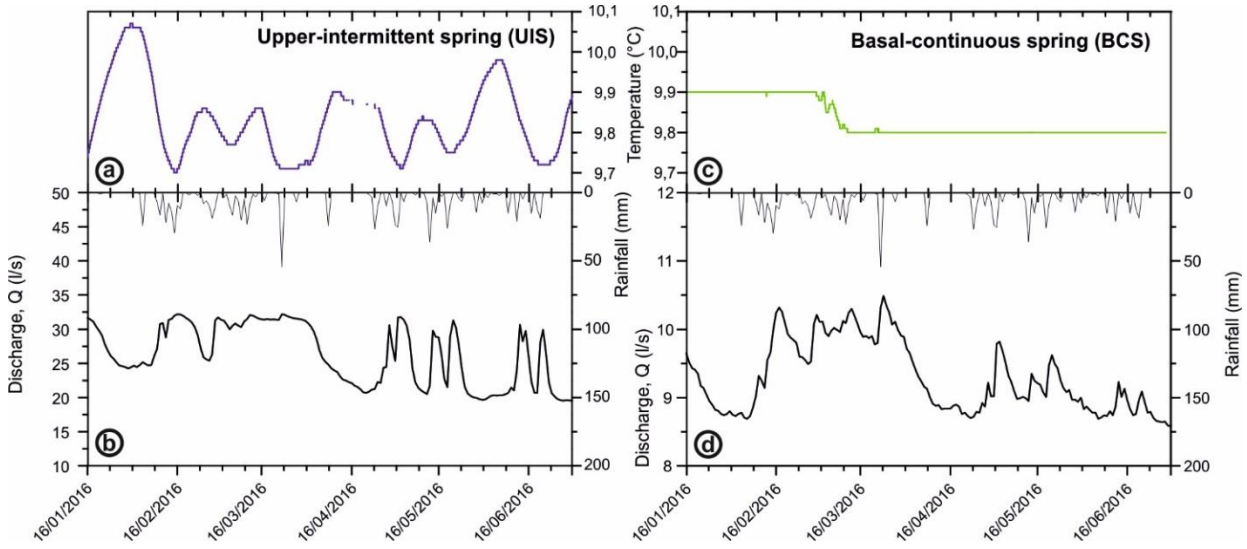

Fig.6.1. Results of discharges (b and d), groundwater temperature (a and c) and rainfall events (b and d) monitored in the upper-intermittent spring (UIS) and basal-continuous spring (BCS) for six months (between 16/01 to 30/06/2016).

Water temperature and discharge recorded at upper-intermittent spring (UIS) and basal-continuous spring (BCS) in the first half of 2016 are related to the rainfall events, show two different behaviours both in the discharge rate and in the groundwater temperature trend (**Fig.6.1**).

UIS show a higher discharge than BCS with a mean of 23.3 L/s and a rapid response to precipitation episodes (**Fig.6.1b**). In the same way, also groundwater temperature of UIS vary frequently from a minimum of 9.7°C to a maximum of 10.7°C; moreover, decreasing rapidly during rainfall episodes with a varying magnitudes (**Fig.6.1a**).

On the other side, BCS discharging a mean of 8.3 L/s and exerting a slow response in the discharge rate, displaying a maximum difference varying between 5.62 to 10.49 L/s (**Fig.6.1d**). Even from the physicochemical point of view this spring outlet shows an opposite behaviour than UIS; in fact, groundwater temperature remains rather stable and is not affected by rainfall events, showing only one step between March 07th and 12rd, where water temperature decrease of 0.1°C, passing from 9.9 to 9.8°C (**Fig.6.1c**). This step, also if in the range of the instrumental error, could be interpreted as result of rapid and concentrated infiltration in the recharge area, generating a general cooling of the basal reservoir.

On the other hand, these results give some indications both on residence (or transit) time of recharge water in the aquifer and on structural organisation of karst system. In UIS, the rapid response of water temperature at recharge events indicates a short transit time of youngest water infiltration, which is quickly drained by conduits systems with high hydraulic conductivity. On the contrary, BCS show a long residence time of groundwater, indicating a deeper and oldest water located in the basal portion of aquifer and characterized by a low hydraulic conductivity.

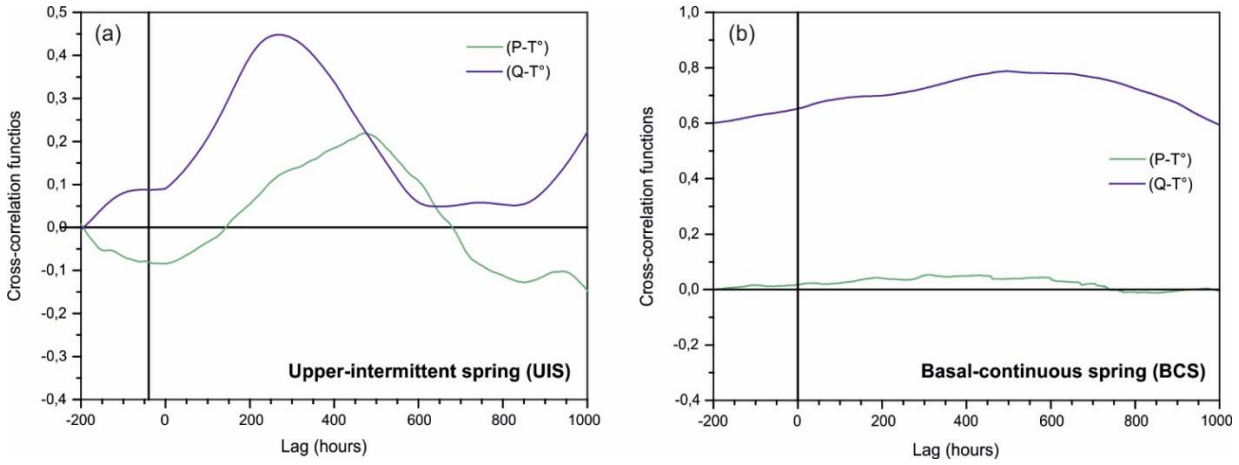

Fig.6.2. Cross-correlation functions of upper-intermittent spring (a) and basal-continuous spring (b); blue lines indicate the precipitations (P) and water temperature (T°) functions, green lines indicate the discharges (Q) and water temperature (T°) functions.

A cross-correlations analysis of precipitation and discharges with the groundwater temperature for UIS and BCS (**Fig.6.2**) confirm the opposite hydrodynamic behaviour of the karst system studied.

Groundwater temperature of UIS present the maximum coefficients r_k of 0.2 (gray line in **Fig.6.2a**), indicating that the input signal from precipitation is significantly reduced during its passage through the system. On other hand, the function shows a rapid response, expressed by the sharp peak, having a time lag of 472 hours (about 19 days). CCF of discharge and groundwater temperature (Q-T°) of UIS are well correlated (r_k=0.45), showing a rapid decrease and a time lag of 269 hours (11 days) (blue line in **Fig.6.2a**). This indicates the existence of quickflow component that regulate the

discharge in UIS, probably connected to conduits network drainage during high-water table condition (HWT).

Cross-correlation function between precipitation and groundwater temperature (P-T°) in the basal-continuous spring (BCS) show a maximum coefficient of r_k=0.05, indicating non-correlation between rainfall and water temperature in this portion of aquifer (green line in **Fig.6.2b**). Indeed, the correlation functions between discharge-groundwater temperature (Q-T°) decrease very slowly after a maximum peak of 0.78 and a time lag of 496 hours (about 21 days) (blue line in **Fig.6.2b**). This slow response of water temperature at the variation of discharge rate indicates the baseflow component, probably linked to fracture networks drainage during the lower water table condition (LWT).

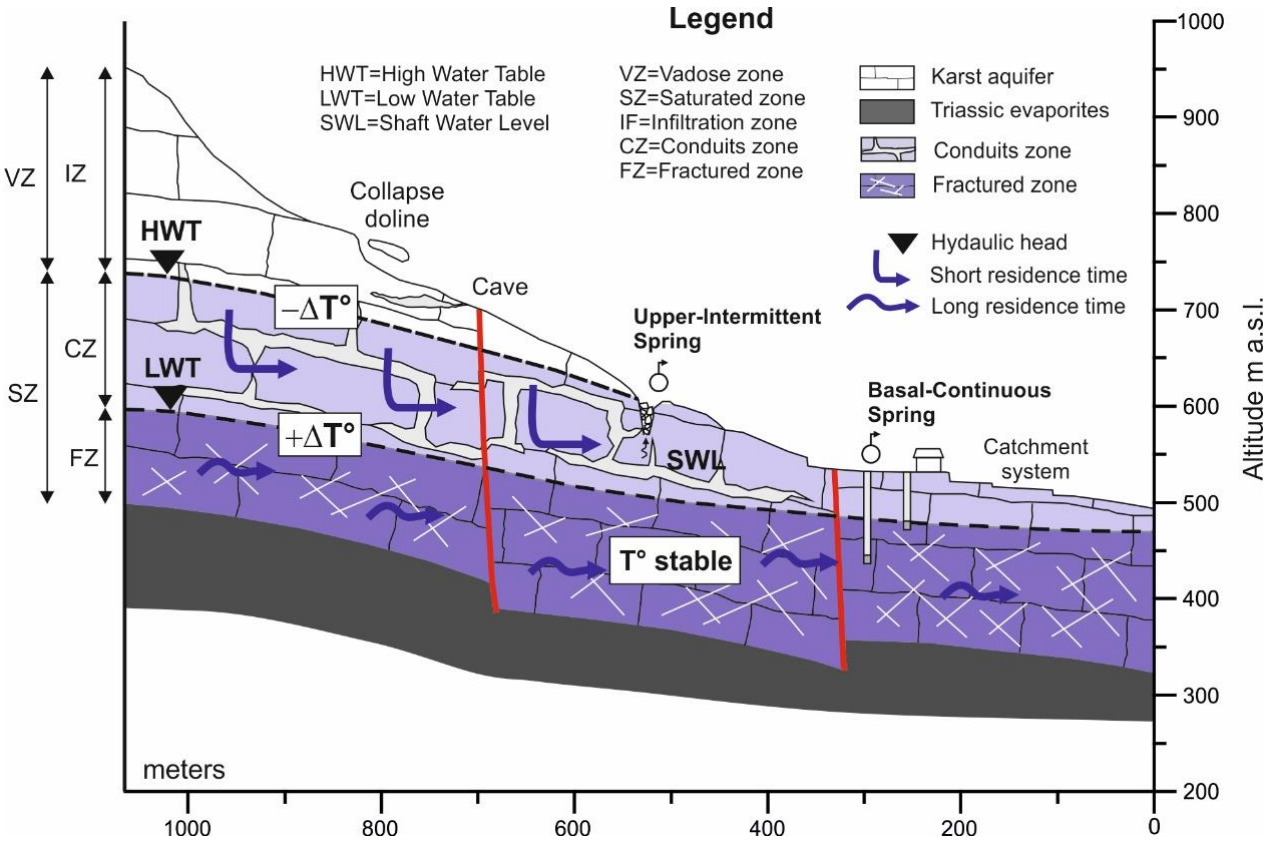

Fig.6.3. Simplified aquifer model during high and low water table condition. Main fractured and conduit zone are also indicating.

6.5. Conclusion

Analysis of the temperature variations of groundwater drained by the UIS and BSC, enables us to make a qualitative analysis of the development of the karstic drainage pattern and the structural organisation of aquifer. Groundwater of two karst outlets record the same mean temperature of 9.9°C but do not present also the same behaviour during the rainfall events. This evidence the distinctive degree of karstification in the carbonate massif, which enables a partial mixing of the groundwater stored in the aquifers with infiltration or "new" and "colder" rainwater.

Indeed, the UIS display higher variations in groundwater temperature showing several peaks of different magnitude and a rapid response after the recharge events (19 days). These data are interpreted as the consequence of high velocity (short residence time) probably linked to water coming from infiltration zone (IZ) that is quickly drained by conduits zone (CZ) until the upper-intermittent spring (**Fig.6.3**).

On the contrary, groundwater of BCS show a stable trend of temperature and a no-correlation with the recharge events, which means a long residence time localized in the basal portion of aquifer. The results indicate that the quickflow component is absent and the drainage is under the "diffuse flow" behaviour (baseflow condition), probably due to high fracturation and poor karstification (fractured zone, FZ).

The degree of karstification influences the flow-path length, water velocity and heat exchange (Anderson, 2005). After a recharge events the karst system reaches a HWT condition and the flow path is relatively short. Hence the heat exchange is low and the groundwater temperature is lower (9.7°C).

During the dry periods the water table decrease and the karst system reaches the LWT condition, indicating a longer flow path. In this case, a favourable heat exchange with higher groundwater temperature (10.1°C).

The fact that the outlets of the same carbonate massif display different responses to the same input highlights differences in the degree of karstification of its aquifer systems and consequently in their hydrogeological behaviour (Líñán Baena et al., 2009).

The trend of groundwater temperature in the two spring outlets seem to indicate a different storage geometry of water linked to structural organisation of karst system: basal aquifer characterized by high fracturation (FZ) and a conduit zone characterized by a well-developed karst network.

Finally, interpretation of groundwater temperature records of a karstic system provides supplemental information about groundwater circulation, drainage components and on the structural organisation of an aquifer, giving results coherent with other techniques used in hydrogeological investigations.

7. General conclusion and outlook

Karst aquifers are often characterised by a rapid and strong response to hydrological events, such as storm rainfall and snowmelt.

There are two and sometimes three types of porosity in a karst aquifer: intergranular pores, fractures, and conduits. The existence of conduits is the big difference and the big problem compared with other aquifer types, which only contain intergranular pores and/or fractures (Ford and Williams, 2007).

Consequently, all karst hydrogeological studies need to consider the conduits. Speleological surveys make it possible to directly observe water flow in caves, but accessible caves are not always present and in any case, only represent a fraction of the total conduit network, mostly the inactive part.

The Apennine chain of central Italy is a mountain range characterized by the presence of extensive outcrops of thick Mesozoic limestone sequences. Above the Triassic evaporitic level can be recognize three superimposed aquifers, having a different permeabilities due mainly to fissures, joints and karst conduits (Boni et al., 1986; Nanni and Vivalda, 2005; Boni and Petitta, 2007, 2008). Starting from the bottom can be found the basal aquifer of Calcare Massiccio complex, the middle aquifer of Maiolica complex and the upper aquifer of Scaglia complex. In this research has been taken into account only Calcare Massiccio and Maiolica Formations, as they represent the most important hydrogeological complex in the Apennine ridge, where occurs the regional flow through very-well developed fissures and karst conduits. In particular, have been analysed several hydrostructures of Umbria-Marche Apennines and their associated karst springs.

In the study area, carbonatic lithotypes covered about the 67% of the considered hydrostructures, of which only the 4.3% is represented by the Massiccio complex (Baq), and 28.8% by the Maiolica complex (Maq). The sub-basins associated to a karst springs showing recharge areas rather small (from 5 km^2 to 11.5 km^2) and the percentage values of outcropping complexes points out as the karst systems in the Umbria-Marche Apennines are controlled by water circulation in the Maiolica and Calcare Massiccio complexes, which are very often hydraulically connected by faults systems or by the lack of Jurassic aquicludes.

The comparison between the effective infiltration and effective rainfall reveals different results. Some karst systems analysed (Scirca, Boschetto and Capo d'acqua) show a good correspondence between the two parameters, indicating the correctness of the evaluations. Hence, these sub-basins can be considered hydrogeologically closed.

On the other hand, the values of effective infiltration in Vaccara and Bagnara karst systems are higher than effective rainfall estimated in the hydrological budget. Probably, this gap is linked to the non-correspondence between the weather stations altitude and the average altitude of sub-basins considered. Furthermore, the effective infiltration of San Giovenale sub-basin is much higher than

effective rainfall estimated in the hydrological budget, implying a not inconsiderable underground feeding from other sectors outside the present hydrostructure. In this case, the groundwater surplus comes from the karst planes of Colfiorito, which is considered as a high infiltration area, since rainwater is collected by the plain, retained at the surface by the low-permeability fluvio-lacustrine complex and channelled by surface runoff towards karst swallow-holes (Mastrorillo et al., 2009).

Therefore, the lack of a rather large network of weather station do not afford a reliable assessment of some recharge area and especially of its effective rainfall estimation. Hence, it is preferable to refer at the effective infiltration values estimated with the direct method of Boni et al*ii* (1986), except of San Giovenale karst basin which does not represent a closed hydrogeological system.

From structural point of view, the hinge zones of the anticlines have a hydrological control, on the groundwater flow, delineating a regional watershed along the Umbria-Marche ridge (*Chapter 2*).

Karst aquifer are highly complex hydrogeological systems. They evolve with time as the CO^2 in the flowing water dissolves the carbonate rock, enlarging a proportion of the initial fractures into conduits and caves. Hence, the orientation and extension of the flow system and conduit network may change with time, making a karst aquifer not unchanging and characterized by a strong spatial heterogeneity (Kovàcs and Perrochet, 2008).

The karst aquifers analysed simulate the drainage as a linear reservoir condition where the discharge follow the exponential form of modified equation of Maillet, though not all systems show the same structural properties.

From the results of recession analysis and time series analysis show two type of aquifers: karst aquifer having a bimodal behaviour and karst aquifer having unimodal behaviour during the depletion periods. The first systems are characterized by two hydrodynamic sub-regimes, where the fracture networks and microfissures (rock matrix) control the slow drainage (baseflow sub-regime) with a recession coefficient of about 10^{-3}, and conduit networks control the fast drainage (quickflow sub-regime) with a recession coefficient of one order of magnitude lower than that of the matrix. This indicate a certain karstification degree (3.7-4 in accord to classification of Malík and Vojtková, 2012), in which a conduit networks of limited extent characterized by few interconnected systems and surrounded by a fractured rock mass irregularly developed with fissures rather opened. These karst aquifers are characterized by the hydrostratigraphic contact between Maiolica and Calcare Massiccio complex (*Chapter 4*). Analysis of hydraulic behaviour of an isolated karst system, having the same geological and hydrogeological characteristics of the previous ones (Giordano karst basin in SW limb of Mt Nerone anticline), confirm the existence of this duality during the recession period. This behaviour is explained better by the model of Fiorillo (2011, 2014), who approximate the aquifer to

the composite reservoir, where the ratio between two different values of the recession coefficients can be related to the inverse of the effective porosity computed along the surface of the water table.
The effective porosity of fractures, measured with a structural and geomechanics methods, results 1.49% whereas the effective porosity of conduits network is about 0.16%. This results, imply as about 90% of total porosity is attributed at fractures porosity and the remaining 10% is gives at conduits networks.
On the other hand, karst systems with unimodal behaviour show a single exponential flow component with low values of recession coefficient and is easily understandable because the groundwater circulation happens only within the Maiolica complex, where the karst is scarcely developed and the water moves through a fracture networks (*Chapter 5*).
The time-series analysis (auto-correlation and cross-correlation functions) give approximately the same results of recession analysis, showing a steep slope in short time-lag (2-13 days) followed by a gentle slope in bimodal systems, and a quite uniform decrease with high values of delay times in unimodal systems.
These differences can be attributed to structural and geological settings of a single hydrostructures that reflects the different components of groundwater systems (Bonacci, 1993).
The hydrostructures characterized by the Maiolica complex present a high fracturation degree and a rock mass slightly karstified, controlling mostly the infiltration and percolation processes. Here, groundwater circulation happens within fracture network and the discharge is dominated by baseflow sub-regime, with a Darcian flow, making hiring a unimodal behaviour at the reservoir.
On the other hand, the aquifers that involving Massiccio complex present a higher karstification degree, through which regulate the water circulation with different flow components (or sub-regimes): a quickflow linked to conduit networks and a baseflow linked to fracture networks and rock matrix. In particular, the recession coefficients of this complex show a conduits networks rather developed, especially in the deeper zones of aquifers (*Chapter 4*). The case of Giordano karst basin suggest that the conduits are large enough and well interconnected each other, but with poorly branched network and arranged in a few systems. Moreover, the water volumes discharged by the two sub-regimes (quickflow and baseflow) show how the fractures network empties about the 70% of the total volume during the recession period, while the remaining 30% is emptied through conduits network.
Fractures networks exert a strong control on fluid circulation through water aquifers, and spatial heterogeneity reflect an irregular distribution of groundwater flow pathways.
The structural analysis shows two main joint sets, oriented at SE-NW (N115°) and NNE-SSW (N20°), and other secondary sets orientated at N220°, N345° and N70°N115° and N20°. These sets constitute

the main pathways that water make from its entry into the aquifer-system (infiltration), reaching the outlet (spring). Probably, this is guaranteed by the high persistence values of fractures (from 0.6 to 4.4 m), penetrating both bedding planes that other secondary sets present in rock mass.

On the other hand, the secondary joint sets detected show a great fracture intensity (low fracture spacing); this is an important characteristic for water-storage of an aquifer system (*Chapter 5*).

The results of DFN models corroborate this interpretation, showing as the fracture systems are made of two main orthogonal fracture sets and other secondary sets, having different structural and hydraulic properties. So, the principal direction of fracture flow is mainly controlled by the dominant systematic joints.

The DFN models have pointed out a difference of hydraulic properties between Calcare Massiccio Formations. In fact, the basal aquifer shows a fracture porosity much greater respect to Maiolica complex (4.3and 1.7 %, respectively), and also the permeability values result well correlated with this trend. Furthermore, the greatest permeability component corresponds to the vertical one, kzz, for both formations analysed. This is probably correlated with the greater vertical connectivity of facture networks than the horizontal one, guaranteed by the high fracture intensity (fracture per meter) and by a generally high dip of joint sets (on average about 85°) (*Chapter 3*).

Finally, monitoring of groundwater temperature of a spring studied (Mt Nerone karst aquifer) show the probably existence of a “high fracture zone” (FZ), between basal Triassic aquiclude and the “conduits zone” (CZ) in the Massiccio complex. Here, the groundwater temperature varies rather rapidly with different magnitude as a rapid response after the recharge events. On the contrary, in the fracture zone (FC) the groundwater shows a stable trend of temperature and a no-correlation with the recharge events (long residence time), which drainage occurs under diffuse flow behaviour (baseflow condition), confirming the results of recession and time series analysis (*Chapter 6*).

Reference

- Agosta, F., Alessandroni, M., Tondi, E., Aydin, A., 2009. Oblique-slip normal faulting along the northern edge of the Majella anticline: inferences on hydrocarbon migration and accumulation. Journal of Structural Geology 31, 690-774.
- Agosta, F., Aydin, A. 2006. Architecture and deformation mechanism of a basin-bounding normal fault in Mesozoic platform carbonates, central Italy. J. Struc. Geol. 28 (8), 1445-1467.
- Alvarez, W., 1989. Evolution of the Monte Nerone seamount in the Umbria-Marche Apennines: 1, Tectonic control of the seamount-basin transition. Boll Soci Geol It. 108, 23-29.
- Amit, H., Lyakhovsky, V., Katz, A., Starinsky, A., Burg, A., 2002. Interpretation of spring recession curves. Ground Water 40 (5), 543–551.
- Anderson, M.P., 2005. Heat as a ground water tracer. Ground Water 43(6): 951–968.
- Anelli, L., Gorza, M., Pieri, M., Riva, M., 1994. Subsurface well data in the Northern Apennines. Mem Soc Geol It. 48, 461-471.
- Angelini, P., Dragoni, W., 1997. The problem of modelling limestone spring: the case of Bagnara (North Apennines, Italy). Groundwater. 35 (4), 612-618.
- Atkinson, T.C., 1977. Diffuse flow and conduit flow in limestone terrain in the Mendip Hills, Somerset (Great Britain). J. Hydrol. 35, 93–103.
- Aydin, A., 2000. Fractures, faults, and hydrocarbon entrapment, migration and flow. Marine and Petroleum Geology. 17 (7), 797-814.
- Aydin, A., Antonellini, M., Tondi, E., Agosta, F. 2010. Deformation along the leading edge of the Maiella thrust sheet in central Italy. J. Struc. Geol. 32 (9), 1291-1304.
- Bai, T., Pollard, D.D., 2000. Fracture spacing in layered rocks: a new explanation based on the stress transition. Journal of Structural Geology 22, 43–57.
- Bailly-Comte, V., Martin, J.B., Jourde, H., Screaton, E.J., Pistre, S., Langston, A., 2010. Water exchange and pressure transfer between conduits and matrix and their influence on hydrodynamics of two karst aquifers with sinking streams. J. Hydrol. 386 (1–4), 55–66.
- Baiocchi, A., Dragoni, W., Lotti, F., Luzzi, G., Piscopo, V., 2006. Outline of the hydrogeology of the Cimino and Vico volcanic area and of the interaction between groundwater and Lake Vico (Lazio Region, Central Italy). Boll Soc Geol It. 125, pp. 187–202.
- Bally, A.W., Burbi, L., Cooper, C., Ghelardoni, R., 1986. Balanced sections and seismic reflection profiles across the Central Apennines. Mem Soc Geol It. 35, pp. 257-310.
- Barchi M., Lemmi M. 1996. Geologia dell'area del Monte Coscerno-Monte Civitella, Valnerina (Umbria Sud- Orientale). Boll. Soc. Geol. It. 115, 601- 624.
- Barchi, M., De Feyter, A., Magnani, M.B., Minelli, G., Pialli, G., Sotera, B.M., 1998. The structural style of the Umbria-Marche fold and thrust belt. Soc. Geol. Ital. Mem., 52, pp. 557–578.
- Barchi, R.M., Alvarez, W., Shimabukuro, D.H., 2012. The Umbria-Marche Apennines as a double orogen: observation and hypothesis. Ital. J. Geosci. Boll. Soc. Geol. It., Vol. 131, No. 2 (2012), pp. 258-271.
- Barton, C., 1995. Fractals in Petroleum Geology and Earth Processes. New York, Plenum Press, p. 317.

- Becker, A., Gross, M.R., 1996. Mechanism for joint saturation in mechanically layered rocks: an example from southern Israel: Tectonophysics, v. 257, p. 223–237.
- Berkowitz, B., 2002. Characterizing flow and transport in fractured geological media: a re- view. Adv.Water Resour. 25, 861–884.
- Billi, A., 2005. Attributes and influence on fluid flow of fractures in foreland carbonates of southern Italy: Journal of Structural Geology, 27 (9), p. 1630–1643. DOI: 10.1016/j.jsg.2005.05.001.
- Birk, S., Liedl, R., Sauter, M., 2004. Identification of localised recharge and conduit flow by combined analysis of hydraulic and physico–chemical spring responses (Urenbrunnen, SW-Germany). J Hydrol 286:179–193.
- Bison, P., Mariotti, C., Pieroni, M., Piovesana, F., Printe, M., Pugi, S., 1995. Valutazione e protezione delle risorse idriche sotterranee nella dorsale carbonatica M. Catria-M. Nerone (Marche). Groundwater Geoengineering 5, 13-24.
- Bonacci, O., 1993. Karst springs hydrographs as indicators of karst aquifers. Hydrol. Sci. J. 38 (1), 51–62.
- Boni, C., Baldoni, T., Banzato, F., Cascone, D., Petitta, M., 2010. Hydrogeological study for identification, characterisation and management of groundwater resources in the Sibillini Mountains National Park (central Italy). Ital J Eng Geol Environ 2 (2010):21–39. DOI:10.4408/IJEGE.2010-02.
- Boni, C., Bono, P., 1982. Prima valutazione quantitativa dell'infiltrazione efficace sui sistemi carsici della piattaforma carbonatici laziale-abruzzese e nei sistemi di facies pelagica umbro-marchigiana-sabina (Italia centrale). Geologia Applicata e idrogeologia. 17, 427-436.
- Boni, C., Bono, P., Capelli, G., 1986. Schema idrogeologico dell'Italia Centrale. Mem Soc Geol It 35: 991–1012. Roma.
- Boni, C., Mastrorillo, M., Cascone, D., Tarragoni, C., 2005. Carta idrogeologica delle dorsali interne umbro-marchigiane (scala 1:50.000). Pubblicazione GNDCI - CNR n°2865, Roma.
- Boni, C., Petitta, M., 2007. Studio idrogeologico per l'identificazione e la caratterizzazione degli acquiferi che alimentano le sorgenti dei corsi d'acqua perenni dei Monti Sibillini, esteso all'intera area del Parco Nazionale. Rapporto definitivo. Contratto di studio e ricerca. Autorità di Bacino del Fiume Tevere-Parco Nazionale dei Monti Sibillini. Dipartimento Scienze della Terra Università di Roma "La Sapienza". Technical Note. p 97.
- Boni, C., Petitta, M., 2008. Redazione informatizzata della cartografia idrogeologica tematica del territorio della Regione Umbria. Contratto di ricerca. Regione Umbria. Dipartimento Scienze della Terra Università di Roma "La Sapienza". Technical Note. p 131.
- Boussinesq, J.M., 1877. Essai sur la théorie des eaux courantes (Theory of Underground Water Flow under a Non-Permanent Regime). Imprimerie nationale.
- Boussinesq, M.J., 1904. Recherches théoriques sur l'écoulement des nappes d'eau infiltrées dans le sol et sur le debit des sources. Journal de mathématiques, 5e, serie 10.
- Box, G., Jenkins, G. 1970., Time series analysis: Forecasting and control. Holden-Day, San Francisco, USA.
- Box, G.E.P., Jenkins, G.M., Reinsel, G.C., 1994. Time Series Analysis: Forecasting and Control. Prentice Hall Inc., Englewood Cliffs, NJ, USA.

- Brodie, R.S., Hostetler, S., 2009. A review of techniques for analysing baseflow from stream hydrographs. Intl Assn Hydrogeol.
- Calamita, F., Cello, G., Invernizzi, C., Paltrinieri, W., 1990. Stile strutturale e cronologia della deformazione lungo la traversa M. S. Vicino—Polverigi (Appennino marchigiano esterno). Studi Geologici Camerti, Vol. Spec. (1990) 69– 86.
- Calamita, F., Coltorti, M., Pieruccini, P., Pizzi, A., 1999. Evoluzione strutturale e morfogenesi plio-quaternaria dell'Appennino umbro-marchigiano tra il Preappennino umbro e la costa adriatica. Boll Soc Geol It. 118, 125–139.
- Capaccioni, B., Didero, M., Paletta, C., Salvadori, P., 2001. Hydrogeochemistry of groundwaters from carbonate formations with basal gypsiferous layers: an example from the Mt Catria-Mt Nerone ridge (Northern Apennines, Italy). Journal of Hydrology. 253, 14-26.
- Capelli, G., Mazza, R., Gazzetti, C., 2005. Strumenti e strategie per la tutela e l'uso compatibile della risorsa idrica nel Lazio. Vol. 78. Bologna: Pitagora.
- Caprari, M., Nanni, T., Scesi, L., 2002. Contributo all'analisi della circolazione idrica, mediante l'applicazione del metodo di Kiràly, in idrostrutture carbonatiche dell'Appennino adriatico. Bollettino della Società Geologica Italiana. 121(1), 99–120.
- Carloni, G.C., 1964. La Geologia dei dintorni di Cingoli (Appennino Marchigiano). Giornale di Geologia 32, 365-401.
- Cavazza, W., Wezel, F.C., (eds). 2003. Geology of Italy. Episodes, 26, 3, 268.
- Centamore, E., Chiocchini, D., Deiana, G., Micarelli, A., Pieruccini, U., 1971. Contributo alla conoscenza del Giurassico dell'Appennino umbro-marchigiano. Studi Geologici Camerti 1, 7-89.
- Centamore, E., Chiocchini, M., Chiocchini, U., Dramis, F., Giardini, G., Jacobacci, A., Martelli, G., Micarelli, A., Potetti, M., 1979. Note illustrative Foglio 301 "Fabriano" alla scala 1:50.000. Serv. Geol. d'It.
- Centamore, E., Deiana, G., 1986. La Geologia delle Marche. Studi Geologici Camerti, vol. spec., p 145.
- Centamore, E., Jacobacci, A., Malferrari, N., Martelli, G., Pieruccini, U., 1972. Carta Geologica d'Italia alla scala 1:50.000, F290 Cagli. Servizio Geologico D'Italia.
- Centamore, E., Jacobacci, A., Malferrari, N., Martelli, G., Pieruccini, U., Valletta, M., 1975. Carta Geologica d'Italia alla scala 1:50.000, F291 Pergola. Servizio Geologico D'Italia.
- Centamore, E., Micarelli, A., 1991. L'ambiente fisico delle Marche: Stratigrafia. Regione Marche, Assessorato Urbanistico, Ed. S.E.L.C.A., Firenze.
- Centamore, E., Soc., Idrotecnico, Valletta, M., 1976. Note illustrative della Carta Idrogeologica F° 291 "Pergola". Servizio Geologico d'Italia, Roma.
- Chang, Y., Wu, J.C., Liu, L., 2015. Effects of the conduit network on the spring hydrograph of the karst aquifer. J. Hydrol. 527, 517–530.
- Chen, Z., Grasby, S.E., Osadetz, K.G., 2004. Relation between climate variability and groundwater levels in the upper carbonate aquifer, southern Manitoba, Canada. Journal of Hydrology. 290, 43–62.
- Chen-Chang, L., Cheng-Haw, L., Hsin-Fu, Y., Hung-I, L., 2010. Modeling spatial fracture intensity as a control on flow in fractured rock. Environ Earth Sci. DOI: 10.1007/s12665-010-0794-x.

- Ciarapica, G., Passeri, L., 2002. The paleographic duplicity of the Apennines. Boll Soc Geol It, 121 (1), 67-75.
- Colacicchi, R., Passeri, L., Pialli, G., 1970. Nuovi dati sul Giurese umbro-marchigiano ed ipotesi per un suo inquadramento regionale. Memorie della Società Geologica Italiana 9, 839-874.
- Cooke, M.L., Simo, J.A., Underwood, C.A., Rijken, P., 2006. Mechanical stratigraphic controls on fracture patterns within carbonates and implications for groundwater flow: Sedimentary Geology, v. 184, p. 225–239. DOI: 10.1016/j.sedgeo.2005.11.004.
- Cooke, R.U., Doornkamp, J.C., 1990. Geomorphology in environmental management: a new introduction. New York: Clarendon Press.
- Covington, M.D., Luhmann, A.J., Gabrovšek, F., Saar, M.O., Wicks, C.M., 2011. Mechanisms of heat exchange between water and rock in karst conduits. Water Resour Res 47(W10514). DOI: 10.1029/2011WR010683.
- Davy, P., Le Groc, R., Darcel, C., Bour, O., de Druzy, J.R., Munier, R., 2010. A likely universal model of fracture scaling and its consequence for crustal hydromechanics. Journal of Geophysical Research 115, B10411. DOI:10.1029/ 2009JB007043.
- De Feyter, A., Koopman, A., Molenaar, N., Van Den Ende, C., 1987. Detachment tectonics and sedimentation, Umbro-Marchean Apennines, Italy. Bollettino della Società Geologica Italiana. 105, 65–85.
- De Feyter, A.J., Menichetti, M., 1986. Back-thrusting in forelimbs of rootless anticlines, with examples from the Umbria-Marche Apennines (Italy).
- de Marsily, G., 1986. Quantitative hydrogeology: groundwater hydrology for engineers. Academic Press Orlando, FL.
- Decandia, F.A., Giannini, E., 1977. Studi geologici nell'Appennino umbro-marchigiano. 2) Le scaglie di copertura. Boll. Soc. Geol. It., 96, 723-734.
- Deiana, G., Cello, G., Chiocchini, M., Galdenzi, S., Mazzoli, S., Pistolesi, E., Potetti, M., Romano, A., Turco, E., Principi, M., 2002. Tectonic evolution of the external zones of the Umbria-Marche Apennines in the Monte San Vicino-Cingoli area. Boll Soc Geol It. 1, 229-238.
- Deiana, G., Pialli, G., 1994. The structural provinces of the Umbro-Marchean Apennines. Mem. Soc. Geol. It., 48, 473-484.
- Delbart, C., Valdés, D., Barbecot, F., Tognelli, A., Chouchoux, L., 2016. Spatial organization of the impulse response in a karst aquifer. J. Hydrol., 537, 18-26.
- Delbart, C., Valdés-Lao, D., Barbecot, F., Tognelli, A., Richon, P., Couchoux, L., 2014. Temporal variability of karst aquifer response time established by the sliding windows cross-correlation method. J. Hydrol. 511, 580–588.
- Demek, J., Embleton, J.F., Andgellert, C., Verstappen, H.T., 1972. Manual of Detailed Geomorphological Mapping (International Geographical Union Commission on Geomorphological Survey and Mapping). Prague: Academia.
- Dershowitz, W.S., Herda, H.H., 1992. Interpretation of fracture spacing and intensity. In: Tillerson, J.R., Wawersik, W.R. (Eds.), Proceedings of the 33rd U.S. Symposium on Rock Mechanics. Rotterdam, Balkema, pp. 757–766.

- Dewandel, B., Lachassagne, P., Bakalowicz, M., Weng, P., Al-Malki, A., 2003. Evaluation of aquifer thickness by analysing recession hydrographs. Application to the Oman ophiolite hard-rock aquifer. J. Hydrol. 274 (1–4), 248–269.
- Di Naccio, D., Boncio, P., Cirilli, S., Casaglia, F., Morettini, E., Lavecchia, G., Brozzetti, F., 2005. Role of mechanical stratigraphy on fracture development in carbonate reservoirs: Insights from outcropping shallow water carbonates in the Umbria-Marche Apennines, Italy. Journal of Volcanology and Geothermal Research 148, 98-115.
- Doerfliger, N., Zwahlen, F., 1995. Action COST 65 – Swiss National Report. Bulletin d'Hydrogéologie de l'Université de Neuchâtel, 14, 3-33.
- Drew, D., Hötzl, H., 1999. Karst Hydrology and Human Activities. International Contributions to Hydrogeology. A. A. Balkema, International Association of Hydrologists, pp. 322, Rotterdam.
- Drogue, C., 1971. Coefficient d'infiltration ou infiltration eficace, sur le roches calcaires, Actes du Colloque d'Hydrologie en Pays Calcaire, Besancon, 15, 121–130.
- Drogue, C., 1972. Analyse statistique des hydrogrammes de décrues des sources karstiques. Journal of Hydrology 15, 49–68.
- Drogue, C., 1974. Structure de certains aquifères karstiques d'après les résultats de travaux de forage. (Structure of certain karst aquifers from drilling data). CR Acad Sci Paris, série III (278):2621–2624.
- Drogue, C., 1980. Essai d'identification d'un type de structure de magasins carbonatés fissurés: application à l'interprétation de certains aspects du fonctionnement hydrogéologique (On the structural identification of carbonate storage fissures: application to certain aspects of hydrological functioning). Mém Hors Sér Soc Géol Fr 11:101–108.
- Eichubl, P., Tyler, W.L., Pollard, D.D., Aydin, A. 2004. Paleo-fluid flow deformation in the Aztec Sandstone at the Valley of Fire, Nevada – evidence for the coupling of hydrogeologic, diagenetic, and tectonic processes. Geological Society of America Bulletin 116, 1120-1136.
- Eisenlohr, L., Király, L., Bouzelboudjen, M., Rossier, Y., 1997. Numerical versus statistical modelling of natural response of a karst hydrogeological system. J. Hydrol. 202 (1–4), 244–262.
- Elter, P., Giglia, G., Tongiorgi, M.&Trevisan, L., 1975. Tensional and compressional areas in the recent (Tortonian to present) evolution of North Apennines, Boll. Geof. teor. Appl., 17, 3–18.
- Engelder, T., Scholz, C., 1981. Fluid flow along very smooth joints at effective pressure up to 200 megapascals. In: Carter, N.L. (Ed.), Mechanical behaviour of crustal rocks Geophysical Monograph Series, vol. 24. AGU, pp. 147-152.
- Farlin, J., Maloszewski, P., 2013. On the use of spring baseflow recession for a more accurate parameterization of aquifer transit time distribution functions. Hydrol. Earth Syst. Sci. 17 (5), 1825–1831.
- Fetter, C.W., 1980. Applied Hydrogeology. Merrill Publishing, Columbus, Ohio.
- Fiorillo, F., 2011. Tank-reservoir drainage as a simulation of the recession limb of karst spring hydrographs. Hydrogeol. J. 19 (5), 1009–1019.
- Fiorillo, F., 2014. The recession of spring hydrographs, focused on karst aquifers. Water Resour. Manage. 28 (7), 1781–1805.
- Fiorotto, V., Caroni, E., 2013. A new approach to master recession curve analysis. Hydrol Sci J 58(5):966–975. DOI: 10.1080/ 02626667.2013.788248

- Ford, D.C., Ewers, R.O., 1978. The development of limestone caves in the dimensions of length and depth. Canadian Journal of Earth Sciences 15, 1783-1798.
- Ford, D.C., Williams, P.W., 1989. Karst Geomorphology and Hydrology. Unwin Hyman, London, 601p.
- Ford, D.C., Williams, P.W., 2007. Karst hydrogeology and geomorphology. Chichester, UK: Wiley.
- Forkasiewicz, J., Paloc, H., 1967. Le régime de tarissement de la Foux de la Vis. Etude preliminaire. Chron. d'Hydrogeol., BRGM 3 (10), 61–73.
- Fu, T.G., Chen, H.S., Zhang, W., Nie, Y.P., Gao, P., Wang, K.L., 2015a. Spatial variability of surface soil saturated hydraulic conductivity in a small karst catchment of southwest China. Environ. Earth Sci. 74 (3), 2381–2391.
- Fu, T.G., Chen, H.S., Zhang, Wang, K.L., 2016. Structure and water storage capacity of a small karst aquifer based on stream discharge in southwest China. Journal of Hydrology. 534, 50-62.
- Galdenzi, S., Menichetti, M., 1989. Evolution of underground karst systems in the Umbria-Marche Appennines in Central Italy. In: Hazslinszky, T. & B.K. Takacsne (eds.) Proceedings, International Congress of Speleology, 10th, August 1989 Budapest, vol.3, 745-747, Budapest Hungary.
- Galdenzi, S., Menichetti, M., 1995. Occurrence of hypogenic caves in a karst region: examples from central Italy. Environmental Geology 26, 39–47.
- Ghasemizadeh, R., Hellweger, F., Butscher, C., Padilla, I., Vesper, D., Field, M., Alshawabkeh, A., 2012. Review: groundwater flow and transport modeling of karst aquifers, with particular reference to the North Coast Limestone aquifer system of Puerto Rico. Hydrogeol. J. 20 (8), 1441–1461.
- Giacopetti, M., Materazzi, M., Pambianchi, G., Posevac, K., 2017. Analysis of mountain springs discharge time series in the Tennecola stream catchment (central Apennine, Italy). Environ Earth Sci (2017) 76:20.
- Gillespie, P., Walsh, J.J., Watterson, J., Bonson, C.G., Manzocchi, T., 2001. Scaling relationships of joint and vein arrays from the Burren, Co. Clare Ireland. J. Struct. Geol. 23, 183-201.
- Goldscheider, N., Drew, D., 2007. Methods in Karst Hydrogeology, edited by: Hydrogeologists, I. A. o., Taylor & Francis Group, 264 pp.
- Gregor, M., Malík, P., 2012. Construction of master recession curve using genetic algorithms. J. Hydrol. Hydromech. 60 (1), 3–15.
- Groshong, R.H., 1988. Low-temperature deformation mechanisms and their interpretation. Geological Society of America Bulletin 100, 1329-1360.
- Gross, M.R., 1993. The origin and spacing of cross joints: examples from the Monterrey Formation, Santa Barbara coastline, California. Journal of Structural Geology 15, 737–751.
- Gross, M.R., Engelder, T., 1995. Strain accommodated by brittle failure in adjacent units of the Monterey Formation, U.S.A.: scale effects and evidence for uniform displacement boundary conditions. Journal of Structural Geology 17, 1303–1318.
- Gross, M.R., Eyal, Y., 2007. Thoroughgoing fractures in layered carbonate rocks. GSA Bulletin 119, 1387-1404.
- Guardiola-Albert, C., Martos-Rosillo, S., Pardo-Igúzquiza, E., Valsero, J.J.D., Pedrera, A., Jimén-Gavilán, P., Liñan Baena, C., 2015. Comparison of recharge estimation methods during a wet period in a karst aquifer. Groundwater. 53(6), 885-895.

- Gudmundsson, A., 2011. Rock Fractures in Geological Processes, first ed. Cambridge University Press, New York.
- Gudmundsson, A., Simmenes, T.H., Larsen, B., Philipp, S.L., 2010. Effects of internal structure and local stresses on fracture propagation, deflection, and arrest in fault zones. Journal of Structural Geology 32, 1643-1655.
- Guerriero, F., Dati, F., Giorgioni, M., Iannace A., Mazzoli, S., Vitale, S., 2015. The role of stratabound fractures for fluid migration pathways and storage in well-bedded carbonates. Ital. J. Geosci., Vol. 134, No.3, pp. 383-395.
- Hanks, C.L., Lorenz, J., Lawrence, T., Krumhardt, A.P., 1997. Lithologic and structural controls on natural fracture distribution and behaviour within the Lisburne Group, north-eastern Brooks Range and North Slope subsurface, Alaska. American Association of Petroleum Geologists Bulletin 81, 1700–1720.
- Healy, R.W., Winter, T.C., La Baugh, J.W., Franke, O.L., 2007. Water budgets: Foundations for effective water-resources and environmental management. Reston, Va: U.S. Geological Survey Circular 1308.
- Heinz, B., Birk, S., Liedl, R., Geyer, T., Straub, K.L., Andresen, J., Bester, K., Kappler, A., 2009. Water quality deterioration at a karst spring (Gallusquelle, Germany) due to combined sewer overflow: evidence of bacterial and micro-pollutant contamination. Environmental Geology. 57(4), 797-808. DOI: 10.1007/s00254-008-1359-0.
- Huang, Q., Angelier, J., 1989. Fracture spacing and its relation to bed thickness. Geological Magazine 126, 355–362.
- Jacobacci, A., Centamore, E., Chiocchini, M., Malferri, N., Martelli, G., Micarelli, A., 1974. Note esplicative della Carta Geologica d'Italia (1:50000). Foglio 290-Cagli. Servizio Geologico d'Italia. Roma.
- Jeannin, P.Y., Sauter, M., 1998. Analysis of Karst Hydrodynamic Behaviour Using Global Approach: A Review, Université de Neuchatel, Neuchatel.
- Jemcov, I., Petrič M., 2009. Measured precipitation vs. effective infiltration and their influence on the assessment of karst systems based on results of the time series analysis. J. Hydrol. 379, 304–314.
- Katsanou, K., Lambrakis, N., Tayfur, G., Baba, A., 2015. Describing the karst evolution by the exploitation of hydrologic time-series data. Water Resour. Manage. 29 (9), 3131–3147.
- Kiraly, L. 1975. Rapport sur l'état actuel des connaissances dans le domaines des caractères physiques des roches karstiques, edited by: Burger, A. and Dubertret, L., Hydrogeology of karstic terrains, Int. Union of Geol. Sci. B, 3, 53–67.
- Király, L., 1998a. Modeling karst aquifers by the combined discrete channel and continuum approach. Bulletin d'Hydrogéologie de l'Université de Neuchâtel, 16, 77-98.
- Király, L., 2002. Karstification and Groundwater Flow. In: Proceedings of the Conference on Evolution of Karst: From Prekarst to Cessation. Postojna-Ljubljana. 155-190.
- Király, L., Matthey, B., Tripet, J.P., 1971. Fissuration et orientation des cavités souterraines. Région de la Grotte Milandre. Bull. Soc. Neuchât. Sci. Nat. 94, 99-114.
- Király, L., Morel, G., 1976. Remarques sur l'hydrogramme des sources karstiques simulé par modéles mathématiques. Bull Centre d'Hydrogéol Univ de Neuchatel (Suisse) 1:37–60.
- Kiraly, L., Perrochet, P., Rossier, Y., 1995. Effect of the epikarst on the hydrograph of karst springs: a numerical approach. Bull. Centre d'Hydrogéol. 14, 199–220.

- Korneva, I., Tondi, E., Agosta, F., Rustichelli, A., Spina V., Bitonte, R., Di Cuia, R., 2014. Structural properties of fractured and faulted Cretaceous platform carbonates, Murge Plateau (Southern Italy). Marine and Petroleum Geology 57, 312-326.
- Kovács, A., 2003. Geometry and hydraulic parameters of karst aquifers: A hydrodynamic modelling approach, PhD thesis, Centre of Hydrogeology, University of Neuchatel, 131 pp., 2003.
- Kovács, A., Perrochet, P., 2008. A quantitative approach to spring hydrograph decomposition. J. Hydro. 352, 16-29.
- Kovács, A., Perrochet, P., Király, L., Jeannin, P.Y., 2005. A quantitative method for the characterisation of karst aquifers based on spring hydrograph analysis. J. Hydrol. 303 (1), 152–164.
- Kovács, A., Sauter, M., 2007. Modelling karst hydrodynamics, in Methods in Karst Hydrogeology, edited by N. Goldscheider and D. Drew, pp. 65–91, Taylor and Francis/Balkema, London, U. K.
- Kresic, N, Bonacci, O., 2010. Spring discharge hydrograph. In Groundwater Hydrology of Springs: Engineering, Theory, Management, and Sustainability. Elsevier ch 4, pp 129–163.
- Kresic, N., Stevanovic, Z., 2010. Groundwater Hydrology of Springs: engineering, theory, management and sustainability. Burlington: Butterworth-Heinemann.
- Kullman, E., 2000. Nové metodické prístupy k riešeniu ochrany a ochranných pásiem zdrojov podzemných vôd v horninoých prostrediach s krasovo—puklinovou priepustnostou (New methods in groundwater protection and delineation of protection zones in fissure-karst rock environment; in Slovak). Podzemná voda 6(2):31–41
- Larocque, M., Mangin, A., Razck, M., Banton, O., 1998. Contribution of correlation and spectral analyses to the regional study of a large karst aquifer (Charente, France). J. Hydrol. 205, 217–231.
- Lavecchia, G., 1985. Il sovrascorrimento dei Monti Sibillini: analisi cinematica e strutturale. Boll. Soc. Geol. It., 104, 161-194.
- Lavecchia, G., Brozzetti, F., Barchi, M., Menichetti, M., Keller, J.V.A., 1994. Seismotectonic zoning in east-central Italy deduced from an analysis of the Neogene to present deformations and related stress fields. Geological Society of America Bulletin 106, 1107–1120.
- Lavecchia, G., Minelli, G., Pialli, G., 1988. The Umbria-Marche arcuate fold belt (Italy). Tectonophysics, 146, 125-137.
- Lavenu, A., Lamarche, J., 2017. What controls diffuse fractures in platform carbonates? Insights from Provence (France) and Apulia (Italy). J. Struct. Geol. xxx, 1-14.
- Lee, C., Farmer I., 1993. Fluid flow in discontinuous rocks. Chapman and Hall, New York.
- Li, L.L., 2009. Study of Effects of Ecological Environment on Regulated Function of Epikarst Water in Typical Karst Area of Southwest, China. Southwest University, Congqing, China.
- Líñán Baena, C., Andreo, B., Mudry, J., Carrasco Cantos, F., 2009. Groundwater temperature and electrical conductivity as tools to characterize flow pattern in carbonate aquifer: The Sierra de las Nieves karst aquifer, southern Spain. Hydrogeol J 17:843–853. DOI: 10.1007/s10040-008-0395-x.
- Lo Russo, S., Amanzio, G., Ghione, R., De Maio, M., 2014. Recession hydrographs and time series analysis of springs monitoring data: application on porous and shallow aquifers in mountain areas (Aosta Valley). Environ Earth Sci. 73:7415-7434.

- Long, J.C.S., Aydin, A., Brown, S., Einstein, H., Hestir, K., Hsieh, P., Myer, L., Nolte, K., Norton, D., Olsson O., Paillet F., Smith, J., Thomsen, L., 1996. Rock fractures and fluid flow. National Academy Press, Washington D.C., 551.
- Lucia, F.J., 1999. Carbonate Reservoir Characterization. Springer-Verlag, New York, USA.
- Maillet, E., 1905. Essais d'Hydraulique souterraine et fluviale (Underground and River Hydrology). Hermann, Paris, 218 pp.
- Malík, P., 2007. Assessment of regional karstification degree and groundwater sensitivity to pollution using hydrograph analysis in the Velka Fatra Mts., Slovakia. Water Resources and Environmental Problems in Karst. Environ Geol 2007 (51):707–711. DOI: 10.1007/s00254-006-0384-0.
- Malík, P., 2015. Evaluating discharge regimes of karst aquifer. In: Stevanović Z. (eds) Karst Aquifers Characterization and Engineering. Springer, Berlin. pp 205–247. DOI: 10.1007/978-3-319-12850-4.
- Malík, P., Vojtková, S., 2012. Use of recession-curve analysis for estimation of karstification degree and its application in assessing overflow/underflow conditions in closely spaced karstic springs. Environ. Earth Sci. 65 (8), 2245–2257.
- Malinverno, A., Ryan, W.B.F., 1986. Extension in the Tyrrhenian Sea and shortening in the Apennines as result of arc migration driven by sinking of the lithosphere. Tectonics 5, 227-245.
- Mandal, N., Deb, S.K., Khan, D., 1994. Evidence for a nonlinear relationship between fracture spacing and layer thickness. Journal of Structural Geology 16, 1275–1281.
- Mangin, A., 1975. Contribution á l'étude hydrodynamique des aquiféres karstiques. PhD Thése, Université de Dijon, p. 124.
- Mangin, A., 1981. Utilisation des analyses correlatoire et spectrale dans l'approche des systemes hydrologiques. Comptes Rendusd'Acad Sci 293:401–404
- Mangin, A., 1984. Pour une meilleure connaissance des systemes hydrologiques h partir des analyses corrflatoire et spectrale, J. Hydrol., 67, 25-43.
- Mangin, A., Pulido-Bosch, A., 1983. Aplicacion de los analisis de correlatorie spectral en el estudio de los acuiferos karsticos. Tecniterrae 51–53.
- Marchegiani, L., Bertotti, G., Cello, G., Deiana, G., Mazzoli, S., Tondi, E., 1999. Pre-orogenic tectonics in the Umbria-Marche sector of the Afro-Adriatic continental margin. Tectonophysics 315, 123-143.
- Marrett, R., Ortega, O., Kelsey, C., 1999. Extent of power-law scaling for natural fractures in rock: Geology, v. 27, no. 9, p. 799–802, DOI:10.1130/0091-7613(1999)027<0799: EOPLSF>2.3.CO;2.
- Martin, J.B., Dean, R.W., 1999. Temperature as a natural tracer of short residence times for groundwater in karst aquifers. In: Palmer AN, Palmer MV, Sasowsky ID (eds) Karst Modeling. Spec.
- Mastrorillo, L., 2001. Elementi strutturali e caratteristiche idro- geologiche della dorsale carbonatica umbro-marchigiana. Mem. Soc. Geol. It., 56, 219-226.
- Mastrorillo, L., Baldoni, T., Banzato, F., Boscherini, A., Cascone, D., Checcucci, R., Petitta, M., Boni, C., 2009. Quantitative hydrogeological analysis of the carbonate domain in the Umbria region. Ital Eng Geol Environ, 1: 137-155.
- Mastrorillo, L., Petitta, M., 2010. Effective infiltration variability in the Umbria-Marche carbonate aquifers of central Italy. Journal of Mediterranean Earth Sciences, 2, 9-18.

- Mastrorillo, L., Petitta, M., 2014. Hydrogeological conceptual model of the Upper River basin aquifers (Umbria-Marche Apennines). Ital. J. Geosci., Vol. 133, No. 3, pp. 396-408. DOI: 10.3301/IJG.2014.12.
- Mauldon, M., Dershowitz, W., 2000. A multi-dimensional system of fracture abundance measures: Geological Society of America Abstracts with Programs, v. 32, no. 7, p. A474.
- Mayaud, C., Wagner, T., Benischke, R., Birk, S., 2014. Single event time series analysis in a binary karst catchment evaluated using a groundwater model (Lurbach system, Austria). J. Hydrol. 511, 628–639.
- Mayer, L., Menichetti, M., Nesci, O., Savelli D., 2003. Morphotectonic approach to the drainage analysis in the North Marche region, central Italy. Quaternary Intern., 101-102, 157-167.
- Mazzoli, S., Deiana, G., Galdenzi, S., Cello, G., 2002. Miocene fault-controlled sedimentation and thrust propagation in the previously faulted external zones of the Umbria-Marche Apennines, Italy. EGU Stephan Mueller Special Publication Series 1, 195-209.
- McGinnis, R.N., Ferrill, D.A., Morris, A.P., Smart, K.J., 2016. Insight on mechanical stratigraphy and subsurface interpretation. In: Krantz, B., Ormand, C., Freeman, B. (Eds.), 3-D Structural Interpretation: Earth, Mind, and Machine, vol. 111. AAPG Memoir, pp. 111-120.
- Meinzer, O.E., 1923. The occurrence of groundwater in the United States with a discussion of principles. USGS Water Supply Paper. 489.
- Menichetti M., Chirenco, M.I., Onac, B., Bottrell, S., 2008. Depositi di gesso nelle grotte del M. Cucco e della Gola di Frasassi, Considerazioni sulla speleogenesi. Mem. Ist. Ital. Speleol., II, 21, 308-325.
- Menichetti, M. 1991. La sezione geologica Cingoli-M. Maggio-Tevere nell'Appennino umbro-marchigiano: analisi cinematica e strutturale. Studi Geologici Camerti 1, 315-328.
- Menichetti, M., 1987. Evoluzione spazio temporale del sistema carsico di Monte Cucco. Atti Conv Naz Spel Bari 1:731-762.
- Menichetti, M., 1989. Hydrogeology of Mount Cucco karst system in Central Italy. 10th Congress International of Speleology. Budapest. 3, 748-750.
- Menichetti, M., 1995. Rapporti tra tettonica giurassica e neogenica nell'area umbro-marchigiana. Atti Conv. «Geodinamica e tettonica attiva del sistema Tirreno-Appennino». Camerino, 9-10 febbraio 1995.
- Menichetti, M., 2008: Assetto strutturale del sistema geotermico di Acquasanta Terme (Ascoli Piceno). Rend. Soc. Geol. It., 1, 118-122.
- Menichetti, M., 2009: Speleogenesis of the hypogenic caves in Central Italy. In: White, W.B. (ed.) Proceedings of the 15th Int. Cong. of Speleology, August 2009 Kerrville, 909-915, Kerrville, U.S.A.
- Menichetti, M., De Feyter, A.J., Corsi, M., 1991. Crop 03dIl tratto della Val Tiberina-Mare Adriatico. Sezione geologica e caratterizzazione tettonico- sedimentaria delle avanfosse della zona umbro-marchigiano-romagnola. Studi Geologici Camerti 1, 279-293.
- Menichetti, M., Salvatori, F., Reichembach, G., 1988. Contribution des essais de multitracages à la definition de l'hydrostructure carbonatique de Monte Cucco et de la source Scirca-Italie-Apennin Central. Annales Scientifiques de l'Université de Besancon, Geologie, Memorie Hors series, no.6, vol.2, 347-364.
- Minissiale, A., Vaselli, O., 2011. Karst spring as "natural" pluviometers: constrains on the isotopic composition of rainfall in the Apennines of central Italy. Applied Geochemistry. 26, 838-852.
- Mohommadi, Z., Shoja, A., 2014. Effect of annual rainfall amount on characteristics of karst spring hydrograph. Carbonates Evaporites, 29: 279-289.

- Nanni, T., Vivalda, P., 2005. The aquifers of the Umbria-Marche Adriatic region: relationship between structural setting and groundwater chemistry. Boll Soc Geol It 124:523–542.
- Narr, W., 1996. Estimating average fracture spacing in subsurface rock. AAPG Bulletin 80, 1565– 1586.
- Narr, W., Suppe, J., 1991. Joint spacing in sedimentary rocks. J. Struct. Geol. 13, 1037-1048.
- Nathan, R.J., McMahon, T.A., 1990. Evaluation of automated techniques for base flow and recession analyses. Water Resour Res 26(7):1465–1473. DOI: 10.1029/WR026i007p01465.
- Nelson, R., 2001. Geologic Analysis of Naturally Fractured Reservoirs, second ed. Gulf Professional Publishing, Woburn.
- Neuman, S.P., 2005. Trends, prospects and challenges in quantifying flow and transport through fractured rocks, Hydrogeol. J., 13, 124–147.
- Oda, M., 1985. Permeability tensor for discontinuous rock masses. Geotechnique 35, 483–495.
- Odling, N.E., Gillespie, P.A., Bourgine, B., Castaing, C., Chiles, J.P., Chistensen, N.P., Fillion, E., Genter, A., Olsen, C., Thrane, L., Trice, R., Aarseth, E., Walsh, J., Watterson, J.J., 1999. Variations in fracture system geometry and their implications for fluid flow in fractured hydrocarbon reservoirs. Petroleum Geosciences 5, 373-384.
- Padilla, A., Pulido-Bosch, A., 1995. Study of karstic aquifers by means of correlation and cross-spectral analysis. J. Hydrol. 168, 73–89
- Padilla, A., Pulido-Bosch, A., Mangin, A., 1994. Relative importance of baseflow and quickflow from hydrographs of karst spring. Ground Water 32 (2), 267-277.
- Palmer, A.N., 1991. The origin and morphology of limestone caves. Geological Society of America Bulletin 103, 1-21.
- Palmstrom, A., 2001. Measurement and Characterization of Rock Mass Jointing. A.A. Balkema Publishers.
- Paloc, H., Margat, J., 1985. Report on hydrogeological maps of karstic terrains, in hydrogeological Mapping in Asia and the Pacific Region (eds W. Grimelmann, K.D. Krampe and W. Struckmeier), International Contributions to Hydrogeology, Vol. 7, Heise, Hannover, pp. 301–15.
- Panagopoulos, G., Lambrakis, N., 2006. The contribution of time series analysis to the study of the hydrodynamic characteristics of the karst systems: application on two typical karst aquifers of Greece (Trifilia, Almyros Crete). J. Hydrol. 329 (3), 368-376.
- Panza, E., Agosta, F., Zambrano, M., Tondi, E., Prosser, G., Giorgioni, M., Janiseck, J.M., 2015. Structural architecture and Discrete Fracture Network modelling of layered fractured carbonates (Altamura Fm., Italy). Ital. J. Geosci., Vol. 134, No. 3, pp. 409-422.
- Pascal, C., Angelier, J., Cacas, M.C., Hancock, P.L., 1997. Distribution of joints: probabilistic modelling and case study near Cardiff (Wales, U.K.). Journal of Structural Geology 19, 1273-1284.
- Pazzaglia, F., Melelli, L., Barchi, M., Piselli, E., Provani, D., 2015. Geological heritage in Valcasana (southeastern Umbria): mass wasting and structural control. Rend. Online Soc. Geol. It., Vol. 34 (2015), pp. 93-96.
- Petras, I., 1986. An approach to the mathematical expression of recession curves. Water SA 12 (3): 145–150.

- Pollard, D.D., Aydin, A., 1988. Progress in understanding jointing over the past century. Geological Society of America Bulletin 100, 1181–1204.
- Posavec, K., Bačani, A., Nakić, Z., 2006. A visual basic spreadsheet macro for recession curve analysis. Ground Water. 44(5):764–767. DOI: 10.1111/j.1745-6584.2006.00226.
- Posavec, K., Parlov, J., Nakić, Z., 2010. Fully automated objective-based method for master recession curve separation. Ground Water 48(4):598–603. DOI: 10.1111/j.1745-6584.2009.00669.
- Price, N.J., 1966. Fault and Joint Development in Brittle and Semibrittle Rocks. Pergamon Press, Oxford.
- Priest, S., 1993. Discontinuity analysis for rock engineering. Springer, Berlin.
- Priest, S., Hudson, J., 1981. Estimation of discontinuity spacing and trace length using scanline. Int J Rock Mech Min Sci Geomech Abstr 18:183–197.
- Pulido-Bosch, A., Padilla, A., Dimitrov, D., Machkova, M., 1995. The discharge variability of some karst springs in Bulgaria studied by time series analysis. Hydrol. Sci. J. 40(4), 517-532.
- Riggs, H.C., 1964. The base-flow recession curve as an indicator of groundwater. Int Assoc Sci Hydrol Publ 63: 352–363.
- Roy, B., Benderitter, Y., 1986. Natural thermal transfer in a superficial fissured carbonate system (in French). Bull Soc Géol France 2 (4):661–666.
- Royden, L.H., 1993. Evolution of retreating subduction boundaries formed during continental collision, Tectonics, 12, 629–638.
- Rustichelli, A., Agosta, F., Tondi, E., Spina, V., 2013. Spacing and distribution of bed-perpendicular joints throughout layered, shallow-marine carbonates (Granada Basin, southern Spain). Tectonophysics 582, 188-204.
- Ryan, M., Meiman J., 1996. An examination of short-term variations in water quality at a karst spring in Kentucky. Ground Water 34, no. 1: 23–30.
- Sahimi, M, 1995. Flow and transport in porous media and fractured rock: from classical methods to modern approaches. VCH, Weinheim, NewYork.
- Sanderson, D.J., Nixon, C.W., 2015. The use of topology in fracture network characterization. J. Struct. Geol. 72, 55-66.
- Sarbu, S.M., Galdenzi, S., Menichetti, M., Gentile, G., 2000. Geology and biology of the Frasassi Caves in Central Italy, an ecological multi-disciplinary study of a hypogenic underground ecosystem. In: Wilkens H, et al., editors. Ecosystems of the world. New York (NY): Elsevier. p. 359-378.
- Sauter, M., 1992. Quantification and forecasting of regional groundwater flow and transport in a karst aquifer (gallusquelle, malm, SW. Germany). Ph.D. thesis, University of Tubingen.
- Sharp, J.M. Jr., 1993. Fractured aquifers/reservoirs: Approaches, problems, and opportunities. In: Banks D, Banks S (eds) Hydrogeology of hard rocks: Memoires 24th Congress, Int Association Hydrogeologists 23–38.
- Sibson, R.H., 1996. Structural permeability of fluid-driven fault-fractures meshes. Journal of Structural Geology 18, 1031-1042.
- Stevanovic, Z., Milanovic, S., Ristic, V., 2010. Supportive methods for assessing effective porosity and regulating karst aquifers. Acta Carsol 39(2):301–311.

- Strijker, G., Bertotti, G., Stefan M. Luthi, S.M., 2012. Multi-scale fracture network analysis from an outcrop analogue: A case study from the Cambro-Ordovician clastic succession in Petra, Jordan. Marine and Petroleum Geology. 38, 104-116.
- Tallaksen, L., 1995. A review of baseflow recession analysis. J. Hydrol. 165 (1), 349–370.
- Tamburini, A., 2016. Structural characterization of a carbonate hydrostructures in the Umbria-Marche Apennines. Rend. Online Soc. Geol. It., Vol. 41, pp. 88-91, 1 fig. DOI: 10.3301/ROL.2016.100.
- Tavani, S., Storti, F., Salvini, F., Toscano, C., 2008. Stratigraphic versus structural control on the deformation pattern associated with the evolution of the Mt. Catria anticline, Italy. Journal of Structural Geology, 30, 664-681.
- Thornthwaite, C.W., 1948. An Approach to a Rational Classification of Climates. Geographical Review. 38: 1, 55–94.
- Thornthwaite, C.W., Mather, J.R., 1957. Instructions and tables for computing potential evapotranspiration and the water balance. Publication in Climatology 10, Drexel Institute of Technology, Centerton, NJ.
- Tucker, M.E., Wright, V.P., 1990. Carbonate sedimentology. Blackwell Scientific Publication, Oxford, p. 468.
- Underwood, C.A., Cooke, M.L., Simo, J.A., Muldoon, M.A., 2003. Stratigraphic controls on vertical fracture patterns in Silurian Dolomite, north-eastern Wisconsin. American Association of Petroleum Geologists Bulletin 87, 121–142.
- van Golf-Racht, T.D., 1982. Fundamentals of Fractured Reservoir Engineering. Elsevier, Amsterdam, 710 p.
- White, W.B., 2003. Conceptual models for karstic aquifers. Speleogenesis Evol. Karst Aquifers 1 (1), 1–6.
- White, W.B., 2007. A brief history of karst hydrogeology: contributions of the NSS. Journal of Cave and Karst Studies. 69(1), 13–26.
- Wilson, C. E., A. Aydin, M. Karimi-Fard, L. J. Durlofsky, S. Amir, E. E. Brodsky, O. Kreylos, Kellogg L.H., 2011. From outcrop to flow simulation: Constructing discrete fracture models from a LIDAR survey: AAPG Bulletin, v. 95, no. 11, p. 1883–1905. DOI: 10.1306/03241108148.
- Wu, H., Pollard, D.D., 1995. An experimental study of the relationship between joint spacing and layer thickness. Journal of Structural Geology 17, 887–905.
- Yevjevich, V., 1972. Stochastic Processes in Hydrology. Water Resources Publications, Fort Collins, CO, 302 pp.
- Zeeb, C., Gomez-Rivas, E., Bons, P.D., Virgo, S., Blum, P., 2013a. Fracture network evaluation program (FraNEP): a software for analysing 2D fracture trace-line maps. Comput. Geosci. 60, 11-22.
- Zhang, Y., Hobbs, B.E., Ord, A., Barnicoat, A., Lin, G., 2003. The influence of faulting on host-rock permeability, fluid flow and ore genesis of gold deposits: a theoretical 2D numerical model. J. Geochem. Explor. 78–79, 279–284.

Karst aquifers of the Umbria-Marche carbonatic ridge (Northern Apenninnes, Italy)

Tamburini A.*, Piacentini D.*, Menichetti M.*

* Dipartimento di Scienze Pure ed Applicate. Università di Urbino "Carlo Bo" - Via Cà le Suore, Urbino. Italy - andrea.tamburini@uniurb.it

LEGEND

- Rain gaugin station
- Town
- Mountain peak
- Hydrographic network

Hydrogeological features

- Karst spring
- Hydrological limit
- Permeability limit
- Tectonic limit
- Recharge area boundary

Structural features

- Incert fault
- Normal fault
- Strike-slip fault
- Thrust fault

Hydrostratigraphic units

- Clayey-marly calcareous of "Scaglia Cinerea" and "Scaglia Variegata" Formations
- Limestone and marly-limestones of the "Scaglia Rossa" and "Scaglia Bianca" Formations
- Marlstones and clayey-marlstones of the "Marne a Fucoidi" Formation
- Limestones and dolomitic limestones of "Maiolica" Formation
- Silicoclastic-marly-calcareous of "Calcari Diaprini", "Calcari e marne a Posidonie" and "Rosso Ammonitico" Formations
- Stratified limestones of the "Corniola", nodular limestones of "Bugarone" and massive limestones of the "Calcare Massiccio" Formations

AGE	Umbria-Marche succession	Hydrogeological Complex	Hydrogeological Behaviour
Terziary			
Oligocene		Clayey-marly calcareous complex	AQUICLUDE
Eocene			
Paleocene		Scaglia complex	AQUIFER
Guide level K-T			
Cretaceous		Marne a Fucoidi complex	AQUICLUDE
		Maiolica complex	AQUIFER
Jurassic		Silicoclastic-marly calcareous complex	AQUICLUDE
Lias inf.		Basal calcarous complex	AQUIFER
Late Trias		Basal marly-clayey calcareous complex	AQUICLUDE

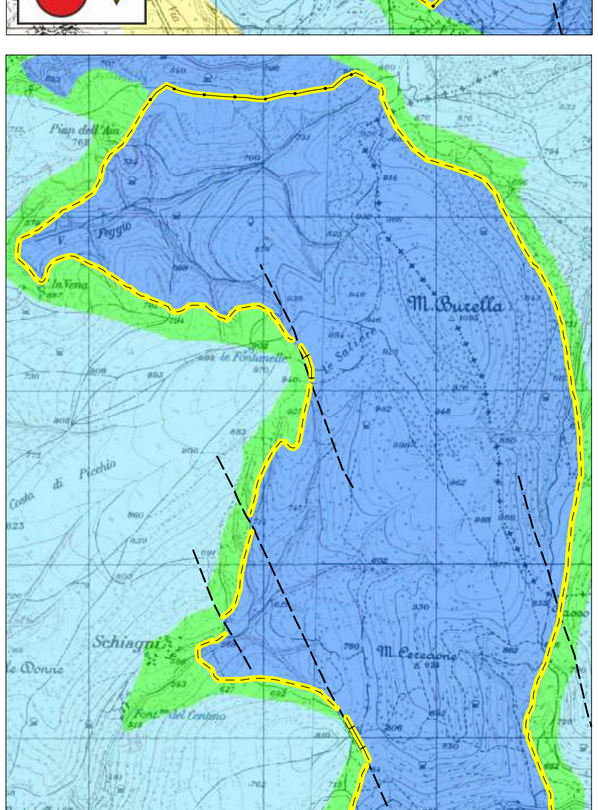

Degrees of spring's discharge reliability based on Iv (index of variability) value

Iv	Symbol	Stability
>30.0		Totally unstable
10.1-30		Very unstable
2.1-10		Unstable
1.0-2.0		Stable

Classification of spring based on average discharge rate (Meinzer 1923)

Discharge	Symbol	Magnitude
10 m³		First
1-10m³		Second
0.1-1 m³		Third
10-100 l/s		Fourth
1-10 l/s		Fifth
0.1-1 l/s		Sixth

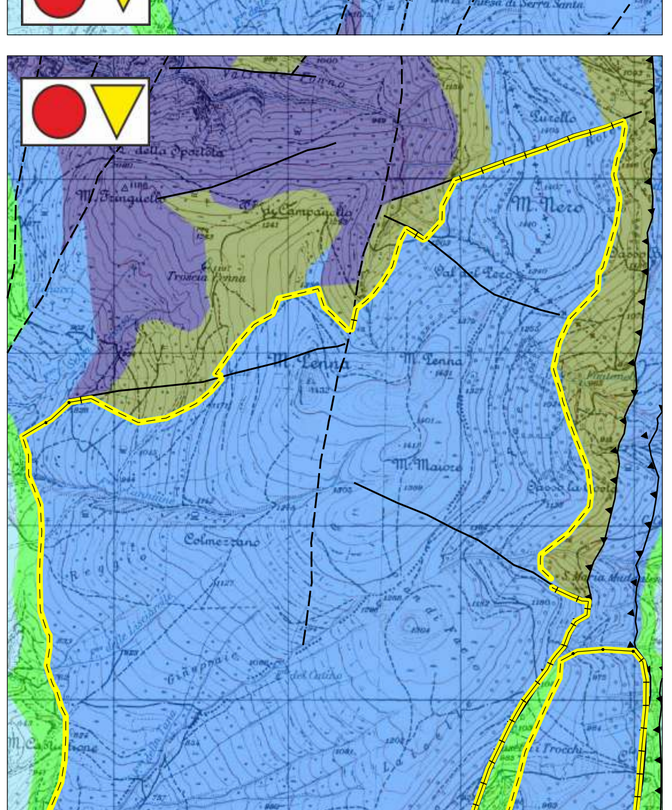

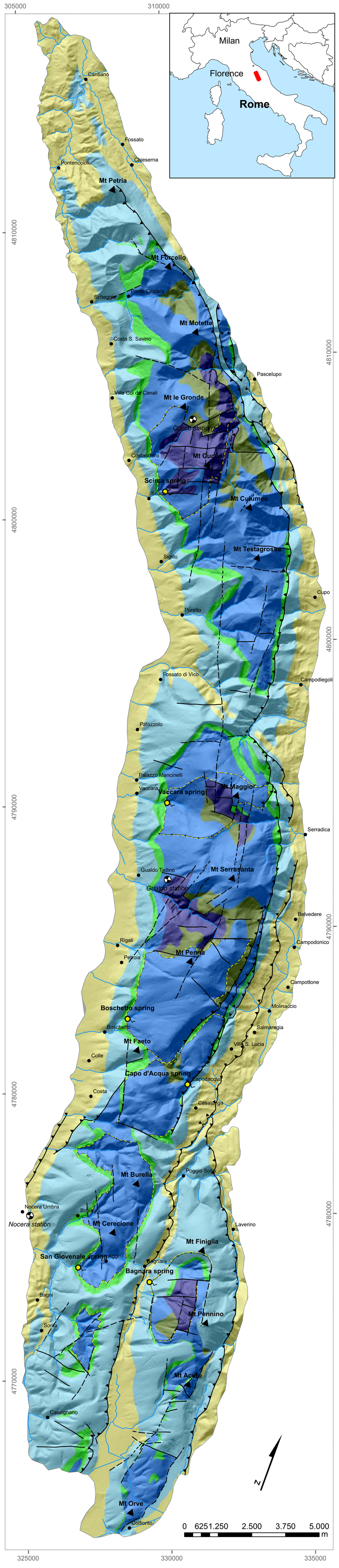

Base map data Regional Technical Map of Umbria, scale 1: 25,000

Geographic Coordinate System W.G.S. 84U.T.M. fuse 33